The influence of autophagy on the fruiting-body development of the filamentous fungus *Sordaria macrospora*

Dissertation
zur Erlangung des mathematisch-naturwissenschaftlichen Doktorgrades
"Doctor rerum naturalium"
der Georg-August-Universität Göttingen

im Promotionsprogramm GAUSS
der Georg-August-University School of Science

vorgelegt von
Oliver Voigt

aus Berlin
Göttingen, 2012

Betreuungsausschuss

Prof. Dr. Stefanie Pöggeler, Abteilung f. Genetik eukaryotischer Mikroorganismen, Institut für Mikrobiologie und Genetik

Mitglieder der Prüfungskommission

Referentin: Prof. Dr. Stefanie Pöggeler, Abteilung f. Genetik eukaryotischer Mikroorganismen, Institut für Mikrobiologie und Genetik

Korreferent: Prof. Dr. Gerhard Braus, Abteilung f. molekulare Mikrobiologie und Genetik, Institut für Mikrobiologie und Genetik

Weitere Mitglieder der Prüfungskommission:

Prof. Dr. Rolf Daniel, Abteilung f. Genomische und Angewandte Mikrobiologie, Institut f. Mikrobiologie u. Genetik

Jun.-Prof. Dr. Kai Heimel, Abteilung f. Mikrobielle Zellbiologie, Institut f. Mikrobiologie u. Genetik

PD Dr. Michael Hoppert, Abteilung f. Allgemeine Mikrobiologie, Institut f. Mikrobiologie u. Genetik

PD Dr. Stefan Irniger, Abteilung f. molekulare Mikrobiologie und Genetik, Institut f. Mikrobiologie u. Genetik

Tag der mündlichen Prüfung: 17.10.2012

Affirmation

I hereby declare, that this thesis was written independently and with no other sources and aids than quoted.

Göttingen, 14.09.2012

Oliver Voigt

Parts of this thesis are essentially accepted for publication or are in manuscript preparation.

Manuscript:

Voigt, O. and Pöggeler, S. Autophagy genes *Smatg8* and *Smatg4* are required for fruiting-body development, vegetative growth and ascospore germination in the filamentous ascomycete *Sordaria macrospora*. *Autophagy (essentially accepted)*.

Manuscripts in preparation:

Voigt, O. and Pöggeler, S. Autophagic kinases SmVPS34 and SmVPS15 are required for viability in the filamentous ascomycete *Sordaria macrospora*. *Manuscript in preparation*.

Voigt, O. and Pöggeler, S. The bZIP transcription factor SmJLB1 regulates the autophagy related genes *Smatg8* and *Smatg4* and is required for perithecia development and vegetative growth in *Sordaria macrospora*. *Manuscript in preparation*.

Further publications in the context of this dissertation:

BLOEMENDAL, S., Y. BERNHARDS, K. BARTHO, A. DETTMANN, **O. VOIGT** *et al.*, 2012 A homologue of the human STRIPAK complex controls sexual development in fungi. Mol Microbiol **84:** 310-323.

Acknowledgements

First of all, my gratitude goes to my doctoral mother Prof. Dr. Stefanie Pöggeler for giving me the opportunity to promote in her department and for the interesting and fruit bearing topic of this thesis. Furthermore, I want to thank her for her excellent supervision and the fact that she taught me a lot (theoretical and practical) and for sharing excitement and frustration concerned with this thesis.

I also want to thank Prof. Dr. Gerhard Braus for being a member of my thesis committee and sharing a sincere interest towards this topic. Additionally, I would like to thank him for giving me advices for better presentations. Also, I want to thank Prof. Dr. Gerhard Braus and Dr. Oliver Valerius for providing the usage of mass spectrometry.

Additionally, I would like to thank Prof. Dr. Michael Thumm and Peter Rube for providing strains, plasmids, antibodies and advice with the Ape1 maturation assay.

Very special thanks go to our charming technical assistant Gertrud Stahlhut for practical advice and her help with the experiments especially in the terminal phase of this thesis. I am sorry your back hurt from all the single spore isolates and thanks for your help with the qRT-PCR-experiments. Once again, thank you.

My gratitude goes to Britta Herzog, Jennifer Gerke, Ronny Lehneck and Stefan Frey for reading the manuscript of this thesis thoroughly. I also want to thank Rebekka Harting and Martin Christmann for their advices regarding western experiments. I have to thank former department members Nicole Nolting, Yasmine “Yäzz” Bernhards, Skander Elleuche and Volker Klix for the nice atmosphere and for welcoming me into this group heartily. Of course I want to thank present department members Britta Herzog, Ronny Lehneck and Stefan Frey and the colleagues of the Braus department and the rest of this institute for the nice atmosphere, the laughs and frustration we shared and of course your helping hands.

I also wanted to thank Dr. Özgür Bayram for “sending me on the right track” by teaching me how to work properly in the laboratory and that he was still open for my questions even after my diploma thesis.

Last but not least I want to thank my parents, “den Dicken”, my hometown friends and especially my girlfriend Kathleen, and I want to say sorry for all the time I had no time ‘cause the lab was calling.

List of abbreviations and acronyms

aa	amino acids
a. dest.	*aqua destillata*
BLAST	Basic Local Alignment Search Tool
BMM	Biomalt Maize Medium
bp	base pairs
CM	Complete Medium
CMS	Complete Medium with Saccharose
d	days
DIC	Differential Interference Contrast
DNA	Deoxyribonucleic Acids
dpi	days past inoculation
EGFP	Enhanced Green Fluorescent Protein
kb	kilo base pairs
kDa	kilo Dalton
o/n	over night
ORF	Open Reading Frame
PCR	Polymerase Chain Reaction
PE	Phosphatidylethanolamine
RNA	Ribonucleic acid
RT	Room Temperature
qRT-PCR	quantitative real-time PCR
SD	Selective Dropout
ssi	single spore isolate
SWG	Sordaria Westergaards Medium
wt	wild type
Y2H	Yeast Two-Hybrid
YEPD	Yeast Extract, Peptone, Dextrose

Common used abbreviations and units of measurement are not enlisted.

Table of contents

Summary

Autophagy, a tightly controlled degradation process in which a eukaryotic cell digests its own proteins and organelles during starvation or stress, has been shown to be involved in various developmental processes. The molecular dissection of autophagy has been mostly performed in the unicellular budding yeast *Saccharomyces cerevisiae*. However, its involvement in developmental processes of multicellular filamentous ascomycetes is largely unknown. Fungal fruiting-body development is a complex cellular differentiation process from a two dimensional mycelium to a three dimensional perithecium that requires specific environmental conditions and is controlled by many developmentally regulated genes. In this study the fungal model organism *S. macrospora* serves as host to investigate the impact of autophagy on the fruiting-body development. *Sordaria macrospora* is a coprophytic filamentous acscomycete which propagates solely sexually being ideal for the addressed question of this thesis. A set of autophagy related genes was chosen to be investigated. Homologous to members of the ascomycete family, the autophagic genes *Smvps34*, *Smvps15*, *Smatg8, Smatg4* and *Smjlb1* were isolated. Deletion of these genes was the first step to elucidate their function in autophagy and thus fruiting-body development. Deletion of the phospholipid kinase *Smvps34* and the protein kinase *Smvps15* resulted in lethality of the transformants as verified by a germination assay. Deletion of genes encoding for a structural component of the autophagosome, *Smatg8,* and *Smatg4,* a cysteine protease processing SmATG8 also impaired fruiting-body development and vegetative growth. Localization of SmATG8 to the autophagosomes and SmATG4 to the cytoplasm is consistent to reports in other ascomycetes. Processing of SmATG8 by SmATG4 was confirmed also by fluorescence microscopy and immuno blotting. In an *S. cerevisiae* Ape1 maturation assay SmATG8 and SmATG4 were capable to rescue the respective yeast deletion strains and indicated a high conservation of these genes among Ascomycota. Abolition of fruiting-body development was caused by the deletion of the bZIP transcription factor *Smjlb1* as well as impairment of vegetative growth. SmJLB1 is localized to the nucleus and expression regulation of at least *Smatg8* and *Smatg4* was affirmed by qRT-PCR experiments indicating the involvement of SmJLB1 in autophagy. The data of this work suggest that autophagy and fruiting-body development in the filamentous ascomycete *S. macrospora* are tightly connected.

Zusammenfassung

Autophagie ist ein Degradationsprozess der streng reguliert ist und in welchem eine eukaryotische Zelle zelleigene Organellen und Proteine bei Nährstoffmangel abbaut. Außerdem konnte gezeigt werden, dass dieser Prozess auch in verschiedene Entwicklungsprozesse involviert ist. Die molekulare Entschlüsselung der Autophagie wurde hauptsächlich in der Bäckerhefe *S. cerevisiae* vorgenommen. Allerdings ist Beteiligung der Autophagie an Entwicklungsprozessen in multizellulären filamentösen Ascomyceten weitestgehend unbekannt. Die Fruchtkörperentwicklung von Pilzen ist ein komplex gestalteter Differenzierungsprozess der von einem zwei-dimensionalem Pilzgeflecht ausgeht das sich zu einem drei-dimensionalem Perithezium entwickelt. Die Fruchtkörperentwicklung erfordert spezifische Umgebungsbedingungen und wird durch viele entwicklungsassoziierten Genen reguliert. In dieser Studie diente der Modellorganismus *Sordaria macrospora* zur Untersuchung des Einflusses der Autophagie auf die Fruchtkörperentwicklung. Der coprophytische filamentöse Ascomycet *S. macrospora* pflanzt sich lediglich sexuell fort, was ihn ideal für die Fragestellung dieser Arbeit macht. Für diese Arbeit wurden eine Reihe konservierter Autophagie bezogener Gene auserwählt. Folgende Gene die homolog zu denen anderer Ascomyceten sind wurden isoliert: *Smvps34*, *Smvps15*, *Smatg8*, *Smatg4*, und *Smjlb1*. Durch die Deletion dieser Gene sollte geklärt werden wie Autophagie in die Fruchtkörperentwicklung involviert ist. Die Deletion des Phospolipidkinase Gens *Smvps34* und des Proteinkinase Gens *Smvps15* führte zur Lethalität von *S. macrospora* was durch eine Auskeimungsuntersuchung belegt wurde. Die Deletion des Gens *Smatg8*, welches eine autophagosomale Strukturkomponente kodiert und des Gens *Smatg4*, das eine Cystein-Protease kodiert, die SmATG8 prozessiert, beeinträchtigte ebenfalls die Fruchtkörperentwicklung und das vegetative Wachstum. Durch Fluoreszenzmikroskopie konnte gezeigt werden, daß SmATG8 in Autophagosomen lokalisiert und SmATG4 vorwiegend im Zytoplasma lokalisiert ist. Die Prozessierung von SmATG8 durch SmATG4 wurde ebenfalls durch Fluoreszenzmikroskopie und Western-blot Analyse bestätigt. Die heterologe Expression von *Smatg8* und *Smatg4* in *S. cerevisiae* und der Ape1 Reifungsuntersuchung zeigte, das die cDNA von *Smatg8* und *Smatg4* den Deletionsphenotyp der jeweiligen Hefedeletionsmutanten aufheben konnte. Somit konnte die Konservierung dieser beiden Gene innerhalb der Ascomyceten gezeigt werden. Die Blockade der Fruchtköperentwicklung wurde durch die Deletion des bZIP Transkriptionsfaktor Gens *Smjlb1* verursacht genauso wie die Beeinträchtigung des vegetativen Wachstums. SmJLB1 ist im Kern lokalisiert und durch qRT-PCR Experimente wurde gezeigt, dass die Autophagiegene *Smatg8* und *Smatg4* durch *Smjlb1* reguliert werden. Dies läßt vermuten, dass *Smjlb1* in den Prozess der Autophagie involviert ist. Die Ergebnisse dieser Arbeit weisen darauf hin, dass Autophagie und Fruchtkörperentwicklung des filamentösen Pilzes *S. macrospora* streng miteinander verknüpft sind.

1. Introduction

1.1 Autophagy in eukaryotes. The acquirement and preservation of nutrients is the most important object, all life forms have to accomplish to guarantee their survival. Especially on a sub-cellular level, mechanisms to endure nutrient deprivation have been developed by evolution. Nutrient homeostasis can be achieved by recycling of aberrant and defective cell constituents. For instance in filamentous fungi, where cellular components such as nuclei of basal hyphae are recycled to maintain nutrient supply and thereby growth of hyphal-tip cells (SHOJI *et al.* 2010). All eukaryotic organisms possess two major degradation pathways for cell recycling and protein homeostasis: autophagy and the ubiquitin-proteasome system. Autophagy accomplishes the non-specific degradation of long-lived cytosolic proteins and cellular organelles. The 26S proteasome is responsible for specific breakdown of short-lived proteins (YORIMITSU and KLIONSKY 2005). Autophagy ("self-eating") is a process of intracellular recycling to overcome nutrient depletion which is consistent in all eukaryotes, from yeast to plants to man (REGGIORI and KLIONSKY 2002).

The mechanism of autophagy is divided into three basic types: microautophagy, macroautophagy and chaperone-mediated autophagy (CMA) (KLIONSKY 2005). CMA allows the degradation of cytosolic proteins with a pentapeptide-consensus motif that are recognized by a chaperone and delivered to the vacuole for direct uptake (KAUSHIK *et al.* 2011; MASSEY *et al.* 2004). Microautophagy is involved in immediate invagination of cytoplasm at the surface of the vacuole/lysosome. Macroautophagy describes the generation of a double membrane vesicle that is degraded after vacuolar fusion. The content of the autophagosome such as amino acids and fatty acids are released into the cytosol and are available for amino-acid synthesis and ATP production (LEVINE and YUAN 2005; SUZUKI *et al.* 2001; UTTENWEILER and MAYER 2008). For micro- and macroautophagy (hereafter autophagy) selective and non-selective pathways have been described. The selective degradation of surplus organelles such as peroxisomes, mitochondria, ribosomes, nuclei and endosomes are termed pexo-, mito-, ribo-, nucleo- and reticulophagy, while specific degradation of protein aggregates and bacteria are named aggre- and xenophagy. During non-selective autophagy a bulk of cytoplasm is degraded which is composed differently of defective proteins and

aberrant organelles (BEAU *et al.* 2008; DUPONT *et al.* 2010; FARRE *et al.* 2008; KANKI *et al.* 2009b; SHOJI *et al.* 2010; TASDEMIR *et al.* 2007; YAMAMOTO and SIMONSEN 2010).

1.2 Autophagy in ascomycetes. In yeast, but not in filamentous fungi, a specific form of autophagy has been described, the cytoplasm-to-vacuole targeting (Cvt) pathway, which transports the hydrolytic enzymes, aminopeptidase I (Ape1) and α-mannosidase (Ams1), to the vacuole (KLIONSKY 2005; KLIONSKY *et al.* 2003). Another pathway using the autophagic machinery is the vacuolar protein sorting (VPS), which delivers the soluble hydrolases carboxypeptidase Y (CPY), proteinase A (Pr A) and proteinase B (Pr B) to the vacuole (HERMAN and EMR 1990). The molecular dissection of autophagy has been mostly performed in the budding yeast *Saccharomyces cerevisiae* and has led to the identification of 33 autophagy-related, or *ATG* genes (CAO *et al.* 2008; KANKI *et al.* 2009a; KLIONSKY *et al.* 2003; OKAMOTO *et al.* 2009). The high degree of conservation of these genes simplified the identification of orthologues in other organisms including filamentous ascomycetes. It has been shown that 24 of these 33 autophagy-related genes are conserved in filamentous fungi (MEIJER *et al.* 2007). The inactivation of conserved *ATG* orthologues in *S. cerevisiae* and higher eukaryotes revealed potentially important functions of autophagy in development, stress-induced adaptation, cellular remodeling and aging (BURSCH 2004; LEVINE and KLIONSKY 2004; SHINTANI and KLIONSKY 2004; TAKEDA *et al.* 2010).

In filamentous ascomycetes, the process of autophagy has been thoroughly investigated in *Podospora anserina*, and the plant pathogens *Magnaporthe grisea*, *Fusarium graminearum, Colletotrichum orbiculare* and *Ustilago maydis* (POLLACK *et al.* 2009). It was demonstrated that autophagy was induced during heterokaryon incompatibility, aerial hyphae and fruiting-body formation as well as in appressorium formation (ASAKURA *et al.* 2009; KERSHAW and TALBOT 2009; LIU *et al.* 2010; NADAL and GOLD 2010; PINAN-LUCARRE *et al.* 2005; PINAN-LUCARRE and CLAVE 2008; PINAN-LUCARRE *et al.* 2003). In *Aspergillus oryzae* and *Aspergillus fumigatus*, autophagy is necessary for conidiation and conidial germination, while autophagy deficiency promotes penicillin production in *Penicillium chrysogenum* (BARTOSZEWSKA *et al.* 2011; KIKUMA and KITAMOTO 2011; KIKUMA *et al.* 2006; RICHIE *et al.* 2007). So far, it is not exactly known how autophagy participates in fungal differentiation processes, but autophagy might be involved in the reconstitution of intracellular components

during development of different cell types. Hyphae that are not in contact with the medium may acquire nutrients through recycling of intracellular components by autophagy (SHOJI and CRAVEN 2011; SHOJI *et al.* 2010).

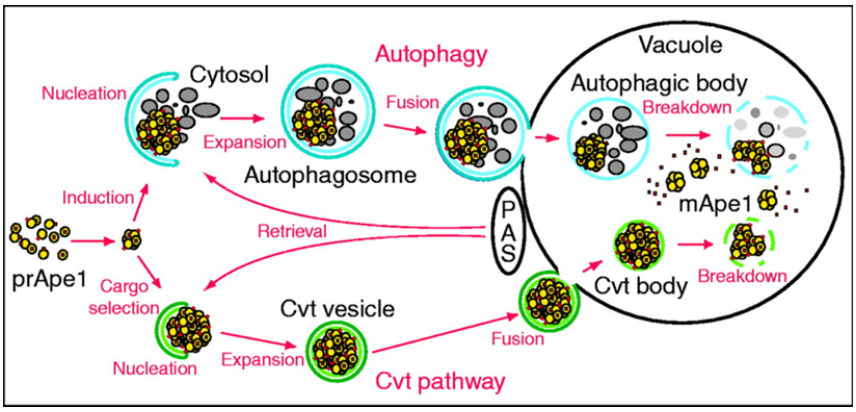

Figure 1. Scheme of autophagy and the Cvt pathway in yeast. Induction of autophagy starts with sensing of starvation signals. During nucleation autophagic proteins are recruited to the PAS and a portion of cytoplasm is sequestered into this double membrane vesicle upon expansion. Subsequent to fusion the inner autophagosome membrane and its contents (autophagic body) are released into the vacuole for breakdown mediated by vacuolar hydrolases. The Cvt pathway is induced by non-starvation conditions, and delivers α-mannosidase and the aminopeptidase 1 precursor to the vacuole using the autophagic machinery. prApe1, aminopeptidase 1 precursor, mApe1, maturated aminopeptidase1, Cvt, cytoplasm to vacuole targeting; Altered according to KLIONSKY (2005).

1.3 The molecular mechanism of autophagy. In the model organism *S. cerevisiae* the autophagosome formation of autophagy is divided into the phases: induction, nucleation, expansion, fusion and breakdown (Fig. 1 and 2). The induction begins with the sensing of nutrient starvation by the Tor kinase. Upon starvation the Tor kinase is inactivated and is no longer able to phosphorylate Atg13. Therefore Atg13 is not hyper phosphorylated and has a higher affinity towards Atg1 leading to complex formation with Atg1, Atg13, Atg17, Atg31 and Atg29 which initiates autophagy (Fig. 2A) (CHEN and KLIONSKY 2011).

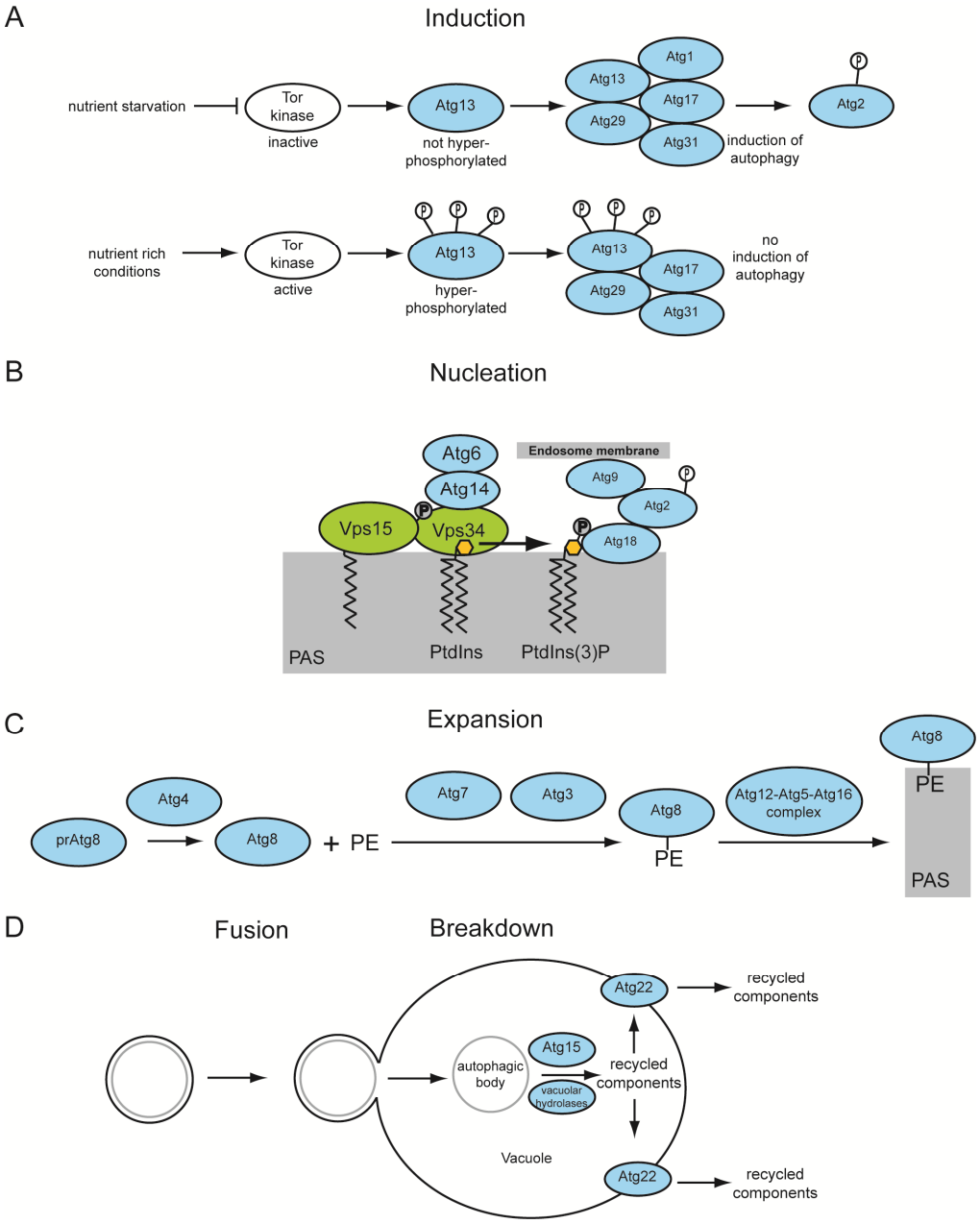

Figure 2. Schematic illustration of the molecular mechanism of autophagy. (A) Induction of autophagy by sensing of nutrient limitation. (B) Nucleation mediated by phosphorylation of phosphatidylinositol at the PAS catalyzed by complex I. (C) Expansion of the phagophore by conjugation of Atg8-PE to PAS via Atg8 and Atg12 conjugation pathways. (D) Fusion of the autophagosome with the vacuole and breakdown of the autophagic body within the vacuole by hydrolases. PAS, phagophore assembly site; PE, phosphatidylethanolamine; PtdIns, phosphatidylinositol; PtdIns(3)P, phosphatidylinositol-3-phosphate. Illustrated according to references stated in chapter 1.3.

The nucleation starts with the accumulation of autophagy related genes at the perivacuolar phagophore-assembly site (PAS) (ABELIOVICH *et al.* 2000; SUZUKI *et al.* 2001). This is regulated by complex I consisting of Vps34, Vps15, Atg14 and Atg6, which phosphorylates phosphatidylinositol at the PAS (for details see chapter 1.4). This induces recruitment of proteins necessary for autophagosome formation (Fig. 2B) (SUZUKI and OHSUMI 2007).

During phagophore expansion, the crescent-like structure sequesters cytoplasm, becoming a double membrane vesicle, the autophagosome (KLIONSKY *et al.* 2003). The Atg8 as well as Atg12 conjugation pathways function similar to the ubiquitin conjugation and are crucial for autophagosome formation. A major structural component of the autophagosome is an Atg8-PE (phosphatidylethanolamine) conjugate whereas Atg4, Atg7 and Atg3 are involved in Atg8-PE conjugation. The Atg12-Atg5-Atg16 protein complex locates the Atg8-PE conjugate at the PAS, involved in the Atg12-Atg5-Atg16 complex assembly are Atg7 and Atg10 (Fig. 2C, for details see chapter 1.5) (GENG and KLIONSKY 2008). It is assumed that the membrane structures for the autophagosome are recruited by Atg9 since localization experiments showed occurrence of Atg9 at the endosome at non-starvation and at the PAS under starvation conditions. Membrane associated Atg9 binds to Atg18 which is localized to the PAS by association to Atg2 and thereby Atg9 delivers membrane structures to the expanding PAS (Fig. 2B) (TANIDA 2011).

Throughout the fusion, the outer autophagosome membrane fuses with the vacuole releasing the inner membrane with the cytoplasmic content called autophagic body into the vacuole. Breakdown of the autophagic body is mediated by vacuolar hydrolases such as the lipase Atg15. The degradation products are released into cytoplasm via permeases for instance Atg22 (Fig. 2D) (BABA *et al.* 1995; EPPLE *et al.* 2001; SURIAPRANATA *et al.* 2000).

1.4 Vps34 and Vps15 mediate nucleation of autophagic proteins for autophagosome formation. The phosphatidylinositol 3-kinase (PI3K) Vps34 and the protein kinase Vps15 are involved in autophagy and vacuolar protein sorting. While Vps15 regulates the activity of Vps34 by phosphorylation, Vps34 catalyzes the phosphorylation of phosphatidylinositol (BUDOVSKAYA *et al.* 2002; YAN and BACKER 2007). Both proteins, Vps34 and Vps15, are present in two different complexes. Complex I consists of Vps15, Vps34, Atg14 and Atg6, and catalyzes the phosphorylation of phosphatidylinositol at the PAS triggering recruitment of proteins necessary for autophagosome expansion (Fig. 3A) (SUZUKI and OHSUMI 2007). Complex II is composed of Vps15, Vps34, Vps38 and Atg6 which phosphorylates phosphatidylinositol at the endosome facilitating vesicle formation needed for vacuolar protein sorting, which delivers the vacuolar hydrolases CPY, Pr A and Pr B to the vacuole (Fig. 3B) (HERMAN and EMR 1990; OBARA and OHSUMI 2011b).

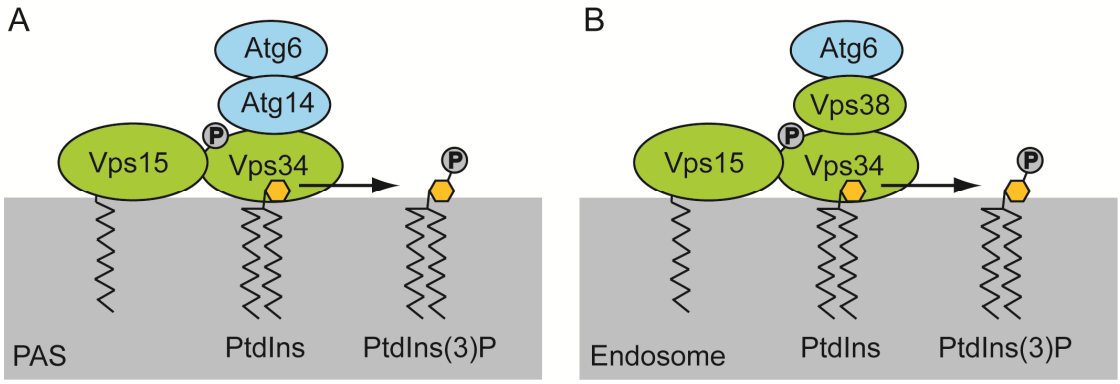

Figure 3. Differentiation between PtdIns 3-kinase complexes I and II. (A) Complex I consisting of Vps15, Vps34, Atg14 and Atg6 phosphorylates phosphatidylinositol at the PAS leading to recruitment of autophagic proteins required for autophagosome formation. In this complex Atg14 determines binding specificity to the PAS (OBARA and OHSUMI 2011a). (B) Proteins Vps15, Vps34, Vps38 and Atg6 form the complex II which generates PtdIns (3)P and the endosome mediating vesicle formation necessary for VPS. Endosome specificity for complex II depends on Vps38. PAS, phagophore assembly site; PtdIns, phosphatidylinositol; PtdIns(3)P, phosphatidylinositol-3-phosphate. Altered according to OBARA and OHSUMI (2011b).

Reports of yeast Atg14 reveal that the N-terminal region of Atg14 contains coiled-coil domains required for the establishment of complex I and the C-terminal end is assumed to play a crucial role in size determination of the autophagosomes. Additionally, the mammalian

Atg14 orthologue contains the Barkor/Atg14(L) autophagosome-targeting sequence (BATS) domain which binds to convex membranes with phosphatidylinositol-(3)-phosphate [PtdIns(3)P] indicating that specificity of complex I towards the PAS is mediated by Atg14 (OBARA and OHSUMI 2011a).

Furthermore, involvement of Vps34 and Vps15 in heterotrimeric G-protein signaling was reported. Regular G-protein signaling occurs at the plasma membrane where inactive Gα-GDP (guanosine diphosphate) is bound to the Gβ and Gγ subunits. An extracellular signal leads to the exchange of GDP by GTP (guanosine triphosphate). The active Gα-GTP is separated from the Gβγ subunit. Gα-GTP and Gβγ can activate effectors located at the plasma membrane and initiate thereby cell response (Fig. 4). In the Vps34/Vps15 *S. cerevisiae* pheromone signaling system, Gα-GDP is bound to Vps15 which again is bound to the inactive Vps34. After pheromone stimuli, an active PI3K complex consisting of Gα-GTP bound to Vps15, and to Vps34 is formed. The active PI3K complex phosphorylates phosphatidylinositol at the endosome (KOELLE 2006). This model of heterotrimeric G-protein signaling contradicts with previous reports of plasma membrane restricted G-protein signaling (Fig. 5) (SLESSAREVA *et al.* 2006).

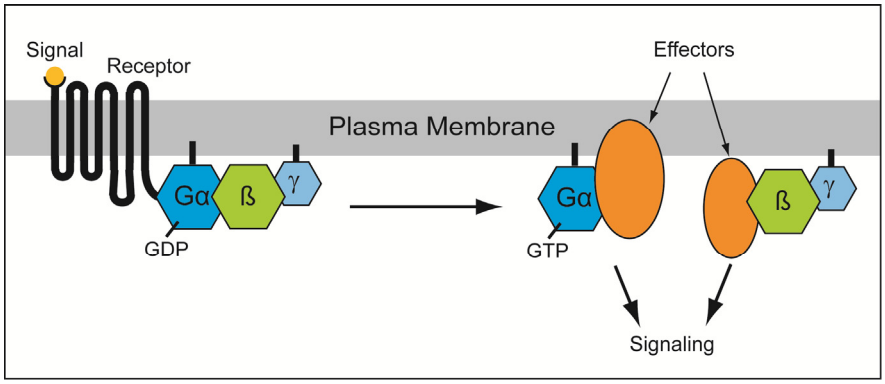

Figure 4. Heterotrimeric G-protein signaling. Inactive GDP-Gαβγ complex is bound to the plasma membrane. An extracellular signal triggers binding of Gα to GTP and separation from Gβγ. Gα-GTP and Gβγ mediate activation of plasma membrane bound effectors which signal a cellular response. GDP, guanosine diphosphate; GTP, guanosine triphosphate; Altered according to KOELLE (2006).

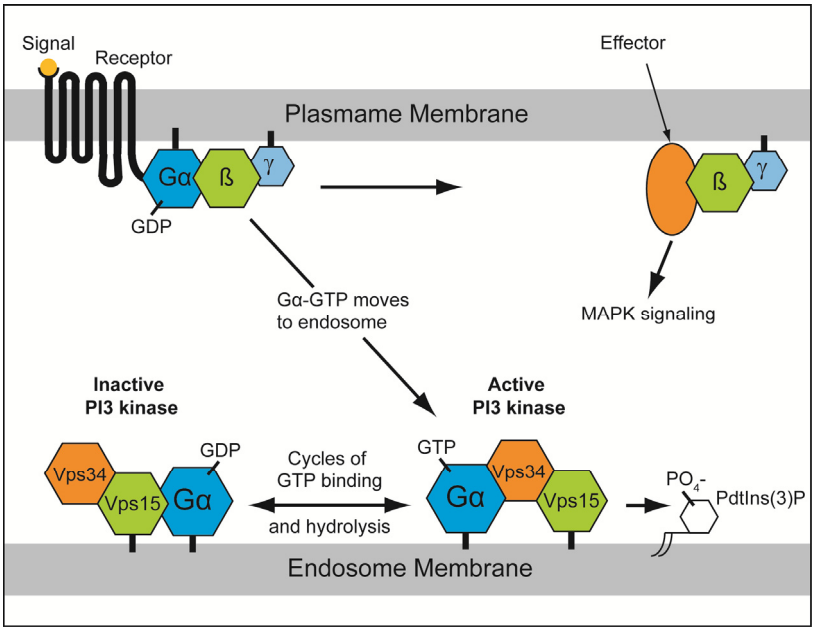

Figure 5. Vps34/Vps15 yeast pheromone signaling. The inactive PtdIns 3-kinase complex Vps34/Vps15/Gα-GDP is stimulated by pheromone signals. This leads to formation of the active PtdIns 3-kinase complex GTP-Gα/Vps34/Vps15 which phosphorylates phosphatidylinositol at the endosome membrane for VPS vesicle formation. GDP, guanosine diphosphate; GTP, guanosine triphosphate; PI3 kinase, phosphatidylinositol 3-kinase; PtdIns(3)P, phosphatidylinositol-3-phosphate; Altered according to KOELLE (2006).

Additionally, human hVps34 is assumed to mediate activation of the mTor kinase (mammalian target of rapamycin), required for nutrient sensing and S6K1 (p70 S6 kinase), required for insulin sensing (YAN and BACKER 2007). Overexpression of hVps34 and also hVps15 led to an activation of S6K1 but it has been shown that hVps34 is not stimulated by insulin but instead by amino-acid and glucose signals. hVps34 seems to regulate mTor and S6K1 activity by sensing amino-acid and glucose levels (BYFIELD *et al.* 2005; NOBUKUNI *et al.* 2005). Taken together, Vps34 and Vps15 are kinases involved in versatile pathways, not solely playing a crucial role for autophagy.

1.5 Atg8 and Atg4 as part of an ubiquitin-like conjugation system are involved in autophagosome formation. In *S. cerevisiae*, two ubiquitin-like-conjugation (ubl) systems are involved in autophagosome formation and expansion (ICHIMURA *et al.* 2000; MIZUSHIMA *et al.* 1998; OHSUMI 2001). The Atg12 and Atg8 conjugation occurs in a pattern similar to ubiquitin conjugation. Ubiquitin is activated by an E1 activating enzyme, transferred to an E2 conjugating enzyme, by the formation of a thioester bond and is afterwards conjugated to the substrate by an E3 ligating enzyme which recognizes the target substrate (Fig.6A) (GENG and KLIONSKY 2008; KERSCHER *et al.* 2006).

In the Atg12 conjugation system, the ubiquitin-like protein Atg12 is covalently attached to Atg5 by the action of the E1-like enzyme Atg7 and the E2-like enzyme Atg10 (Fig. 6B) (SHINTANI *et al.* 1999; TANIDA *et al.* 1999). In the second conjugation system, the ubiquitin-like protein Atg8 is first C-terminally processed to a glycine-exposed form by the cysteine protease Atg4. In *S. cerevisiae* Atg4 cleaves off a C-terminal amino acid, an arginine, and thereby exposes a glycine residue, which is crucial for interaction with Atg7, Atg3 and phosphatidylethanolamine (PE). After Atg8 is processed by Atg4, it is activated by Atg7 (E1-like enzyme) and conjugated to Atg3 (E2-like enzyme) via a thioester bond. Atg8 is subsequently bound covalently to PE with an amide bond. This is achieved by a protein complex consisting of Atg12, Atg5 and Atg16 which is assumed to act as an E3-like enzyme. The ATG12-Atg5-Atg16 complex is responsible for lipidation of Atg8 and precise localization of the Atg8-PE conjugate to the PAS (Fig. 6C) (FUJITA *et al.* 2008; GENG and KLIONSKY 2008; HANADA *et al.* 2007; ICHIMURA *et al.* 2000; SATOO *et al.* 2009).

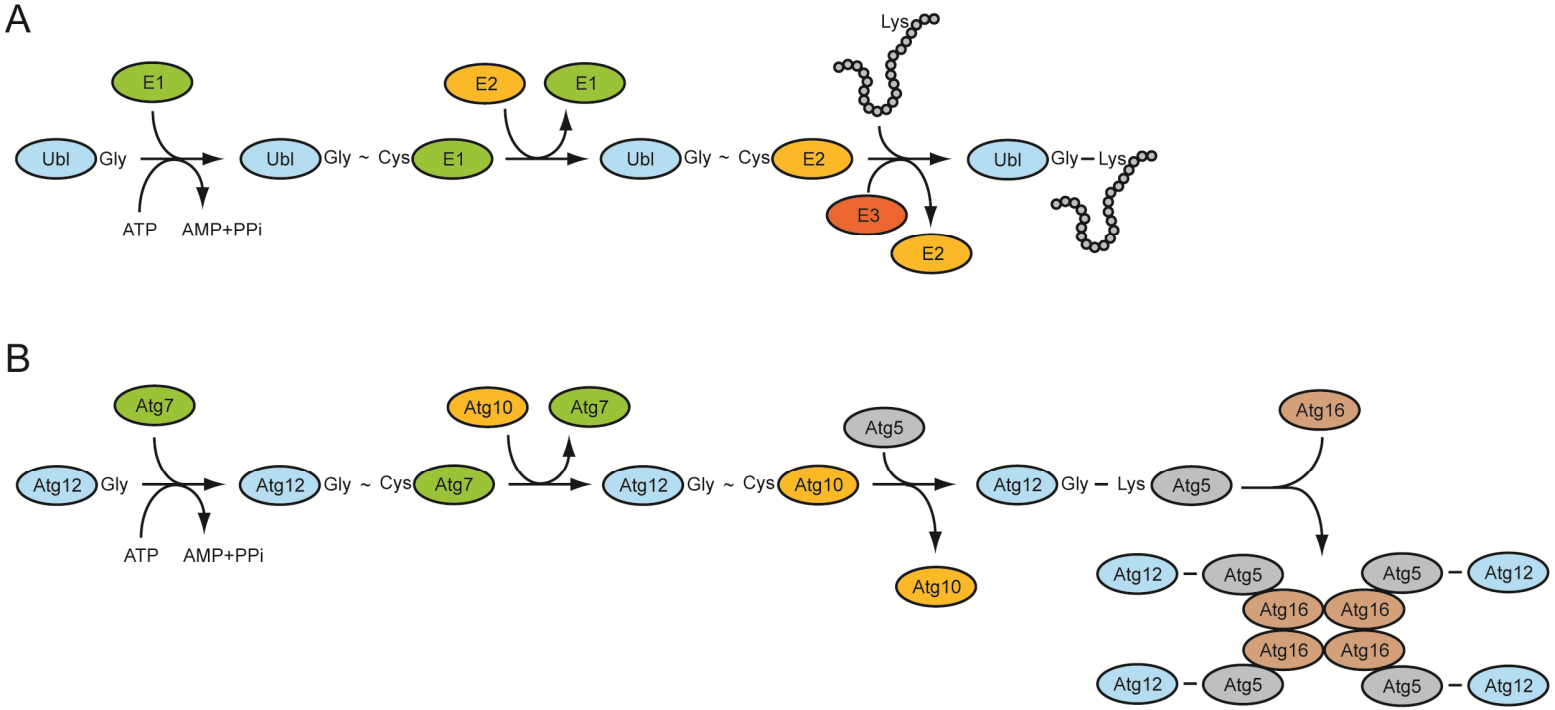
A
E1
Ubl
Gly
ATP
AMP+PPi
Ubl
Gly ~ Cys
E1
E2
E1
Ubl
Gly ~ Cys
E2
Lys
E3
E2
Ubl
Gly – Lys
B
Atg7
Atg12
Gly
ATP
AMP+PPi
Atg12
Gly ~ Cys
Atg7
Atg10
Atg7
Atg12
Gly ~ Cys
Atg10
Atg5
Atg10
Atg12
Gly – Lys
Atg5
Atg16
Atg12 – Atg5
Atg16
Atg16
Atg16
Atg16
Atg12 – Atg5
Atg5 – Atg12
Atg5 – Atg12

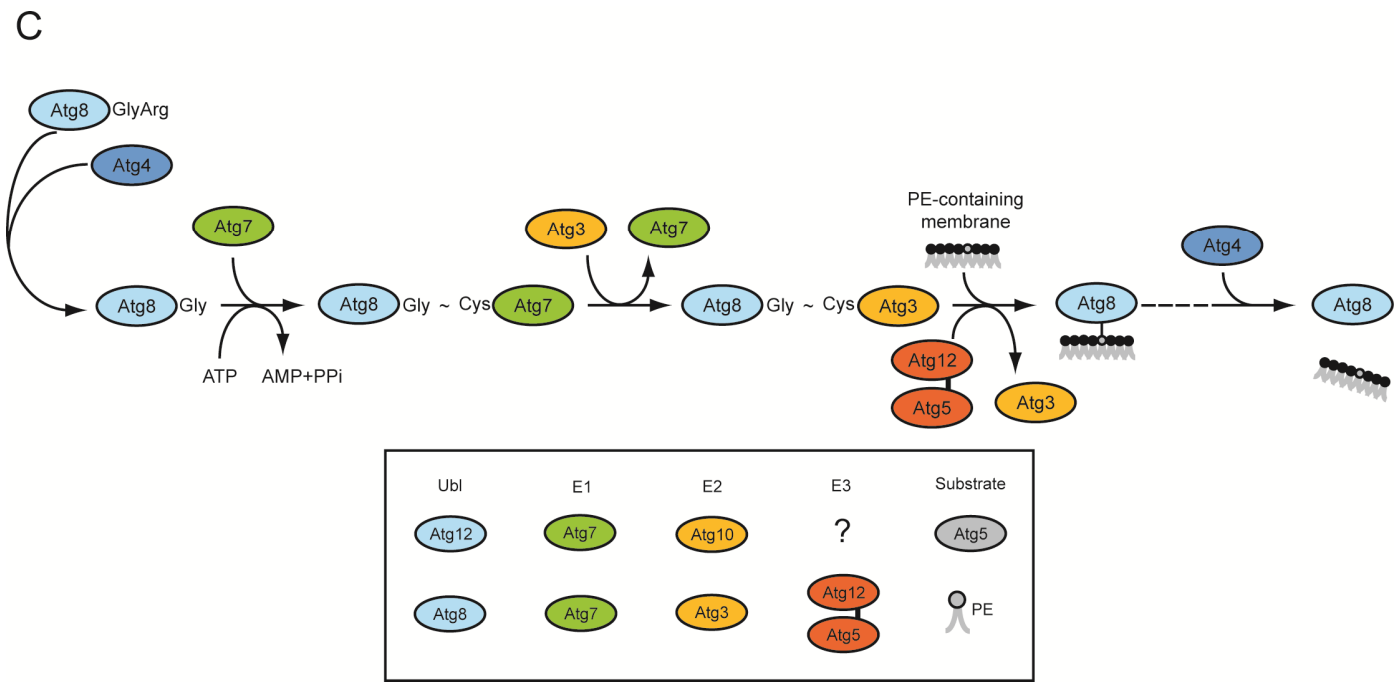

Figure 6. Ubiquitin and autophagy related conjugation systems in yeast. (A) Under ATP consumption, ubiquitin is bound via a thioester bond of its glycine residue to the cysteine residue of the activating enzyme E1. Afterwards ubiquitin is bound to the conjugating enzyme E2 also by the formation of a thioester bond. The ligating enzyme E3 mediates binding of the ubiquitin glycine residue to a lysine of the targeted substrate. (B) In a similar manner, Atg12 is activated by Atg7, bound to Atg10, an E2-like enzyme and transferred to its target substrate Atg5. The E3-like enzyme of this conjugation system has yet to be identified. (C) After processing of Atg8 by the Atg4 protease, Atg7 acts also as an E1-like enzyme for Atg8. The conjugating enzyme for Atg8 is Atg3. The ligation of Atg8 to its target substrate PE is mediated by the protein complex consisting of Atg12-Atg5-Atg16 which acts as an E3-like enzyme. Recycling of Atg8 occurs by its deconjugation from the outer autophagosome membrane and is mediated by Atg4. PE, phosphatidylethanolamine; Altered according to GENG and KLIONSKY (2008).

The Atg8-PE conjugate is a structural component of the inner and outer autophagosome membrane (ICHIMURA *et al.* 2000; KIRISAKO *et al.* 2000; OHSUMI 2001). Atg8 is considered as an ubiquitin-like protein due to its crystal structure but shares no amino-acid sequence identity with ubiquitin (GENG and KLIONSKY 2008; SUGAWARA *et al.* 2004).

In addition to processing newly synthesized Atg8, Atg4 acts as a deconjugating enzyme and facilitates the recycling of Atg8 from the membrane to maintain a sufficient level of Atg8 (KIRISAKO *et al.* 2000; YU *et al.* 2012). The deconjugation of Atg8 by Atg4 is crucial for appropriate autophagy functioning, as reported for *Homo sapiens* (SATOO *et al.* 2007). Additionally, Atg4 recycles Atg8 which is lipidated incorrectly, meaning that Atg4 cleaves Atg8 when Atg8-PE is integrated into incorrect membranes (NAKATOGAWA *et al.* 2012). Hence, the interplay of Atg8 and Atg4 is indispensable for autophagy.

1.6 The role of the bZIP transcription factor IDI-4 in autophagy and programmed cell death. In filamentous fungi, a mechanism called heterokaryon incompatibility is induced when hyphae of two individuals of unlike genotype are fusing. While sexual mating detection is regulated by mating type loci, vegetative incompatibility is mediated by *het* loci (heterokaryon incompatibility) (COPPIN *et al.* 1997; SAUPE 2000). The *het* loci avoid presence of heteroallelism in a heterokaryon and cause cell death of heterokaryotic cells with different *het* alleles (SAUPE 2000). Although, there is an evolutionary advantage of heterokaryon formation and therefore acquirement of new genetic information, genotype maintenance seems to have benefits also. It is assumed that heterokaryon incompatibility is protective against horizontal transfer of mycoviruses and parasites as well as the exploitation by aggressive genotypes (GLASS and KANEKO 2003; SAUPE 2011).

Heterokaryon incompatibility initiates programmed cell death (PCD) and thus cell lysis of the affected hyphae carrying different *het* loci (DEMENTHON *et al.* 2004). The “induced during cell death by incompatibility” reaction is executed by type II PCD which is considered as non-apoptotic and is associated with autophagy (PINAN-LUCARRE *et al.* 2003).

In *P. anserina* a bZIP transcription factor, termed IDI-4 (induced during incompatibility), was described to initiate autophagy and cell death. Overexpression of IDI-4 leads to cell death and an elevated expression of the *idi-7* gene, an orthologue of the yeast *ATG8* gene (DEMENTHON *et al.* 2004). Since IDI-4 expression is induced by rapamycin and nitrogen

starvation, it is assumed to be regulated by the Tor kinase (DEMENTHON *et al.* 2003). On the other hand positive self-regulation of *idi-4* was confirmed as well (DEMENTHON *et al.* 2004).

Numerous of IDI-4 orthologues have been described in ascomycetes which are all very similar in sequence to the *S. cerevisiae* Gcn4 bZIP transcription factor. In *S. cerevisiae* the function of Gcn4 has been studied intensively and it has been shown that it is a main regulator of the amino-acid starvation response (ARNDT and FINK 1986). Similarities among orthologues from filamentous ascomycetes are mainly restricted to the bZIP domain and have been described for *Neusospora crassa* (CPC1), *A. nidulans* (CpcA), *A. fumigatus* (CpcA), *A. niger* (CpcA) and *M. grisiae* (MG00602 4) whereas JlbA of *A. nidulans* also has been described as bZIP transcription factor which seems to be more similar to IDI-4 than Gcn4 (HOFFMANN *et al.* 2001; SASSE *et al.* 2008; STRITTMATTER *et al.* 2001; TIAN *et al.* 2011; WANKE *et al.* 1997).

It was demonstrated that the basic region of the Gcn4 bZIP domain is capable of binding the specific Gcn4 protein recognition element (GCRE). By binding to this motif with the sequence 5'-(A)TGA(G/C)TCA(T)-3' the expression of Gcn4 regulated genes is upregulated (ARNDT and FINK 1986; HOLLENBECK and OAKLEY 2000). In addition, Gcn4 is able to bind several variants if this motif (TGATTCA, TGACTCT, TGACTGA, TGACTAT and ATGACTCT) (NATARAJAN *et al.* 2001). The promoter of the *A. nidulans jlbA* gene was also shown to contain a CPRE (CpcA protein recognition element) which is similar to the GCRE motif of Gcn4 (STRITTMATTER *et al.* 2001). For the promoter region of *cpcA*, a *GCN4* orthologue in *A. niger*, it was reported that it contains a CPRE motif as well, indicating that not only the regulated genes but the regulators are controlled by such motifs (WANKE *et al.* 1997).

In a work of DEMENTHON *et al.* (2005) it was shown that *idi-7* (*ATG8*) is positively regulated by IDI-4 and that it also contains a motif similar to the GCRE sequence in its upstream promoter region. *In vitro* experiments revealed that the bZIP domain of IDI-4 binds to the GCRE-like pseudo palindromic sequence ATGANTCAT of the *idi-7* promoter (DEMENTHON and SAUPE 2005). In addition, IDI-4 regulates its own expression positively but it was not reported that this regulation is mediated by a GCRE like motif present in the *idi-4* promoter (DEMENTHON *et al.* 2004).

Thus, IDI-4 is a bZIP transcription factor which regulates *idi-7* transcription via a GCRE-like motif and is therefore involved in autophagic processes.

1.7 *Sordaria macrospora*: a model organism for fruiting-body development. The haploid filamentous ascomycete *Sordaria macrospora* is an excellent fungal model organism to study multicellular fruiting-body development, since it solely grows vegetatively or sexually (KÜCK *et al.* 2009). Additionally, the genome of 40 Mb is completely sequenced, allowing simple identifications of orthologues known from other organisms (NOWROUSIAN *et al.* 2010). Furthermore, this organism can be used for conventional genetic analysis due to the large sized ascospores which can be effortlessly isolated under a stereo microscope.

S. macrospora is a coprophytic and homothallic (self-fertile) fungus that naturally lives on herbivore dung. It lacks an asexual cycle, but every strain is able to complete the sexual cycle without a mating partner. Thus, in contrast to heterothallic (self-sterile) ascomycetes, recessive mutations can be directly tested for defects in fruiting-body development.

The fruiting-body (perithecia) formation can be divided into three morphologically differing steps: ascogonia-, protoperithecia- and perithecia-genesis (LORD and READ 2011). Under laboratory conditions the *S. macrospora* lifecycle is completed within 7 days. After spore germination *S. macrospora* grows as a two-dimensional mycelium and under given conditions (e.g. temperature, light- or biotin sensing) hyphal tips start branching and adhere with each other signifying the entry into the sexual-developmental stages. At day 3 of the development, the sexual cycle starts with the formation of ascogonial coils which are completely enclosed by sterile hyphae to form a globular premature structure, a prefruiting body (protoperithecium). Consecutive cell differentiation allows the generation of an outer-pigmented peridial tissue and ascus initials on the interior. After a self-fertilization event, karyogamy and meiosis, the mature perithecia are formed containing asci with sexual ascospores (Fig. 7) (ENGH *et al.* 2010; LORD and READ 2011; NOLTING *et al.* 2009; READ 1983; READ and BECKETT 1985).

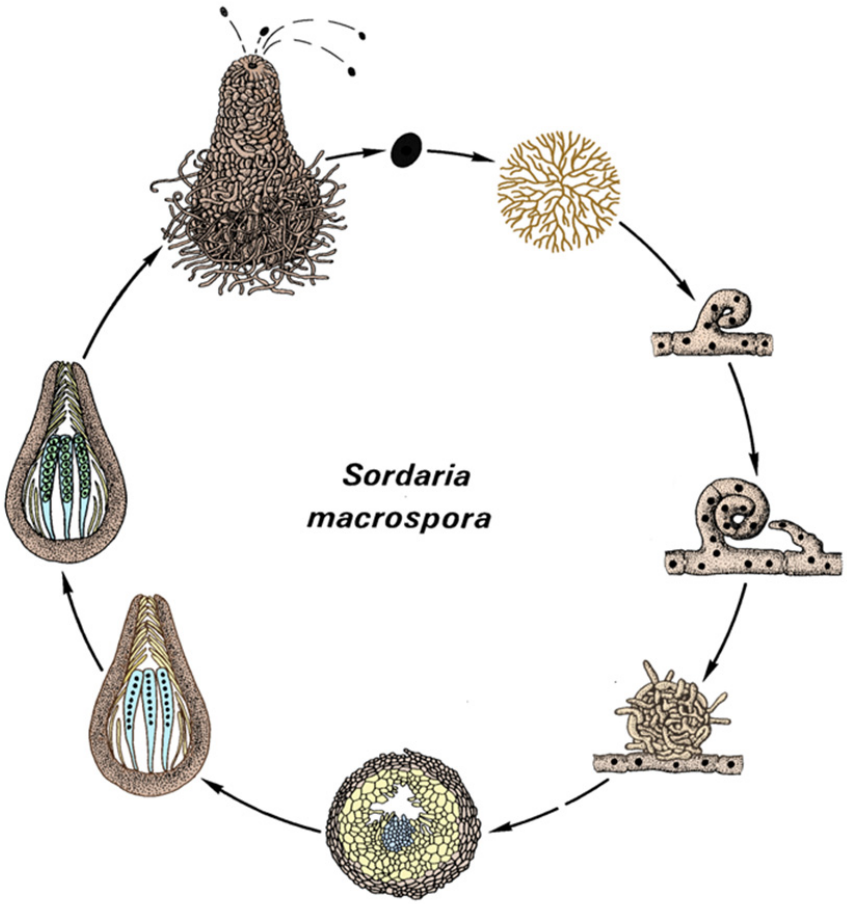

Figure 7. Lifecycle of the filamentous ascomycete *S. macrospora*. After germination of a single ascospore, a network of two dimensional mycelium is formed. 3 days after germination primary sexual structures the ascogonial coils are developed. These are successively surrounded by sterile hyphae to form protoperithecia at day 5 of the lifecycle. Providing ideal conditions, after 7 days mature perithecia are developed containing 130-150 asci each with 8 ascospores. Altered according to KÜCK (2005).

Perithecia have pear- or light-bulb like shape and contain about 130-150 asci, each harbouring 8 ascospores. In general the size of *Sordaria sp.* perithecia equals to 1.0 mm in height and 0.5 mm in width and the ascospores are released through an ostiole pore at the distal end of the perithecial neck (READ AND BECKER1983; READ 1985; ENGH *et al.* 2010; NOLTING *et al.* 2009; PÖGGELER and KÜCK 2004; PÖGGELER and KÜCK 2006).

1.8 Aim of this work. The elucidation of the impact of autophagy on the fruiting-body development in the ascomycete *S. macrospora* was the central aim of this work. For this purpose orthologues of the kinases Vps34 and Vps15, the transcription factor IDI-4, the structural component of the autophagosomes Atg8 and its processing/deconjugating protein Atg4 should be isolated. Alignment analyses are supposed to reveal their conservation among ascomycetes. Furthermore, their influence on sexual development should be investigated by gene replacement of *Smvps34*, *Smvps15*, *Smatg8*, *Smatg4* and *Smjlb1*. Subsequently the phenotypes of the generated deletion mutants were supposed to be analysed with respect to fruiting-body development, vegetative growth and germination efficiency. Localization experiments with fluorescently labelled versions of SmATG8, SmATG4 and SmJLB1 should be used to enlighten their sub-cellular localization.

By means of qRT-PCR of *Smjlb1*, *Smatg8* and *Smatg4* in wt and the Δ*Smjlb1* deletion mutant, transcriptional expression of these genes are supposed to be revealed as well as the involvement of *Smjlb1* in autophagy. Complementation of yeast *ATG8* and *ATG4* deletion strains with respective *S. macrospora* cDNA is supposed to confirm conservation of these genes between both ascomycetes using an Ape1 maturation assay. Via Y2H and GFP-Trap experiments, already described and non-described interaction partners of SmATG8 should be found. In a further Y2H screen, interaction partner of SmATG7 are supposed to be revealed as well. Processing of SmATG8 by SmATG4 is supposed to be confirmed by western blot and microscopical analysis using different SmATG8-EGFP fusion protein versions.

2. Materials and Methods

2.1 Strains

Table 1 enlists strains used in this study with their geno- and phenotypic characteristics and source. Enlistment of strains is ordered by context of organism.

Table 1. Strains used and generated in this study.

Strain	Characteristics	Source
Escherichia coli		
Mach 1	Δ*recA139; endA1; tonA; Φ80ΔlacM15;* Δ*lacX74; hsdR*(r_K -m_K+); wild type strain derivate; recipient strain for vector amplification	Invitrogen
Saccharomyces cerevisiae		
PJ69-4A	*MATa; trp1-901; leu2–3112; ura3–52; his3–200; ga14Δ; ga18OΔ; LYS2::GALl-HIS3; GAL2-ADE2; met2::GAL7-lacZ;*	James *et al.* (1996)
WCG4a	*MATα; his3-11,15; leu2-3,112; ura3-52;*	W. Heinemeyer, Stuttgart[a]
atg8Δ	*MATα; his3-11,15; leu2-3,112; ura3-52; atg8Δ::KAN;*	M. Thumm, Göttingen[b]
atg4Δ	*MATα; his3-11,15; leu2-3,112; ura3-52; atg4Δ::HIS5;*	M. Thumm, Göttingen[b]
Y187	*MATα; ura3-52; his3-200; ade2-101; trp1-901; leu2-3,112; gal4Δ; metΔ; gal80Δ; MEL1; URA3::GAL1$_{UAS}$-GAL1$_{TATA}$-lacZ*	Clontech

Strain	Characteristics	Source
AH109	*MATa; trp1-901; leu2-3,112; ura3-52; his3-200; ade2-101; gal4Δ; gal80Δ; LYS2::GAL1$_{UAS}$-GAL1$_{TATA}$-HIS3; GAL2$_{UAS}$GAL2$_{TATA}$-ADE2; URA3::MEL1$_{UAS}$- MEL1 $_{TATA}$ -lacZ; MEL1*	Clontech
WCG4a + pRS426-met25	*MATα; his3-11;15 leu2-3,112; ura3-52* + pRS426-met25	This study
atg8Δ + pRS426-met25	*MATα; his3-11,15; leu2-3,112; ura3-52; atg8Δ::KAN* + pRS426-met25	This study
atg8Δ + pRS315-EGFP-Atg8	*MATα; his3-11,15; leu2-3,112; ura3-52; atg8Δ::KAN; EGFP-ATG8* under control of an endogenous promoter	This study
atg8Δ + pRS-met-Smatg8	*MATα; his3-11,15; leu2-3,112; ura3-52; atg8Δ::KAN; Smatg8* under control of a *MET25* promoter	This study
*atg4*Δ + pRS426-met25	*MATα; his3-11,15; leu2-3,112; ura3-52; atg4Δ::HIS5* + pRS426-met25	This study
*atg4*Δ + pRS316-Atg4	*MATα; his3-11,15; leu2-3,112; ura3-52; atg4Δ::HIS5*; *atg4* under control of an endogenous promoter	This study
*atg4*Δ + pRS-met-Smatg4	*MATα; his3-11,15; leu2-3,112; ura3-52; atg4Δ::HIS5*; *Smatg4* under control of a *MET25* promoter	This study
Y187 + pBD-Smatg8	*MATα; ura3-52; his3-200; ade2-101; trp1-901; leu2-3,112; gal4*Δ*; met*Δ*; gal80*Δ*; MEL1; URA3::GAL1$_{UAS}$-GAL1$_{TATA}$-lacZ; GAL4* binding domain *N*-terminally fused to *Smatg8* under control of an *alcohol-dehydrogenase* (*adh*) promoter	This study

Strain	Characteristics	Source
Y187 + pBD-Smatg4	*MATα; ura3-52; his3-200; ade2-101; trp1-901; leu2-3,112; gal4Δ; metΔ; gal80Δ; MEL1; URA3::GAL1$_{UAS}$-GAL1$_{TATA}$-lacZ*; *GAL4* binding domain *N*-terminally fused to *Smatg4* under control of an *adh* promoter	This study
Y187 + pGBKT7	*MATα; ura3-52; his3-200; ade2-101; trp1-901; leu2-3,112; gal4Δ; metΔ; gal80Δ; MEL1; URA3::GAL1$_{UAS}$-GAL1$_{TATA}$-lacZ*; + pGBKT7	This study
AH109 + pAD-Smatg8	*MATa; trp1-901; leu2-3,112; ura3-52; his3-200; ade2-101; gal4Δ; gal80Δ; LYS2::GAL1$_{UAS}$-GAL1$_{TATA}$-HIS3; GAL2$_{UAS}$GAL2$_{TATA}$-ADE2; URA3::MEL1$_{UAS}$- MEL1 $_{TATA}$ -lacZ; MEL1*; *GAL4* activation domain *N*-terminally fused to *Smatg8* under control of an *adh* promoter	This study
AH109 + pAD-Smatg4	*MATa; trp1-901; leu2-3,112; ura3-52; his3-200; ade2-101; gal4Δ; gal80Δ; LYS2::GAL1$_{UAS}$-GAL1$_{TATA}$-HIS3; GAL2$_{UAS}$GAL2$_{TATA}$-ADE2; URA3::MEL1$_{UAS}$- MEL1 $_{TATA}$ -lacZ; MEL1*; *GAL4* activation domain *N*-terminally fused to *Smatg4* under control of an *adh* promoter	This study
AH109 + pGADT7	*MATa; trp1-901; leu2-3,112; ura3-52; his3-200; ade2-101; gal4Δ; gal80Δ; LYS2::GAL1$_{UAS}$-GAL1$_{TATA}$-HIS3; GAL2$_{UAS}$GAL2$_{TATA}$-ADE2; URA3::MEL1$_{UAS}$- MEL1 $_{TATA}$ -lacZ; MEL1*; + pGADT7	This study

Strain	Characteristics	Source
AH109 + pAD-RanBPM	*MATa; trp1-901; leu2-3,112; ura3-52; his3-200; ade2-101; gal4Δ; gal80Δ; LYS2::GAL1$_{UAS}$-GAL1$_{TATA}$-HIS3; GAL2$_{UAS}$GAL2$_{TATA}$-ADE2; URA3::MEL1$_{UAS}$- MEL1 $_{TATA}$ -lacZ; MEL1*; *GAL4* activation domain *N*-terminally fused to *ranBPM* under control of an *adh* promoter	This study
Sordaria macrospora		
S48977	Wild type	U. Kück, Bochum,[c]
S66001	Δ*ku70::nat*^{R}	Pöggeler and Kück (2006)
S23442	mutation in *fus1-1* gene; brownish ascospores	U. Kück, Bochum,[c]
ΔSmvps34/Smvps34	primary heterokaryotic transformant; Δ*Smvps34::hyg*^{R}/ *Smvps34*/Δ*Smku70::nat*^{R}	This study
ΔSmvps15/Smvps15	primary heterokaryotic transformant; Δ*Smvps15::hyg*^{R}/ *Smvps15*/Δ*Smku70::nat*^{R}	This study
ΔSmjlb1	Δ*Smjlb1::hyg*^{R}; ssi	This study
ΔSmjlb1::Smjlb1^{ect}	Δ*Smjlb1::hyg*^{R}; *Smjlb1*^{ect}; *nat*^{R}; ssi	This study
ΔSmjlb1::Smjlb1-egfp^{ect}	Δ*Smjlb1::hyg*^{R}; *Smjlb1-egfp*^{ect}; *nat*^{R};	This study
ΔSmatg8	Δ*Smatg8::hyg*^{R}; ssi	This study
ΔSmatg8::Smatg8^{ect}	Δ*Smatg8::hyg*^{R}; *Smatg8*^{ect}; *nat*^{R}; ssi	This study
ΔSmatg8::egfp-Smatg8^{ect}	Δ*Smatg8::hyg*^{R}; *egfp-Smatg8*^{ect}; *nat*^{R}; ssi	This study
ΔSmatg8::egfp-Smatg8-DsRed-SKL^{ect}	Δ*Smatg8::hyg*^{R}; *egfp-Smatg8-DsRed-SKL*^{ect}; *nat*^{R}	This study
ΔSmatg8::DsRed-SKL^{ect}	Δ*Smatg8::hyg*^{R}; *DsRed-SKL*^{ect}; *nat*^{R}	This study
ΔSmatg4	Δ*Smatg4::hyg*^{R}; ssi	This study
ΔSmatg4::Smatg4^{ect}	Δ*Smatg4::hyg*^{R}; *Smatg4*^{ect}; *nat*^{R}; ssi	This study
ΔSmatg4::egfp-Smatg8^{ect}	Δ*Smatg4::hyg*^{R}; *egfp-Smatg8*^{ect}; *nat*^{R}	This study
ΔSmatg4::Smatg8-egfp^{ect}	Δ*Smatg4::hyg*^{R}; *Smatg8-egfp*^{ect}; *nat*^{R}	This study
ΔSmatg4::egfp-Smatg8^{G116ect}	Δ*Smatg4::hyg*^{R}; *egfp-Smatg8*^{G116ect}; *nat*^{R}	This study

Strain	Characteristics	Source
ΔSmatg4::Smatg4-egfp^{ect}	Δ*Smatg4::hyg*^{R}; *Smatg4-egfp*^{ect}; *nat*^{R}	This study
ΔSmatg4::DsRed-SKL^{ect}	Δ*Smatg4::hyg*^{R}; *DsRed-SKL*^{ect}; *nat*^{R}	This study
wt::Smatg8-egfp^{ect}	*Smatg8-egfp*^{ect}; *nat*^{R}	This study
wt::egfp-Smatg8mut^{ect}	*egfp-Smatg8mut*^{ect}; *nat*^{R}	This study

hyg^{R}, hygromycin resistant; *nat*^{R}, nourseothricin resistant.

[a], Institute of Biochemistry, University of Stuttgart, Germany.

[b], Department of Biochemistry II, Georg-August-University Göttingen, Germany.

[c] Department of General and Molecular Botany, Ruhr-University Bochum, Germany.

2.2 Plasmids

Table 2 enlists plasmids utilized or constructed in this study along with their features, vector backbones and sources. Enlistment of plasmids is ordered by context of experiments.

Table 2. Plasmids used and generated in this study.

Plasmid	Features/Inserts	Source
vector backbones		
pRS426	*URA3*	Christianson *et al.* (1992)
pRSnat	*URA3*; *nat*-cassette	Klix *et al.* (2010)
pDS23-EGFP	*egfp* under control of *gpd* promoter and *trpC* terminator of *A. nidulans*; *URA3*; *nat*-cassette	Nowrousian unpublished
p1783	*egfp* under control of *gpd* promoter and *trpC* terminator of *A. nidulans*; *hph*-cassette	Pöggeler *et al.* (2003)
pRS426-met25	*met25* promoter; *URA3*; *amp*^{R}	Mumberg *et al.,* 1994
pGBKT7	*TRP1*; *GAL4-BD*; kan^{R}	Clonetech
pGADT7	*LEU2*; *GAL4-AD*; amp^{R}	Clonetech

Plasmid	Features/Inserts	Source
deletion experiments		
pRS-ΔSmvps34	946 bp of flanking and 53 bp of the ORF its 5'-region and 378 bp of ORF and 396 bp of 3'-flanking region of *Smvps34* disrupted by *hph*-cassette in pRS426	This work
pRS-ΔSmvps15	1069 bp of the 5'-ORF region and 1001 bp of 3'-ORF region of *Smvps15* interrupted by the *hph*-cassette in pRS426	This work
pRS-ΔSmjlb1	1107 bp of the 5'-flanking region and 1169 bp of 3'-flanking region of *Smjlb1* interrupted by the *hph*-cassette in pRS426	This work
pRS-ΔSmatg8	1023 bp of the 5'-flanking region and 1021 bp of 3'-flanking region of *Smatg8* interrupted by the *hph*-cassette in pRS426	This work
pRS-ΔSmatg4	1031 bp of 5'-flanking region and 468 bp of 3'-region plus 214 bp flanking region of *Smatg4* disrupted by the *hph*-cassette in pRS426	This work
complementation experiments		
pRS-Smjlb1-comp	*Smjlb1* plus 1107 bp of 5'-and 1169 bp of 3'-flanking region in pRSnat	This work
pRS-Smatg8-comp	*Smatg8* plus 1023 bp of 5'-and 1021 bp of 3'-flanking region in pRSnat	This work
pRS-Smatg4-comp	*Smatg4* plus 1031 bp of 5'-and 214 bp of 3'-flanking region in pRSnat	This work

Plasmid	Features/Inserts	Source
yeast complementation experiments		
pRSmet-Smatg8	*Smatg8* under control of *met25* promoter; *URA3*; *amp*^{R};	This work
pRSmet-Smatg4	*Smatg4* under control of *met25* promoter; *URA3*; *amp*^{R};	This work
pRS315-EGFP-Atg8	*LEU2*; amp^R; *EGFP-ATG8* under control of endogenous promoter	M. Thumm, Göttingen[a]
pRS316-Atg4	*URA3*; amp^R; *atg4* under control of endogenous promoter	M. Thumm, Göttingen[a]
protein interaction studies		
pBD-Smatg8	*TRP1*; *GAL4-BD*; kan^R; *Smatg8*	This work
pBD-Smatg4	*TRP1*; *GAL4-BD*; kan^R; *Smatg4*	This work
pAD-Smatg8	*LEU2*; *GAL4-AD*; amp^R; *Smatg8*	This work
pAD-Smatg4	*LEU2*; *GAL4-AD*; amp^R; *Smatg4*	This work
pAD-RAN-Bpm	*LEU2*; *GAL4-AD*; amp^R; *RanBPM*	Tucker *et al.* (2009)
localization studies		
pRS-Smjlb1-egfp	*Smjlb1* excluding stop codon in pDS23-EGFP	This work
pRS-Smatg4-egfp	*Smatg4* excluding stop codon in pDS23-EGFP	This work
pRS-egfp-Smatg8	1023 bp of the 5'-flanking region of *Smatg8*; *egfp* exluding stop codon; *Smatg8* without start codon and 1021 bp of 3'-flanking region of *Smatg8* in pRSnat	This work
pRS-Smatg8-egfp	*Smatg8* excluding stop codon in pDS23-EGFP	This work
pRS-egfp-Smatg8mut	*Smatg8* excluding stop codon in pDS23-EGFP; AA 115-118 substituted with alanine	This work

Plasmid	Features/Inserts	Source
pRS-egfp-Smatg8^{G116}	*Smatg8* C-terminally truncated (aa 1-116) in pDS23-EGFP	This work
pRS-egfp-Smatg8-DsRedSKL	1023 bp of the 5'-flanking region of *Smatg8*; egfp exluding stop codon; *Smatg8* without start codon and 1021 bp of 3'-flanking region of *Smatg8* and *DsRed-SKL* under control of *gpd* promoter and *trpC* terminator of *A. nidulans* in pRSnat	This work
pDsRed-SKL	*DsRed-SKL* under control of *gpd* promoter and *trpC* terminator of *A. nidulans* in pRHN1	

gpd promoter, glycerin aldehyde 3-phosphate dehydrogenase promoter; *trpC* terminator, anthranilate synthase terminator; *amp*^{R}, ampicillin resistance; *kan*^{R}, kanamycin resistance; *hph*, hygromycin B phosphotransferase.
[a], Department of Biochemistry II, Georg-August-University Göttingen, Germany.

2.3 Primers

Table 3 registers starter oligomers used for amplification, sequencing or qRT-PCR applied in this study. Oligomer sequences are stated in 5'-3' direction as well as their binding positions. Enlistment of oligomers is ordered by context of experiments.

Table 3. Primers used in this study.

Oligomer name	Specific sequence (5'-3')	Binding position
	sequencing	
ov-vps34-f2	CTACGTCCGGAAAGCCTGCAT	2809-2788 (ORF of *Smvps34*)
ov-vps34-r2	ATGCCCATCATGGAGCCCTTT	1-21 (ORF of *Smvps34*)

Oligomer name	Specific sequence (5'-3')	Binding position
vps15-f1	ATGGGTCAGGGTTTCTCTTTGACTGCC	1-27 (ORF of *Smvps15*)
vps15-r1	TCACCTGATGATAAGCACCA	4721-4702 (ORF of *Smvps15*)
jlb1-seq-f	ATGCACCTGTCTCTCGATCA	1-20 (ORF of *Smjlb1*)
jlb1-seq-r	CTACCTCCCCTGCCTAGCCA	669-650 (ORF of *Smjlb1*)
atg8-seq-f	ATGAGATCCAAGTTTAAGGAC	1-20 (ORF of *Smatg8*)
atg8-seq-r	TTACGCAGTCTCGAAATCGC	503-484 (ORF of *Smatg8*)
atg4-seq-f	ATGACGTCCTCGCGACCTGG	1-20 (ORF of *Smatg4*)
atg4-seq-r	TTATGCTCCTAGAGCGGTTT	1798-1770 (ORF of *Smatg4*)
	deletion/complementation experiments	
vps34-5f	GTAACGCCAGGGTTTTCCCAGTCACGACGCCTTCATGGCTATCTGACGTCCG	1920-1948 (pRS426 overhang); (-)877-(-)855 (5'-region of *Smvps34*)
vps34-5r	CAAAAAATGCTCCTTCAATATCAGTTAACGGATAGTCAAGCTGGTCGGA	(-)337-(-)366 (*hph* 3'-region overhang); 53-34 (ORF of *Smvps34*)
vps34-3f	GAGTAGATGCCGACCGGGAACCAGTTAACGGGTATATCCTCGGCCGCGA	1386-1414 (*hph* overhang); 2432-2451 (ORF of *Smvps34*)
vps34-3rA	GCGGATAACAATTTCACACAGGAAACAGCGCAGATCTTCAAGCGGTTGA	2197-2169 (pRS426 overhang); 3205-3186 (3'-region of *Smvps34*)
vps15-5f	GTAACGCCAGGGTTTTCCCAGTCACGACGATGGGTCAGGGTTTCTCACT	1920-1948 (pRS426 overhang); 1-20 (ORF of *Smvps15*)
vps15-5r	CAAAAAATGCTCCTTCAATATCAGTTAACATCTTGTCAAAGTCGTTCCA	(-)337-(-)366 (*hph* 3'-region overhang); 1069-1050 (ORF of *Smvps15*)
vps15-3f	GAGTAGATGCCGACCGGGAACCAGTTAACGAGAATCCGGTCCATCACGG	1386-1414 (hph overhang); 3783-3802 (ORF of *Smvps15*)
vps15-3r	GCGGATAACAATTTCACACAGGAAACAGCTCACCTGATGATAAGCACCA	2197-2169 (pRS426 overhang); 4721-4702 (ORF of *Smvps15*)
jlb1-5f2	GTAACGCCAGGGTTTTCCCAGTCACGACGTGTATGGCTGGTTCAAGTCA	1920-1948 (pRS426 overhang); (-)1108-(-)1089 (5'-region of *Smjlb1*)

Oligomer name	Specific sequence (5'-3')	Binding position
jlb1-5r	CAAAAAATGCTCCTTCAATATCAGTTAACGGATGG TTGTGGTGGTACCG	(-)337-(-)366 (*hph* 3'-region overhang); (-)20-(-)1 (5'-region of *Smjlb1*)
jlb1-3f	GAGTAGATGCCGACCGGGAACCAGTTAACAGAGAC GTACCTGTTGTGTT	1386-1414 (*hph* overhang); 670-689 (3'-region of *Smjlb1*)
jlb1-3r2	GCGGATAACAATTTCACACAGGAAACAGCGGTACG GACGACAAGACCAA	2197-2169 (pRS426 overhang); 1169-1150 (3'-region of *Smjlb1*)
atg8-5f	GTAACGCCAGGGTTTTCCCAGTCACGACGGACGAC TTCACAGTGACATC	1920-1948 (pRS426 overhang); (-)1015-(-)996 (5'-region of *Smatg8*)
atg8-5r	CAAAAAATGCTCCTTCAATATCAGTTAACGATCTCA TTTTGGCGGTTTG	(-)337-(-)366 (*hph* 3'-region overhang); 8-(-)12 (ORF and 5'-region of *Smatg8*)
atg8-3f	GAGTAGATGCCGACCGGGAACCAGTTAACGATTTC GAGACTGCGTAATC	1386-1414 (*hph* overhang); 505-486 (ORF and 3'-region of *Smatg8*)
atg8-3r	GCGGATAACAATTTCACACAGGAAACAGCGACGCA GCCCTTTGTTTCCC	2197-2169 (pRS426 overhang); 1506-1487 (3'-region of *Smatg8*)
atg4-5f	GTAACGCCAGGGTTTTCCCAGTCACGACGATATCG TTTGCCGCTTGGTC	1920-1948 (pRS426 overhang); (-)1031-(-)1012 (5'-region of *Smatg4*)
atg4-5r	CAAAAAATGCTCCTTCAATATCAGTTAACGAATCTC TTGAATGCCCAGA	(-)337-(-)366 (*hph* 3'-region overhang); (-)20-(-)2 (5'-region of *Smatg4*)
atg4-3f	GAGTAGATGCCGACCGGGAACCAGTTAACAGGTAT AGCCGGGTGAGTCC	1386-1414 (*hph* overhang); 1322-1341 (ORF of *Smatg4*)
atg4-3r	GCGGATAACAATTTCACACAGGAAACAGCAGAGTC CTTTGTTCTATCAT	2197-2169 (pRS426 overhang); 2003-1984 (3'-region of *Smatg4*)
hph-f	GTTAACTGATATTGAAGGAGCATTTTTTGG	1- 29 (ORF of *hph*)
hph-r	GTTAACTGGTTCCCGGTCGGCATCTACTC	1414-1386 (ORF of *hph*)
	deletion/complementation verification	
ov-vps34-f	GGTCAATGGTTACCAGCTC	1904-1886 (ORF of *Smvps34*)
ov-vps34-r	GTAAGCACCGAAGACTTGTCCG	1104-1125 (ORF of *Smvps34*)

Oligomer name	Specific sequence (5'-3')	Binding position
vps-34-5D2	TCGAGATCGCCATTTGCGTCG	(-) 946-(-)926 (5'-region of *Smvps34*)
vps-34-3D2	ATATGGTGGCATGAGCAGGC	3249-3231 (3'-region of *Smvps34*)
vps-15-5D1	GCTGAAGTGGGCCACCTGGG	(-)637-(-)618 (5'-region of *Smvps15*)
vps-15-3D1	CAGGGTTGGTCGCAGTCACG	5338-5319 (3'-region of *Smvps15*)
vps-15-5D2	CATCTTCCTTACCCTAGTCGC	1229-1249 (ORF of *Smvps15*)
vps-15-3D2	GCATAGCGCACGAACTTTGG	3521-3502 (ORF of *Smvps15*)
jlb1-5D1b	ACTTTTCGATGCGGCTACAGTGC	(-)2491-(-)1913 (5'-region of *Smjlb1*)
jlb1-3D1a	GTGTAGGTAGTCTCATGTTGTTTTG	2007-1314 (3'-region of *Smjlb1*)
jlb1-5D2a	AACACAACAATGAGCATGGACATGG	121-145 (ORF of *Smjlb1*)
jlb1-3D2a	CTCCCTCTTAATCTGATCCACCTCC	579-555 (ORF of *Smjlb1*)
atg8-5D1	CGAACGGAGAAGGCGGACAC	(-)1219-(-)1200 (5'-region of *Smatg8*)
atg8-3D1	CAGTTGCGATACATTACAAC	1674-1655 (3'-region of *Smatg8*)
atg8-ver-f	CAAGTTTAAGGACGAGCACCCCTTC	9-33 (ORF of *Smatg8*)
atg8-ver-r	GAAGGTGTTCTCGCCCGAGTATGTG	482-458 (ORF of *Smatg8*)
atg4-5D1	CTGCATGAAAGGTAAAGAGG	(-)1384-(-)1365 (5'-region of *Smatg4*)
atg4-3D1	CTCTGGCTGACAATATTTCC	2353-2334 (3'-region of *Smatg4*)
atg4-ver-f	ATGACGTCCTCGCGACCTGGTGGCAC	1-26 (ORF of *Smatg4*)
atg4-ver-r	ATCGACTGAGGTAACTGTAGAGTTG	1321-1297 (ORF of *Smatg4*)
tC1	CACCGCCTGGACGACTAAACC	(-)268-(-)288 (5'-region of *hph*)
tc1-o	CCTGGACGACTAAACCAAAA	(-)273-(-)292 (5'-region of *hph*)
h3	GTACTCGCCGATAGTGGAAACC	970-991 (ORF of *hph*)
h3-o	GATGGCTGTGTAGAAGTACT	955-974 (ORF of *hph*)
	yeast complementation experiments	
atg8-cf	*ACTAGT*ATGAGATCCAAGTTTAAGGA	generation of *Spe*I restriction site; 1-20 (ORF of *Smatg8* cDNA)

Oligomer name	Specific sequence (5'-3')	Binding position
atg8-cr	*GTCGAC*TTACGCAGTCTCGAAAT	generation of *Sal*I restriction site; 503-487 (ORF of *Smatg8* cDNA)
atg4-cf	*ACTAGT*ATGACGTCCTCGCGACCTGG	generation of *Spe*I restriction site; 1-20 (ORF of *Smatg4* cDNA)
atg4-cr	*GTCGAC*TTATGCTCCTAGAGCGGTTT	generation of *Sal*I restriction site; 1548-1529 (ORF of *Smatg4* cDNA)
	protein interaction studies	
atg8-Hf	*CATATG*AGATCCAAGTTTAAGGACGA	generation of *Nde*I restriction site; 4-23 (ORF of *Smatg8* cDNA)
atg8-Hr	*GAATTC*GCTTACGCAGTCTCGAAATCGC	generation of *Eco*RI restriction site; 366-347 (ORF of *Smatg8* cDNA)
atg4-Hf3	*GAATTCCCC*ATGACGTCCTCGCGACCTGG	generation of *Eco*RI restriction site; 1-20 (ORF of *Smatg4* cDNA)
atg4-Hr3	*CTCGAGG*GTTATGCTCCTAGAGCGGTTT	generation of *Xho*I restriction site; 1548-1529 (ORF of *Smatg4* cDNA)
atg4-Hr	*GTCGACGC*TTATGCTCCTAGAGCGGTTT	generation of *Sal*I restriction site; 1548-1529 (ORF of *Smatg4* cDNA)
	qRT-PCR-experiments	
jlb1-RT-f	TGCACCTGTCTCTCGATCAC	2-21 (ORF of *Smjlb1*)
jlb1-RT-r	TTACTGCTGCTTCCGGAGTT	194-175 (ORF of *Smjlb1*)
atg8-RT-f	GGCCAGTTCGTTTACGTCAT	241-260 (ORF of *Smatg8*)
atg8-RT-r	GTGTTCTCGCCCGAGTATGT	478-459 (ORF of *Smatg8*)
atg4-RT-f	GTCTTTGGCGTACGAAGAGC	489-508 (ORF of *Smatg4*)
atg4-RT-r	GTTTGCGAGAAGGCTTTGAC	738-719 (ORF of *Smatg4*)
ssu-f	ATCCAAGGAAGGCAGCAGGC	*N.crassa* gDNA SC8 93867-93886
ssu-r	TGGAGCTGGAATTACCGCG	*N.crassa* gDNA SC8 94028-94046

Oligomer name	Specific sequence (5'-3')	Binding position
	localization studies	
jlb1-gf	*AGATCT*ATGCACCTGTCTCTCGATCA	generation of *Bgl*II restriction site; 1-20 (ORF of *Smjlb1*)
jlb1-gr	*AAGCTT*CCTCCCCTGCCTAGCCATAG	generation of *Hin*dIII restriction site; 666-647 (ORF of *Smjlb1*)
atg8-egfp-5r	GTGAACAGCTCCTCGCCCTTGCTCACCATTTTGGCG GTTTGCTTTGATG	1-29 (*egfp* overhang); (-)20-(-)1 (5'-region of *Smatg8*)
atg8-egfp-3f	TCACTCTCGGCATGGACGAGCTGTACAAGAGATCC AAGTTTAAGGACGA	689-717 (*egfp* overhang); 4-23 (ORF of *Smatg8*)
atg8-egfp-3r	GCGGATAACAATTTCACACAGGAAACAGCGTGTAC TACCTATCATGTAT	2197-2169 (pRSnat overhang); 1004-985 (3'-region of *Smatg8*)
atg8-gf	*GCGAGATCT*ATGAGATCCAAGTTTAAGGAC	generation of *Bgl*II restriction site; 1-21 (ORF of *Smatg8*)
atg8-gr	*CGCAAGCTT*CGCAGTCTCGAAATCGCCGA	generation of *Hin*dIII restriction site; 500-481 (ORF of *Smatg8*)
atg8-gr2	*CGCAAGCTT*CGCAGTCTCGGCGGCGGCGGCGGTGTT CTCGCCCGAGTAT	generation of *Hin*dIII restriction site; 500-461 (ORF of *Smatg8*; substitutes aa's 115-118 to alanine)
atg4-gf	*GCGCCATGGCC*ACGTCCTCGCGACCTGGTGG	generation of *Bgl*II restriction site; 4-23 (ORF of *Smatg4*)
atg4-gr	*CGCCCATGGC*TGCTCCTAGAGCGGTTTCTC	generation of *Hin*dIII restriction site; 1786-1767 (ORF of *Smatg4*)
atg8pegfp-5r	GCCGAAGGTGTTCTCGCCCG	485-466 (ORF of *Smatg8*)
atg8pegfp-3f	TCACATACTCGGGCGAGAACACC TTCGGCTAATCCATATCCTCTCTA CC	457-485 (overhang to ORF of *Smatg8*) 501-520 (ORF and 3'-region of *Smatg8*)
atg8-5f3	GTAACGCCAGGGTTTTCCCAGTCACGACGTTTATGT TGTAATAGACGGG	1920-1948 (pRSnat overhang); (-)972-(-)953 (5'-region of *Smatg8*)
atg8-org-5r2	GTGTACTACCTATCATGTATTTCTA	1004-980 (3'-region of *Smatg8*)
atg8-org-3f	AGCTTAGAAATACATGATAGGTAGTACACGTACAG TGACCGGTGACTCT	976-1004 (overhang to 3'-region of *Smatg8*); 1-20 (*Pgpd*)

Oligomer name	Specific sequence (5'-3')	Binding position
MiPe-r2	GCGGATAACAATTTCACACAGGAAACAGCTCGAGT GGAGATGTGGAGTG	2197-2169 (pRSnat overhang); 766-746 (*TtrpC*)
egfp-f	ATGGTGAGCAAGGGCGAGGAGCTGTTCAC	1-29 (ORF of *egfp*)
egfp-r	CTTGTACAGCTCGTCCATGCCGAGAGTGA	717-689 (ORF of *egfp*)

ORF, open reading frame; *hph*, hygromycin B phosphotransferase;

[a], Department of Biochemistry II, Georg-August-University Göttingen, Germany.

[b], Underlined sequences represent 29 bp overhangs for homologous recombination in *S. cerevisiae* and letters in italics indicate generation of restriction sites.

2.4 Chemicals and Materials. 3-amino-1,2,4-triazole (Sigma-Aldrich, A8056-100G), acetic acid (Carl Roth GmbH and Co, 3738.2), acrylamide = Rotiphorese® Gel 30 (37,5:1) (Carl Roth GmbH and Co, 3029.1), adenine (Sigma-Aldrich, 01830-50G), agar-agar (Carl Roth GmbH and Co, 5210.2), agar-agar SERVA high gel-strength (SERVA, 11396.03), agarose (Biozym Scientific GmbH, 840004), albumin bovine (Sigma-Aldrich, A9647-50G), ammonium chloride (VWR International, BDH0208-500G), ammonium sulfate (AppliChem, A1032,1000), ampicillin (Sigma-Aldrich, A9518-25G), arginine (AppliChem, A3709,0250), bacto-yeast-extract (Oxoid LTD., LP0021), bio malt maize extract (Brau-Partner Kling, 115), biotin (Sigma-Aldrich, B4501-1G), boric acid (Carl Roth GmbH and Co, 6943.1), bromophenol blue (AppliChem, A3640,0005), calcium chloride dihydrate (Carl Roth GmbH and Co, 5239.1), chloroform (Merck Millipore, 1024451000), citric acid monohydrate (Carl Roth GmbH and Co, 3958.1), copper (II) sulfate 5-hydrate (Carl Roth GmbH and Co, P024.1), maize flour (Mühle Levers, N/A), CSM-Ade-His-Leu-Trp-Ura (MP Biomedicals, 4550-122), DAPI (4'-6-diamidino-2-phenylindole) (AppliChem, A1001,0010), desoxynucleotid triphosphate (dNTPs) (Thermo Scientific, R0191), Difco™ Skim Milk (BD Biosciences, 232100), Difco™ Yeast Nitrogen Base w/o amino acids and ammonium sulfate (BD Biosciences, 233520), dimethylformamide (Carl Roth GmbH and Co, T921.1), DMSO = dimethyl sulfoxide (Merck Millipore, 1029310500), DTT (1,4-Dithiothreitol) (AppliChem, A1101,0025), EDTA (ethylenediamine tetraaceticacid disodium salt dihydrate) (Carl Roth GmbH and Co, 8043.2), electro-poration cuvettes (VWR International, 732-1137), ethanole (VWR International, 20821.321), ethidium bromide (Sigma-Aldrich, 46065), Flat Optical 8-Cap Strip 0,2 ml (Biozym, 712100), formaldehyde (Carl Roth GmbH and Co, 4979.2),

formamide (Sigma-Aldrich, 47670), formic acid (Merck Millipore, 1002641000), galactose (AppliChem, A1131,0500), Gene Ruler DNA Ladder Mix (Thermo Scientific, SM0331 or SM0311), GeneScreen Hybridization Transfer Membrane (PerkinElmer Lifesciences, NEF988001PK), glass beads Ø 0.25-0.5 mm (Carl Roth GmbH and Co, A553.1), glass beads Ø 2.85-3.45 mm (Carl Roth GmbH and Co, A557.1), glucose (AppliChem, A3617,1000), glycerin (VWR International, 24388.295), HEPES (4-(2-hydroxyethyl)-1-piperazineethanesulfonicacid) (Carl Roth GmbH and Co, 9105.4), histidine (Merck Millipore, 1.04351.0025), hydrochloric acid (Carl Roth GmbH and Co, 4625.2), hydrogen peroxide 30% (H_2O_2) (Merck Millipore, 8.22287.2500), hygromycin B (Merck, 400051-10MU), IPTG (isopropyl-β-D-galactopyranoside) (Carl Roth GmbH and Co, 2316.3), iron(II) chloride (Carl Roth GmbH and Co, 231-753-5), iron(II) sulfate heptahydrate (Sigma-Aldrich, 31236), isopropanol (AppliChem, A0900,2500GL), kanamycin sulfate (Sigma-Aldrich, 60615), leucine (AppliChem, A1426,0100), lithium acetate (Carl Roth GmbH and Co, 5447.1), magnesium chloride hexahydrate (Merck Millipore, 1.05833.1000), magnesium sulfate heptahydrate (Carl Roth GmbH and Co, P027.2), manganese(II) chloride tetrahydrate (Carl Roth GmbH and Co, T881.1), manganese(II) sulfate monohydrate (Carl Roth GmbH and Co, 4487.1), methanol (VWR International, 20864.320), MOPS = 3-(N-morpholino)-propane sulfonic acid (AppliChem, A2947,0500), Nonident® P40 (AppliChem A2239,0025), nourseothricin (WernerBioAgents, 5004000), PEG 6000 (Sigma-Aldrich, 81255), phenol (AppliChem, A1153,0500), PMFS = phenylmethylsulfonyl fluoride (Sigma-Aldrich, P-7626), potassium acetate (Merck Millipore, 1.04820.1000), potassium chloride (AppliChem, A3582,1000), potassium dihydrogen phosphate (Merck Millipore, 1.04873.1000), potassium hydroxide (Carl Roth GmbH and Co, 6751.1), potassium nitrate (Merck Millipore, 1.05063.1000), PVDF western blotting membranes (Roche, 03010040001), RNA Loading Dye (2x) (Thermo Scientific, R0641), SDS = sodium dodecyl sulfate (Carl Roth GmbH and Co, 4360.2), sodium acetate (Carl Roth GmbH and Co, 6773.2), sodium chloride (AppliChem, A3597,1000), sodium dihydrogen phosphate monohydrate (Merck Millipore, 1.06346.1000), sodium hydroxide (VWR International, 28244.295), sodium molybdate-dihydrate (Sigma-Aldrich, 31439), sorbitol (Carl Roth GmbH and Co, 6213.1), ß-mercaptoethanol (Carl Roth GmbH and Co, 4227.1), sterile filter 0.45/0.2 µm (Sarstedt, 83.1826/83.1826.001), sucrose (AppliChem, A4734,1000), TEMED = N,N,N',N'-tetramethylethylenediamine (Carl Roth

GmbH and Co, 2367.3), Tris = tris-hydroxymethyl-aminomethane (Carl Roth GmbH and Co, AE15.2), Tris/HCl (Carl Roth GmbH and Co KG, 9090.3), Trizol (Invitrogen,15596026), tryptone/peptone (Carl Roth GmbH and Co, 8952,2), tryptophan (MP Biomedicals, 4061-012), Tween 20® (AppliChem, A4974,0100), uracil (MP Biomedicals, 4061-212), Whatman paper B002 580x600 mm (Schleicher & Schuell, 88-3852), X-ray films (Fujifilm, 4741019236), xylene cyanol (AppliChem, A4976,0005), zinc chloride (Sigma-Aldrich, 14424), zinc sulfate heptahydrate (Carl Roth GmbH and Co, K301.1).

2.5 Enzymes. Calf Intestine Alkaline Phosphatase = CIAP (Thermo Scientific, EF0341), DNase I (Thermo Scientific, EN0521), natuzym (Schliessmann, 5090), HotstarTaq Master Mix (Qiagen, 203443), lysozyme (SERVA, 28262.03), Moltaq (Molzym GmbH and Co, P-010-1000), Pfu polymerase (Promega GmbH, M7741), Phusion® Hot Start High-Fidelity DNA Polymerase (New England Biolabs, M0530S), restriction endonucleases (Thermo Scientific), RNase A (AppliChem, A2760,0100), T4 DNA ligase (Thermo Scientific, EL0011).

2.6 Kits. CloneJET PCR Cloning Kit (Thermo Scientific, K1231), High Prime DNA Labeling and Detection Starter Kit II (Roche Diagnostics GmbH, 1585614), HiSpeed Plasmid Midi Kit (Qiagen, 12643), LumiMax Superoxide Anion Detection Kit (Agilent Technologies, 204525), QIAGEN PCR Cloning Kit (Qiagen, 231124), QIAprep Spin Miniprep Kit (Qiagen, 27106), QIAquick Gel Extraction Kit (Qiagen, 28704), QIAquick PCR Purification Kit (Qiagen, 28104), qPCR Mastermix for SYBR GreenI (Eurogentec, RT-SN2X-03T), Transcriptor High Fidelity cDNA Synthesis Kit (Roche, 05091284001).

2.7 Media and Solutions

2.7.1 Culture media

E. coli

LB: 1% (w/v) tryptone/peptone, 0.5% yeast extract, 0.5% NaCl, pH 7.2; 1.5% (w/v) agar-agar for solid medium; addition of ampicillin (120 µg/ml) or kanamycin (60 µg/ml) for selection.

SOB: 2% (w/v) tryptone/peptone, 0.5% (w/v) yeast extract, 10 mM NaCl, 2.5 mM KCl, 10 mM $MgCl_2$, 10 mM $MgSO_4$, pH 7.5.

TB: 0.3% (w/v) HEPES, 0.22% (w/v) $CaCl_2$ monohydrate, 1.86% (w/v) KCl, 0.66% (w/v) $MnCl_2$ monohydrate, pH 6.7.

S. cerevisiae

YEPD: 2% (w/v) tryptone, 1% (w/v) yeast extract, 2% (w/v) glucose, pH 5.8; 1.5% (w/v) SERVA-agar for solid medium.

YEPDA: YEPD + 0.003% (w/v) adenine, pH 6.5.

SD: 0.17% (w/v) Difco™ Yeast Nitrogen Base w/o amino acids and ammonium sulfate, 2% (w/v) glucose, 0.064% (w/v) CSM-Ade-His-Leu-Trp-Ura (0.002% (w/v) L-methionine, 0.005% (w/v) L-arginine hydrochloride, L-isoleucine, L-lysine hydrochloride, L-phenylalanine, L-tryptophan, L-tyrosine each, 0.008% (w/v) L-aspartic acid, 0.01% (w/v) L-leucine and L-threonine, 0.014% (w/v) L-valine), pH 5.8; 1.5% (w/v) SERVA-agar for solid medium. Selection of transformants occurred by exclusion of respective amino acid(s).

S. macrospora

BMM: 0.8% bio malt maize extract and maize flour (25 g/l), pH 6.5; 1.5% (w/v) agar-agar for solid medium; addition of hygromycin B (110 U/ml) or nourseothricin dihydrogen sulfate (50 µg/ml) for selection.

BMM + Sodium acetate: BMM + 0.5% (w/v) sodium acetate (sporulation induction).

SWG: 1x Westergaard´s (0.1% (w/v) KNO_3, 0.1% (w/v) KH_2PO_4, 0.05% (w/v) $MgSO_4$ heptahydrate, 0.01% (w/v) NaCl, 0.01% (w/v) $CaCl_2$, 0.01% (v/v) trace element-stock solution [5% (w/v) citric acid ($C_6H_8O_7$ monohydrate) 5% (w/v) $ZnSO_4$ heptahydrate, 1% (w/v) $Fe(NH_4)_2(SO_4)_2$ hexahydrate, 0.25% (w/v) $CuSO_4$ pentahydrate, 0.05% (w/v) $MnSO_4$ monohydrate, 0.05% (w/v) H_3BO_3, 0.05% (w/v) Na_2MoO_4 dihydrate] 0.1% (v/v) chloroform),

2% (w/v) glucose, 0.1% (w/v) arginine, 0.1% (v/v) biotin-stock solution (0.01% in 50% ethanol), pH 6.5; 1.5% (w/v) agar-agar for solid medium; addition of hygromycin B (110 U/ml) or nourseothricin dihydrogen sulfate (50 µg/ml) for selection.

CMS: 1% (w/v) glucose, 0.2% (w/v) tryptone/peptone, 0.2% (w/v) yeast extract, 0.15% (w/v) KH_2PO_4, 0.05% (w/v) KCl, 0.05% (w/v) $MgSO_4$ heptahydrate, 0.37 % (w/v) NH_4Cl, 10.8% (w/v) sucrose, 0.01% (v/v) trace element-stock solution (10 mg/l $ZnSO_4$, 10 mg/l $Fe(II)Cl_2$, 10 mg/l $MnCl_2$), pH 6.5; 1.5% (w/v) agar-agar for solid medium.

MM + starch: 0.1% (w/v) soluble starch, 1.8 mM KH_2PO_4, 1.7 mM K_2HPO_4 trihydrate, 8.3 mM urea, 1 mM $MgSO_4$ heptahydrate, 0.01% (v/v) trace element-stock solution, 5 mM biotin, pH 6.6-6.8; 1.5% (w/v) SERVA-agar for solid medium.

2.7.2 Solutions

adenine-stock solution: 0.002% adenine in a. dest.
BDI solution: 50 mM glucose, 10 mM EDTA, 25 mM Tris/HCl, 0.2% lysozyme
BDII solution: 0.4 M NaOH + 2% (w/v) SDS (1:1)
BDIII: 3 M potassium acetate, 1.8 M formic acid
buffer I: 0.25 M HCl
buffer II: 0.5 M NaOH
buffer III: 1.5 M NaCl, 0.5 Tris, pH 7.4
dNTP-mix (10 mM): 10 mM dATP, dCTP, dGTP, dTTP each in a. dest.
EtBr-stock solution: 10 mg/ml ethidium bromide in a. dest.
histidine-stock solution: 0.002% histidine in a. dest.
leucine-stock solution: 0.003% leucine in a. dest.
lithium acetate (10x): 1 M lithium acetate, pH 7.5
loading dye (6x): 0.25% (w/v) xylene cyanol FF, 0.25% (w/v) bromophenol blue, 40% (w/v) saccharose
MOPS buffer (10x): 0.2 M MOPS, 50 mM sodium acetate, 10 mM EDTA, pH 7.0

protein-buffer solution: 100 mM Tris, 200 mM NaCl, 2 mM EDTA, 10% (v/v) glycerin, 0.3% (v/v) Nonident P40, 1 mM DTT, 1 mM PMSF

protoplast buffer (PPB): 13 mM Na_2HPO_4, 45 mM KH_2PO_4, 0.6 M KCl, pH 6.0

***S.macrospora* lysis buffer**: 10 mM Tris/HCl, 1 mM EDTA, 100 mM NaCl, 2% SDS, pH 8.0

Smash and Grab lysis buffer: 2% (v/v) Triton X-100, 1% (w/v) SDS, 100 mM NaCl, 10 mM Tris (pH 8.0), 1 mM EDTA

SDS-PAGE-running buffer: 1.5% (w/v) Tris, 9.4% (w/v) glycine, 20% (w/v) SDS, pH 8.3

TBE (10x): 1 M Tris/HCl, 1 M boric acid, 20 mM EDTA, pH 8.3

TBST: 150 mM NaCl, 10 mM Tris/HCl, 0.1% (v/v) Tween® 20 pH 7.5

TE(D): 10 mM Tris, 1 mM EDTA, pH 7.5

TPS: 1 M sorbitol, 80 mM $CaCl_2$, pH 7.4

trace element-stock solution: 5% (w/v) citric acid ($C_6H_8O_7$ monohydrate), 5% (w/v) $ZnSO_4$ heptahydrate, 1% (w/v) $Fe(NH_4)_2(SO_4)_2$ hexahydrate, 0.25% (w/v) $CuSO_4$ pentahydrate, 0.05% (w/v) $MnSO_4$ monohydrate, 0.05% (w/v) H_3BO_3, 0.05% (w/v) Na_2MoO_4 dihydrate

transferring buffer: 1.5% (w/v) glycerin, 10 mM Tris/HCl, 10% (v/v) methanol, pH 8.1-8.5

uracil-stock solution: 0.002% uracil in a. dest.

2.8 Strains and culture conditions. Cloning and amplification of recombinant plasmids was achieved in an *E. coli* Mach1 strain under standard culture conditions (SAMBROOK and RUSSELL 2001). All fungal strains used and generated during this work are enlisted in Tab. 1. All plasmids used in this study are listed in Tab. 2. Depending on the experimental setup *S. macrospora* was cultivated in Biomalt Maiz Medium (BMM), complete medium containing 10.8% saccharose (CMS) and fruiting-body development inducing SWG medium (ELLEUCHE and PÖGGELER 2008; NOWROUSIAN *et al.* 1999). *S. cerevisiae* was inoculated in YEPD or SD minimal medium supplemented with appropriate amino acids and grown at 30°C (AMBERG *et al.* 2005). *S. macrospora* was grown in petri dishes at 27°C in liquid medium for genomic DNA and protein extraction (NOWROUSIAN and CEBULA 2005). For RNA isolation *S. macrospora* was grown either vegetatively or sexually in liquid cultures. Growth in petri dishes induced sexual development and grown in flasks shaken at 130 rpm vegetative growth was induced. Basic, not described, molecular-biological/micro-biological methods have been conducted according to SAMBROOK and RUSSELL (2001).

2.9 Transformation procedures

2.9.1 Preparation and transformation of competent *E. coli* and *S. cerevisiae* cells. Production of chemo-competent *E. coli* cells was conducted as follows: 2-5 colonies of *Mach1* cells were grown o/n in SOB at 20-30 rpm and 20°C to an OD_{600} of 0.6. After 10 minutes incubation on ice, cells were centrifuged for 10 minutes at 2,500 g at 4°C. The supernatant was discarded and the pellet was resuspended in TB, kept on ice for 10 minutes and centrifuged for 10 minutes at 2,500 g and 4°C. Discarding of the supernatant was followed by addition of TB and DMSO. After 10 minutes of incubation on ice cells were aliquoted and frozen in liquid nitrogen and stored at -80°C.

Transformation of chemically competent *E. coli* cells was achieved by standard transformation protocols whereas plasmid DNA was added to thawed competent cells and incubated for 20 minutes on ice (SAMBROOK and RUSSELL 2001). After a one minute heat shock at 42°C, cells were incubated on ice for 2 minutes followed by the addition of LB and incubation for 45 minutes at 37°C and 200 rpm. Cells were plated on solid LB medium with respective antibiotics.

For preparation of electro-competent *S. cerevisiae* cells, a culture was grown o/n to an OD_{600} of 1.0-1.2, pelleted and resuspended in a LiAc:TE(D):H_2O solution (1:1:8) followed by an incubation at 30°C and 100 rpm for 45 minutes. Addition of DDT was followed by 15 minutes incubation at 30°C and 100 rpm. After centrifugation done twice, cells were washed with a. dest. and 1 M sorbitol and ready for usage.

S. cerevisiae transformations were carried out by electroporation using an Eppendorf Electroporator 2510 (Eppendorf). 40 µl of competent cells and DNA were added to an electroporation cuvette, electro shocked at 1.5 kV, resuspended in 600 µl sorbitol and plated on solid SD medium excluding the according amino acid for selection (BECKER and LUNDBLAD 2001).

2.9.2 Protoplastation and transformation of *S. macrospora*. Protoplastation was conducted according to (PÖGGELER *et al.* 1997). Cultures of *S. macrospora* were grown for 3 days in 115x15 mm petri dishes containing liquid BMM, harvested, protoplasted in PPB containing 20 mg/ml natuzym and incubated for 3 hours at 27°C and 100-125 rpm. Using a frit, protoplasts were separated from hyphal debris and eluted into a 50 ml falcon tube. Protoplasts

were washed two times with 10 ml PPB by centrifugation at 4,400 rpm for 5 minutes. Protoplasts were resuspended in 100 µl TPS per transformation-setup and incubated on ice for 10 minutes subsequent to addition of 20 µg DNA. A PEG6000 solution (25% [w/v] PEG6000 in PPB) was added to the transformation-setup and mixed by repetitive gentle inverting of the reaction tube followed by 20 minutes incubation at RT. The protoplast suspension was spread on solid CSM medium with a volume of 36 ml and incubated o/n at 27°C. The regenerated protoplasts were covered with 9 ml top-agar (4.7% [w/v] NaCl and 0.8% [w/v] SERVA-agar), while for selection, the top-agar contained the fivefold concentration of antibiotics used in regular medium. In general, *S. macrospora* transformants were selected on BMM or SWG media containing nourseothricin dihydrogen sulfate (50 µg/ml) or hygromycin B (110 U/ml).

2.10 Methods regarding nucleic acids

2.10.1 Isolation of plasmid DNA of *E. coli*. Plasmid extractions were conducted using either the QIAprep Spin Miniprep Kit, the HiSpeed Plasmid Midi Kit or the plasmid extraction protocol according to Birnboim and Doly (BIRNBOIM and DOLY 1979). DNA extractions using Qiagen mini or midi plasmid preparation kits occurred to the manufacturer's manuals.

Applying the Birnboim and Doly protocol, a 5 ml LB *E. coli* culture was grown o/n at 37°C and harvested at 500 rpm for 5 min. Subsequent to the addition of 200 µl BDI solution (containing 7 µl RNase [stock: 1mg/ml in a. dest.]) the pellet was resuspended by vortexing and incubated at RT for 5 min. After the addition of 200 µl BDII solution the suspension was mixed by inverting and incubated for 5 minutes on ice. The same procedure was conducted after the addition of 200 µl BDIII solution. Subsequent to 15 min centrifugation at 13,000 rpm, the supernatant was transferred to a new reaction tube and undergone an isopropanol precipitation. For this purpose, 750 µl isopropanol (-20°C) was added to the supernatant and incubated for 20 minutes at -20°C, centrifuged for 10 minutes at 13000 rpm. After discarding the supernatant the pellet was washed with 500 µl of 70% ethanol, dried using a concentrator (Eppendorf) and resuspended in 100-200 µl distilled water.

2.10.2 Isolation of plasmid DNA of *S. cerevisiae*. Yeast plasmid extraction occurred using the QIAprep Spin Miniprep Kit or the Smash and Grab protocol according to HOFFMAN and

WINSTON (1987). Qiagen miniprep kit isolation occurred to manufacturer's manuals except that 0.3 g of glass beads (Ø 0.25-0.5 mm) were added to the P1 buffer and cells were disrupted by vortexing.

The Smash and Grab protocol was conducted as follows: Yeast cultures were grown o/n in 5-10 ml medium and pelleted by centrifugation for 5 minutes at 13,000 rpm. After discarding the supernatant the pellet was washed in in 500 µl a. dest. and centrifuged at 13,000 rpm for 2 minutes. Discarding the supernatant was followed by resuspending of the pellet in residual liquid through vortexing. 200 µl lysis Buffer, 200 µl phenol/chloroform solution and 0.3 g of small glass beads were added and vortexed in a thermomixer (Eppendorf) for 8 min at 1,400 rpm at 8°C. After centrifugation, for 15 minutes at 13,000 rpm, 200-300 µl of the upper, aqueous layer were transferred in a fresh reaction tube. To get rid of the residual phenol an optional isopropanol precipitation was performed depending on the purpose of the extracted DNA.

2.10.3 Isolation of genomic DNA and RNA of *S. macrospora*. Extraction of *S. macrospora* gDNA was conducted according to a phenol/chloroform extraction described by LECELLIER and SILAR (1994) or a modified sodium acetate/isopropanol precipitation. Therefore, in petri dishes grown mycelium was harvested into a 2.0 ml reaction tube and frozen at -80°C, followed by the addition of 600 µl lysis buffer and 6-8 glass beads (Ø 2,85-3,45 mm). Mycelium was broken using a TissueLyser (Eppendorf) for 5 minutes at 30 Hz. Addition of 500 µl phenol was followed by brief vortexing and centrifugation at 13,000 rpm for 10 minutes. The upper, aqueous phase was transferred to another 2.0 ml reaction tube and mixed with 500 µl phenol and 500 µl chloroform and briefly vortexed. After centrifugation the upper, aqueous layer was transferred to a new 2.0 ml reaction tube and 1.0 ml chloroform was added followed by vortexing and centrifugation. The upper, aqueous layer was transferred into a 1.5 ml reaction tube and underwent an isopropanol precipitation as described previously, except that the pellet was dried under a flow box and not in a concentrator to preserve the gDNA.

Extraction of gDNA using a sodium acetate/isopropanol precipitation protocol was conducted as stated: Harvesting and breaking the mycelium was conducted as described before, followed by incubation at 70°C for 30 minutes. Subsequent to addition of 200 µl of

3 M sodium acetate (pH 5.2) the samples were incubated for 10 minutes at -80°C. After centrifugation at 13,000 rpm for 10 minutes the supernatant was mixed with the same amount of isopropanol, incubated for 10 minutes at RT and centrifuged for 10 min at 13,000 rpm. The pellet was washed with 70% ethanol, dried under a flow box and dissolved in distilled water.

Isolation of RNA was conducted modified respective to ELLEUCHE and PÖGGELER (2009). The harvested mycelium (grown as described previously) was mortared powdery using liquid nitrogen and mixed with 1 ml Trizol. After centrifugation for 10 minutes at 13,000 rpm and 4°C, 200 µl chloroform was added to the supernatant and mixed, the new generated upper phase was blended with the same amount of isopropanol. After 10 minutes incubation at RT the RNA was pelleted by centrifugation for 10 min at 13,000 rpm and 4°C and dried under a flow box. To dissolve the RNA pellet, 120 µl a. dest. were added and the reaction tube incubated for 30 minutes at 1000 rpm and 60°C.

2.10.4 Purification of DNA fragments using gel extraction, sodium-acetate precipitation and micro dialyzes. DNA fragment isolation from agarose gels was conducted using the QIAquick Gel Extraction Kit (Qiagen) according to the manufacture's manuals. Sodium-acetate precipitation and dialysis of nucleic acids was conducted for desaltation of DNA, present in reaction buffers. For sodium-precipitation 50 µl DNA was mixed with 50 µl a. dest., 20 µl 3 M sodium acetate (pH 5.2) and 100 µl isopropanol and incubated at -80°C for 20 minutes. Subsequent to a 10 minutes centrifugation at 13,000 rpm the DNA pellet was washed with 70% ethanol. Using micro-dialysis membranes (Millipore, 0.02 µm pore size), nucleic acids were pipetted on membranes floating on a. dest. in a petri dish, incubated for 10 minutes at RT and removed off the membrane via pipetting.

2.10.5 Hydrolysis and ligation of nucleic acids. Depending on the experimental setup, plasmid, genomic or via PCR amplified DNA was hydrolyzed according to manufacturer's manuals (Thermo Scientific) in setups of a volume of 10-100 µl.

For ligation reactions the QIAGEN PCR Cloning Kit (Qiagen) or T4 ligase (Thermo Scientific) were used. Utilizing the QIAGEN PCR Cloning Kit reactions were setup according to the manufacture's manuals. The reaction setup conducted with T4 ligase was arranged as follows: 1 µl T4 ligase, 2 µl 10x ligation buffer, 1 µl vector DNA and 16 µl PCR amplicon

(dialyzed). Reaction was incubated at RT for 30 minutes to 2 hours. Prior to ligation, vectors were dephosphorylated using Calf intestine alkaline phosphatase (CIAP, Thermo Scientific) according to a setup of: 2.5 µl 10x CIAP buffer, 1 µl CIAP and 21.5 µl vector DNA, with an incubation at 37°C for 10 minutes followed by a CIAP inactivation at 75°C for 10 minutes.

2.10.6 Gelelectrophoresis of nucleic acids. DNA fragments were mixed with 6x loading dye and separated in 1% agarose gels (1% [w/v] agarose in 1x TBE buffer) using a Mupid® gelelectrophoresis chamber with a voltage of 70-135 V. As electrophoresis buffer 0.5x TBE buffer was used. DNA was visualized under UV light subsequent to incubation in a 1 µg/ml ethidium bromide solution. RNA fragments were separated in 1.2 % 1x MOPS-agarose gels containing 5% formaldehyde at 80-100 V using a Mupid® gelelectrophoresis chamber. 1x MOPS served as electrophoresis buffer. Visualization of RNA occurred using UV light and prior to gel loading, the RNA was mixed in a 1:1 ratio with 2x RNA loading dye containing ethidium bromide and incubated for 10 min at 65°C. As standards, Gene Ruler DNA Ladder Mix or Gene Ruler DNA Ladder 1 kb were utilized.

2.10.7 PCR and colony PCR. PCR amplification of *S. macrospora* gDNA and cDNA was performed with either HotStarTaq Master Mix Kit (Qiagen), Phusion High-Fidelity DNA polymerase (New England Biolabs) or Pfu polymerase (Promega GmbH). Molzyme MolTaq polymerase (Molzym GmbH & Co. KG) was used for verification PCR or colony PCR on *S. macrospora* gDNA, on *E. coli* or *S. cerevisiae* plasmid DNA. All polymerases were applied according to the manufacturer's manuals.

2.10.8 cDNA synthesis and quantitative real-time PCR. To rid isolated RNA of gDNA, it was treated with DNaseI according to the manufacturer's manual. For reverse transcription, Transcriptor High Fidelity cDNA Synthesis kit was used to manufacturer's manual, with 2 µg of RNA as template. All quantitative real-time PCR experiments were performed at least 3 times utilizing 3 biologic independent replicates. Quantitative real-time runs were performed using a Mastercycler® ep realplex (Eppendorf) and the qPCR Mastermix for SYBR GreenI (PÖGGELER *et al.* 2006). The usage of primer pair jlb1-RT-f/jlb1-RT-r amplified a 193 bp fragment of *Smjlb1*, primer pair atg8-RT-f/atg8-RT-r amplified a 170 bp fragment of *Smatg8*

and primer pair atg4-RT-f/atg4-RT-r amplified a 250 bp fragment of *Smatg4*. Amplification of a 180 bp fragment encoding for the small rRNA subunit of *S. macrospora* with primer pair ssu-f/ssu-r served as normalization reference of Ct values. If given by experimental setup the data significance was analyzed using the REST application (PFAFFL *et al.* 2002).

2.10.9 Southern blotting and hybridization. DNA in interest of investigation was hydrolyzed in a 40-60 µl restriction setup and separated gelelectrophoretically. The gel was washed in buffer I (0.25 M HCl) for ten minutes, in buffer II (0.5 M NaOH) for 25 minutes and in buffer III (1.5 M NaCl, 0.5 Tris, pH 7.4) for 30 minutes. Using a capillary blot, the DNA was transferred to a GeneScreen Hybridization Transfer Membrane (PerkinElmer) and linked to the membrane via 5 minutes exposure to UV radiation. Using the High Prime DNA Labeling and Detection Starter Kit II (Roche) according to the manufacturer's manual the DNA-DNA hybridization and detection reaction was achieved. Exposition duration of membranes treated with detection agents towards X-ray films was 20 minutes to 2 hours.

2.11 Protein regarding methods

2.11.1 *S. macrospora* protein extraction. For protein extraction *S. macrospora* was grown in BMM liquid medium at 27°C for 3-6 days. Subsequent to mortaring of the mycelium in liquid nitrogen, it was mixed with protein buffer solution by thorough vortexing. After centrifugation (depending on mycelium volume 10 minutes at 13000 rpm or 20 minutes at 7500 rpm), the supernatant was transferred into a new reaction tube.

2.11.2 Yeast Two-Hybrid protein interaction studies. Bait plasmids pBD-Smatg8 and pBD-Smatg4 were constructed by cloning an amplified cDNA fragment using primer pair atg8-Hf/ atg8-Hr and atg4-Hf3/atg4-Hr, respectively, into vector pGBKT7 (Clonetech, 630443). To generate the prey vector pAD-Smatg8 the *Smatg8* amplicon was cloned into the vector pGADT7 (Clonetech, 630442). For cloning of the pAD-Smatg4 prey plasmid, primers atg4-Hf3/atg4-Hr3 were utilized. Bait plasmids were transformed into the *S. cerevisiae* strain Y187 and prey plasmids into *S. cerevisiae* strain AH109, by a lithium acetate transformation

protocol and selected on SD-Trp and SD-Leu, respectively (GIETZ *et al.* 1992). Mating of transformants was performed in YPDA liquid medium over night at 30°C and mated cells were selected on SD-Trp/Leu solid medium. Interaction was verified on SD-Ade/Leu/Trp solid medium. To determine whether the bait proteins are expressed appropriately for an interaction to be detected, a test based on interaction of the *GAL4* binding domains with the protein RanBPM was used (TUCKER *et al.* 2009).

For verification of SmATG8 and SmATG4 interaction strains carrying the respective bait or prey plasmids were directly mated and observed for interaction displayed by growth on SD-Ade/Leu/Trp or SD-His/Ade/Leu/Trp medium. A protein-protein interaction study of SmATG8 was conducted, also. Here, a Y187 strain carrying pBD-Smatg8 was mated against the AH109 strain harboring a *S. macrospora* cDNA library cloned into pGADT7. Plasmids were extracted of yeast clones indicating protein-protein interaction. Obtained plasmids were transformed into *E. coli*, purified and sequenced at the Göttinger Genom Labor (G2L). A BLASTP search in the *S. cerevisiae* (SGD: http://www.yeastgenome.org/cgi-bin/blast-sgd.pl) or the *N. crassa* (*N. crassa* Database: http://www.broadinstitute.org/annotation/genome/neurospora/Blast.html) databases revealed functions of the putative interaction partner of SmATG8.

2.11.3 Protein interaction studies using GFP-Trap®. Confirmation of Y2H interaction studies was conducted via GFP-Trap representing an *in vivo* and homologous expression method using *S. macrospora* protein extracts. For this purpose, the EGFP-SmATG8 fusion protein was used as bait. 20-40 µl GFP-Trap agarose beads where washed three times in 500 µl dilution buffer (10 mM Tris/HCl [pH 7.5], 150 mM NaCl, 0.5 mM EDTA, 1 mM PMSF, 1x protease inhibitor cocktail) at 300 rpm and 4°C for 2 minutes. Subsequent to the addition of protein extract to the GFP-Trap beads, samples were incubated at 4°C for 3 hours in a spinning wheel to evoke end-over-end mixing. After centrifugation at 2,000 rpm and 4°C for 2 minutes, the supernatant was discarded and the pellet was washed two times with 500 µl dilution buffer. Agarose beads were resuspended in 20-100 µl 5x SDS-sample buffer and boiled at 95°C for 10 minutes. The obtained supernatant, after centrifugation at 3000 rpm and 4°C for 2 minutes, was transferred into a new reaction tube. After brief separation in a SDS-PAGE gel the protein containing bands were cut and underwent a trypsin

digestion. The peptides were analyzed via mass spectrometry in the AG Braus by Dr. Oliver Valerius using the LCQ DecaXP mass spectrometer (Thermo Scientific).

2.11.4 Immuno Blotting. For detection of EGFP-SmATG8, SmATG8-EGFP, SmATG8mut-EGFP and EGFP-SmATG8^{G116} fusion proteins *S. macrospora* protein extracts were separated in a 15% SDS-PAGE and blotted to a PVDF membrane (BLOEMENDAL *et al.* 2012; LAEMMLI 1970; TOWBIN *et al.* 1979). Immunodetection of the fusion proteins was achieved with a monoclonal mouse anti-EGFP antibody (Santa Cruz Biotechnology, sc-9996, 1:5000). As secondary antibody a goat anti-mouse Horse Radish Peroxidase-linked (HRP) antibody (Dianova, 115-035-003, 1:5000) was used. Detection of signals was performed using the enhanced chemiluminescent reaction (Stratagene).

The aminopeptidase I (Ape1) maturation assay in *S. cerevisiae* was carried out as described by HARDING *et al.* (1995) using the polyclonal rabbit anti-Ape1 antibody (M. Thumm, Göttingen, 1:2500) and as secondary antibody HRP-linked anti-rabbit antibody (Invitrogen, G21234, 1:2500) was used. After stripping of the nitrocellulose membrane by incubating it for 1 h at RT in a solution of 0.2% Ponceau S dissolved in 3% TCA, and subsequent blocking, the calibration of the Western blot was performed by immunodetection with a monoclonal anti-mouse anti-actin antibody (Novus, NB100-74340, 1:2500) and secondary HRP-linked goat anti-mouse antibody (Dianova, 115-035-003, 1:2500).

2.12 Generation of the *S. macrospora Smvps34*, *Smvps15, Smatg8*, *Smatg4* and *Smjlb1* deletion strains. The generation of the deletion (and complementation) constructs was conducted using the homologous recombination mechanism of *S. cerevisiae* (COLOT *et al.* 2006). Deletion cassettes of *Smvps34*, *Smvps15, Smatg8*, *Smatg4* and *Smjlb1*were constructed in a similar manner and primers (Tab. 3) are named alike and solely the gene description changes (e.g. atg8-5f, atg4-5f or vps-34-3r, vps15-3r). 5'- and 3'-regions of *Smvps34*, *Smvps15, Smatg8*, *Smatg4* and *Smjlb1* were amplified from wt gDNA using the primer pair gene-5f/gene-5r and gene-3f/gene-3r. During the PCR amplification, specific 29-bp overhangs either homologous to the *S. cerevisiae* shuttle vector pRS426 as described by CHRISTIANSON *et al.* (1992) or to the hygromycin-resistance cassette were added to the 5'-and 3'-flank. The *hph* cassette was amplified using the primer pair hph-f/hph-r and plasmid pCB1003 served as

template. The three PCR amplicons obtained and the *Eco*RI/*Xho*I linearized vector pRS426 were co-transformed into the *S. cerevisiae* strain PJ69-4A as described by JAMES *et al.* (1996) in which the fragments were fused by homologous recombination. The resulting plasmids pRS-Δvps34, pRS-Δvps15, pRS-Δatg8, pRS-Δatg4 and pRS-Δjlb1 (Tab. 2) were isolated and served as a template for the amplification of the deletion cassettes with primer pairs gene-5f/gene-3r. Subsequently, 3.1 kb *Smvps34*, 3.4 kb *Smvps15*, 3.4 kb *Smatg8*, 3.4 kb *Smatg4* and 3.3 kb *Smjlb1*deletion cassettes were transformed into the *S. macrospora* Δku70 strain which is enhanced in homologous recombination events (PÖGGELER and KÜCK 2006). As *S. macrospora* transformants are often heterokaryotic and carry both transformed and nontransformed nuclei, single spore isolates were generated from the primary transformants. Additionally single spore isolates are generated to eliminate the *Δku70::nat*^{R} background. For that purpose single spore isolates containing both nourseothricin and hygromycin resistances were crossed with the *S. macrospora* spore-color mutant fus1-1 (S23442). From hybrid perithecia, spores were isolated and selected with hygromycin, to obtain homokaryotic deletion strains absent of the *Δku70::nat*^{R} background. The confirmation of the desired gene deletion was achieved by PCR using certain primer pairs. Deletion verification occurred in a similar manner for heterokaryotic ΔSmvps34/Smvps34, ΔSmvps15/Smvps15 as well as homokaryotic ΔSmatg8, ΔSmatg4 and ΔSmjlb1 and is explained by the example of *Smatg8* deletion. To verify the integration of the deletion cassette at the targeted *Smatg8* locus, primer pairs atg8-5D1/tC1 and atg8-3D1/h3-o were used and primer pair atg8-ver-f/atg8-ver-r was used to confirm the presence of *Smatg8* in the *S. macrospora* wt and complemented strain as well as the absence of *Smatg8* in the homokaryotic ΔSmatg8 deletion strain.

2.13 Generation of the *S. macrospora, Smatg8*, *Smatg4* and *Smjlb1*complementation strains. To complement the phenotype of ΔSmatg8, ΔSmatg4 and ΔSmjlb1 mutants, plasmids pRS-Smatg8-comp, pRS-Smatg4-comp and pRS-Smjlb1-comp (Tab. 2) were constructed by amplifying the 5'-and 3'-regions together with the entire coding regions of *Smatg8*, *Smatg4* and *Smjlb1* with primer pairs atg8-5f/atg8-3r, atg4-5f/atg4-3r and jlb1-5f2/jlb1-3r2 from wt gDNA, respectively. Amplified fragments were integrated into the *Eco*RI linearized vector pRSnat as described by KLIX *et al.* (2010) by homologous recombination in *S. cerevisiae*. The plasmid pRS-Smatg8-comp, pRS-Smatg4-comp and pRS-Smjlb1-comp was transformed into

deletion strains ΔSmatg8, ΔSmatg4 and ΔSmjlb1, respectively. Complemented transformants were selected on medium containing nourseothricin and inspected for perithecia development. The reintegration of the ectopic copy of the desired wild type gene was confirmed by PCR using the primer pair atg8-ver-f/atg8-ver-r for the ΔSmatg8::Smatg8^{ect}, atg4-ver-f/atg4-ver-r for ΔSmatg4::Smatg4^{ect} and jlb1-5D2a/jlb1-3D2a for the ΔSmjlb1::Smjlb1^{ect} strains, respectively.

In addition, *Smatg8* and *Smatg4* deletion and complementation events were confirmed by Southern hybridization. Southern blotting was performed according to standard techniques according to SAMBROOK and RUSSELL (2001). Hybridization was done with DIG High Prime DNA Labeling and Detection Starter Kit II (Roche). DNA probes were obtained by PCR with primers hph-f and hph-r (Tab. 3), and labeling and detection was executed according to the manufacturer's protocol.

2.14 Analytic procedures

2.14.1 Sequence analysis and oligonucleotide synthesis. Primers used in this study were synthesized by MWG Biotech AG and are enlisted in Tab 3. DNA sequencing was performed by the G2L-sequencing service of the "Göttinger Genom Labor" (Georg-August-University Göttingen). Molecular weights and isoelectric points of proteins were calculated with programs from the ExPASy Proteomics Server (http://www.expasy.org). Protein sequence alignments were performed using the ClustalX program as described by THOMPSON *et al.* (1997) and visualized using GeneDoc (NICHOLAS *et al.* 1997). Protein and nucleotide sequences of *VPS34*, *VPS15*, *ATG8*, *ATG4* and *idi-4* were obtained from the public databases at NCBI (http://www.ncbi.nlm.nih.gov/entrez/) or by BLAST searches of the complete sequenced genomes at the Broad Institute (http://www.broad.mit.edu/annotation/fungi/fgi/).

2.14.2 Isolation of *S. macrospora* genes *Smvps34*, *Smvps15*, *Smatg8*, *Smatg4* and *Smjlb1*. For the isolation of the *S. macrospora* autophagy genes *Smvps34* (*SMAC01337*), *Smvps15* (*SMAC04753*), *Smatg8* (*SMAC02305*), *Smatg4* (*SMAC08321*) and *Smjlb1* (*SMAC08510*), a TBLASTN search of the *S. macrospora* genomic sequence, published by NOWROUSIAN *et al.* (2010) was performed. The search was conducted using the amino-acid sequence of

S. cerevisiae Vps34 (YLR240W), Vps15 (YBR097W), Atg8 (YBL078C) and Atg4 (YNL223W), respectively. The search for a *S. macrospora* homologue of the *P. anserina* IDI-4 was performed using the Pa_6_10650 amino-acid sequence.

2.14.3 Phenotypical analysis of *S. macrospora*. Determination of growth velocity of the *S. macrospora* strains was performed as described by NOLTING and PÖGGELER (2006). For microscopic analysis, *S. macrospora* was inoculated on objective slides coated with 1-2 ml SWG medium or on a cellophane layer on solid SWG or BMM medium and incubated at 27°C (BLOEMENDAL *et al.* 2012). For macroscopic analysis *S. macrospora* was grown on solid SWG or BMM medium with a volume of 25 ml. The examination of the foraging abilities of *S. macrospora* strains, using a plug test was performed according to JOSEFSEN *et al.* (2012): an agar plug with a diameter of 5 mm was put into an empty petri dish and incubated for 5 days in a damp chamber at 27°C. Mycelial growth was visualized using a Digital Microscope VHX-500F (Keyence) or an AxioImager M1 microscope (Zeiss). Crossing of *S. macrospora* strains was achieved by putting agar plugs two of different strains (one strain carrying a spore-color mutation) on opposite sides of petri dishes containing solid BMM or SWG medium. After 7-14 days of incubation hybrid perithecia were formed at the crossing zone indicated by asci with a 4:4 ratio of black to brown ascospores. These spores were isolated on preparation plates (5% agar in a. dest.) and transferred to BMM solid medium containing 0.5% sodium acetate which induces germination. *S. macrospora* crossing was utilized to generate single spore isolates of sterile *Smvps34*, *Smvps15*, *Smatg8*, *Smatg4* and *Smjlb1* deletion mutants, hybrid perithecia of sterile ΔSmatg8, ΔSmatg4 and ΔSmjlb1 strains and germination-efficiency determination of sterile *Smatg8*, *Smatg4* and *Smjlb1*deletion mutants. The same experimental setup was used to verify that *Smvps15* and *Smvps34* are required for viability of *S. macrospora*. To determine germination efficiency of ascospores from hybrid perithecia, deletion and complementation strains were crossed with a fus1-1 strain (S23442, a spore-color mutant).

A total of 100 spores of each color were isolated from hybrid perithecia and inoculated on BMM supplemented with 0.5% of sodium acetate which was repeated at least three times. Germinated spores were counted after 1, 2, and 3 days. Obtained colonies were then transferred to hygromycin selective media to elucidate whether the ascospore isolates carried a

wt or knockout phenotype. To conduct hyphal fusion studies, strains were grown on a cellophane layer placed on solid MM + starch medium. Strains were incubated for 2-4 days and hyphal fusion events were examined 5-10 mm distant to the hyphal growth front. For visualization of asco rosettes perithecia were cracked open on object slides into a drop of water, the perithecia hull was removed and asci were covered with a cover slide to evoke asco-rosette formation.

2.14.4 Light and fluorescence microscopy. For the visualization of hyphae, ascogonia and protoperithecia an AxioImager M1 microscope (Zeiss) was utilized. A Photometrics CoolSNAP$^2_{HQ}$ camera (Roper Scientific) was used to obtain the images. EGFP fluorescence was visualized with the filter combination chroma filter set 49002 (exciter ET470/40x, emitter ET525/50 m and beamsplitter T495LP), DAPI with filter set 49000 (exciter D350/50x, emitter ET460/50nm and beamsplitter T400LP) and detection of DsRED and FM4-64 dye was achieved with a chroma filter set 49005 (excitation/emission filter ET545/30/ET620/60, beam splitter T570lp) and an X-cite 120 PC lamp (EXFO). Image editing was performed with MetaMorph (VisitronSystems), Adobe-Photoshop CS2 and -Illustrator CS2. Staining with DAPI was conducted by applying 50-100 µl of DAPI dissolved in fixation solution (3.7% formaldehyde, 0.2% Triton X-100, 50 mM phosphate buffer pH 7.0, 1 M K_2HPO_4, 1 M KH_2PO_4) directly on the mycelium as well as staining with FM4-64 (Invitrogen, F34653) using 20-40 µl of a FM4-64 (1 µg/ml a. dest.) solution.

Egfp-fusion constructs were integrated ectopically into the genome of wt and deletion strains. To examine the localization of SmATG8, an EGFP-SmATG8 fusion protein under its native promoter and terminator was constructed. The 5'-flanking region of *Smatg8* was amplified using wt gDNA as template and the primer pair atg8-5f/atg8-egfp-5r (Tab. 3). The forward primer atg8-5f contains a 29 bp overhang to the pRSnat vector and the reverse primer atg8-egfp-5r an overhang to the *egfp* gene. The *egfp* gene without stop codon was amplified using the primer pair EGFP-f/EGFP-r and p1783 as described by PÖGGELER *et al.* (2003) served as template. Primer pair atg8-egfp-3f/atg8-egfp-3r was used for the amplification of the coding region of *Smatg8* without the start codon and its 3'-flanking region. Both primers have overhangs homologous to the 3'-end of *egfp* and to the pRSnat vector, respectively. The fragments were fused in *S. cerevisiae* via homologous recombination and plasmid pRS-egfp-

Smatg8 was obtained. For localization of a C-terminal SmATG8-EGFP fusion protein, the plasmid pRS-Smatg8-egfp was constructed. Using the primer pair atg8-gf/atg8-gr *Smatg8* was amplified excluding the stop codon and atg8-gf generated a *Bgl*II overhang as well as atg8-gr a *Hin*dIII overhang. The by PCR obtained fragment was cloned into the *Bgl*II/*Hin*dIII linearized pDS23-EGFP (Nowrousian, unpublished), a pRS426 derivative with *egfp* under control of *gpd* promoter and *trpC* terminator of *A. nidulans* (Tab. 2). The construction of a C-terminal SmATG4-EGFP fusion encoded by plasmid pRS-Smatg4-egfp was conducted in the same manner with the primer pair atg4-gf/atg4-gr.

For generation of an EGFP-SmATG8mut fusion protein encoded by plasmid pRS-egfp-Smatg8mut, the putative SmATG4 processing site of SmATG8 was mutagenized. To amplify the mutated version of *Smatg8* the primer pair atg8-gf/atg8-gr2 was used to substitute the amino-acid residues 115-118 of SmATG8 to alanine. This fragment was cloned also into pDS23-EGFP. Plasmid pRS-egfp-Smatg8^{G116} encodes the putatively processed form of SmATG8 that lacks amino acids 117-121 and exposes a C-terminal G116. It was generated using primer pair atg8-5f/atg8p5r and atg8p-3f/atg8-3r, respectively, with pRS-egfp-Smatg8 as template. Fragments consisting of *Smatg8* 5'-flanking region, *egfp* and a truncated *Smatg8* as well as the 3'-region of *Smatg8* were amplified. The obtained fragments were cloned into pRSnat via homologous recombination in *S. cerevisiae*. To study the involvement of *Smatg8* and *Smatg4* in pexophagy, the plasmid pRS-egfp-Smatg8-DsRed-SKL encoding both an EGFP-SmATG8 and a DsRED-SKL fusion protein was generated. Primer pair atg8-5f3/atg8-org-5r amplified a fragment consisting of *Smatg8* 5'-region, egfp, *Smatg8* and its 3'-flanking region using pRS-egfp-Smatg8 as template. A fragment containing a *gpd* promoter, *DsRed-SKL* and a *trpC* terminator was amplified using the primer pair atg8-org-3f/MiPe-r2 and pDsRed-SKL as described by ELLEUCHE and PÖGGELER (2008) as a template. Both fragments were cloned into pRSnat by homologous recombination in *S. cerevisiae*. Generation of a C-terminal SmJLB1-EGFP fusion construct was achieved in the same manner as for SmATG8-EGFP and SmATG4-EGFP while using the primer pair jlb1-gf/jlb1-gr. The constructed plasmid was termed pRS-Smjlb1-egfp.

2.15 Measures of safety. Genetic engineering experiments of security level 1 have been conducted according to the guide lines of the genetic engineering law (GenTG) stated on 16.12.1993 (recently altered by Art. 12 G v. 29.7.2009 I 2542).

3. Results

3.1 Characterization of *Smvps34* and *Smvps15*

3.1.1 Identification of *Smvps34* and *Smvps15*. For the isolation of a gene coding for the phosphatidylinositol 3-kinase (PI3K) homologue *VPS34* in *S. macrospora,* a TBLASTN search in the *S. macrospora* genome published by NOWROUSIAN *et al.* (2010) was performed using amino-acid sequence of Vps34 of *S. cerevisiae* (YLR240W). *SMAC*01337 with an ORF of 2809 bp encoding a protein of 891 aa length was identified. Two predicted introns of 64 bp and 69 bp size were confirmed by cDNA sequencing. The protein has a calculated mass of 100.8 kDa with an isoelectric point (pI) of 6.15. Because it shares an identity of 35% with Vps34 of *S. cerevisiae* (P22543), *SMAC*01337 (CCC07770.1) has been named *Smvps34*. In an amino-acid alignment of related Ascomycota it is shown that SmVPS34 shares an overall identity of 95, 74, 66, 54, and 53% with orthologues of *N. crassa* (Q7SHZ6), *P. anserina* (B2AUR5), *Magnaporthe oryzae* (G4NKI8), *A. nidulans* (Q5B421), and *A. oryzae* (Q2U4A1), respectively. In an alignment using solely the amino-acid sequence of the phosphoinositide 3-kinase domain, conservation is remarkably higher (Fig. 8). The C-terminal PI3K domain of SmVPS34 shares an identity of 56% with *S. cerevisiae* and 96, 85, 75, 69 and 68% with *N. crassa*, *P. anserina*, *M. oryzae*, *A. nidulans* and *A. oryzae*, respectively.

The homologue of Vps15, a regulatory subunit of Vps34, was identified, using the *S. cerevisiae* (YBR097W) amino-acid sequence in a TBLASTN search in the genome of *S. macrospora*. The 4831 bp ORF of *SMAC04753* (CCC11771.1) encodes a putative Vps15 protein of 1474 aa, with a calculated molecular mass of 166.2 kDa and an isoelectric point of 7.0. By sequencing of the cDNA, splicing of two introns of 65 bp and 340 bp was confirmed.

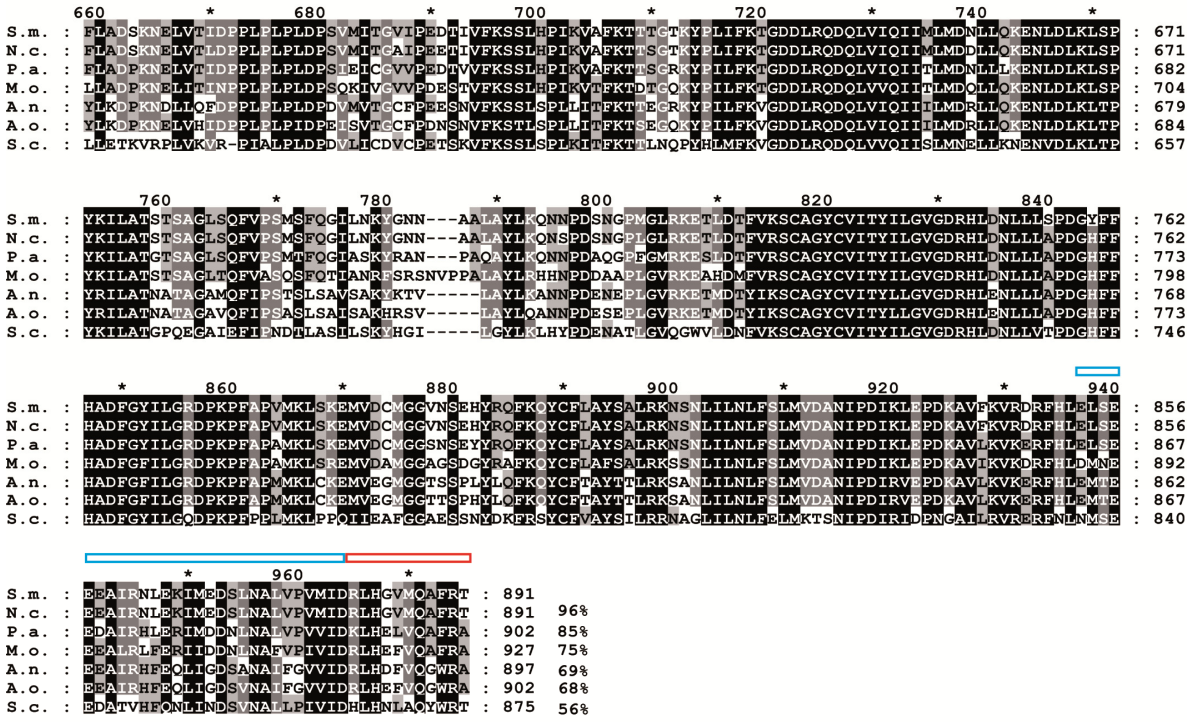

Figure 8. Alignment of multiple sequences of the Vps34 phosphoinositide 3-kinase class II, catalytic domain. The ClustalX alignment was generated with the following sequences: S.m., *Sordaria macrospora*, F7VQI8; N.c., *Neurospora crassa*, Q7SHZ6; P.a., *Podospora anserina*, B2AUR5; M.o., *Magnaporthe oryzae*, G4NKI8; A.n., *Aspergillus nidulans*, Q5B421; A.o., *Aspergillus oryzae*, Q2U4A1; S.c. *Saccharomyces cerevisiae*, P22543. The amino-acid residues responsible for interaction of Vps34 with Vps15 are highlighted by a blue box above the alignment (aa 837-864). C-terminal residues (aa 865-875) crucial for Vps34 kinase activity are highlighted by a red box above the alignment. The identical amino acids, conserved in the phosphoinositide 3-kinase domains, are shaded in black; residues conserved in at least 6 of 7 sequences are shaded in dark grey and residues conserved in at least four sequences are shaded in light grey. Amino-acid identities in % are given at the right margin.

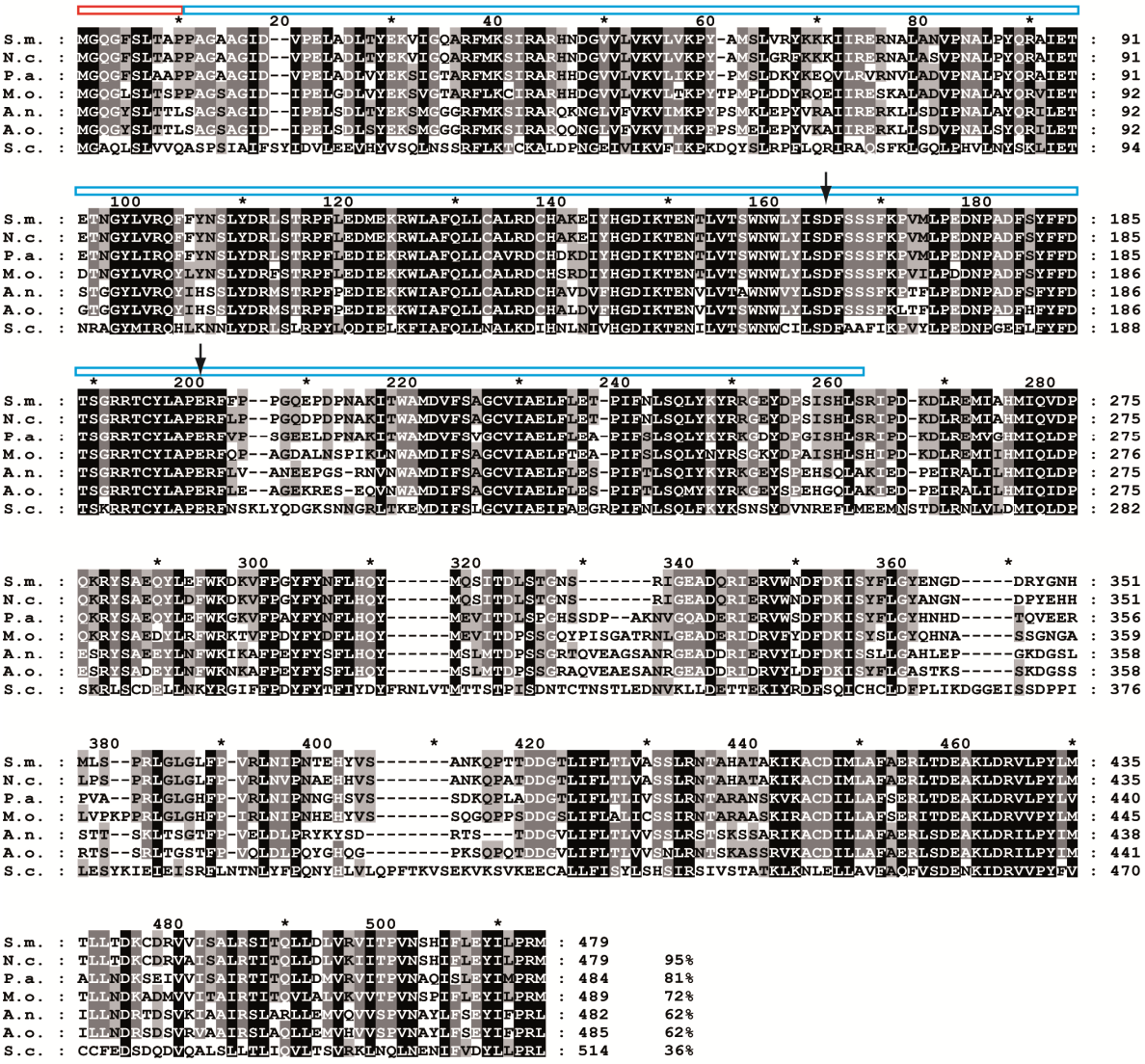

Figure 9. Alignment of multiple sequences of the protein kinase domain of Vps15 from members of the Ascomycota. Using the following sequences the ClustalX alignment was generated: S.m., *Sordaria macrospora*, F7W2C1; N.c., *Neurospora crassa* Q7S9P0; P.a., *Podospora anserina*, B2B2X0; M.o., *Magnaporthe oryzae*, G4N5A1; A.n., *Aspergillus nidulans*, Q5BFV4; A.o., *Aspergillus oryzae*, Q2UHC8; S.c. *Saccharomyces cerevisiae*, P22219. The N-terminal amino-acid residues of the myristoylation consensus site (aa 1-10) are highlighted by a red box above the alignment. The serine/threonine kinase domain residues (aa 11-262) as described by PANARETOU *et al.* (1997) crucial for Vps34 phosphorylation are highlighted by a blue box above the alignment. Arrows indicate two conserved residues important for kinase activity (HERMAN *et al.* 1991b). The identical amino acids, conserved in the N-terminal protein kinase region of Vps15, are shaded in black; residues conserved in at least 6 of 7 sequences are shaded in dark grey and residues conserved in at least four sequences are shaded in light grey. Amino-acid identities in % are given at the right margin.

Since the *S. macrospora* protein displayed a 24% aa identity when compared to *S. cerevisiae* Vps15 (P22219), *SMAC04753* was denoted *Smvps15*. A full length amino-acid alignment of SmVPS15 and orthologues of members of the phylum Ascomycota was performed. The alignment revealed identities of 88, 55, 42, 42 and 27% with *N. crassa* (Q7S9P0), *M. oryzae* (G4N5A1), *A. nidulans* (Q5BFV4), *A. oryzae* (Q2UHC8) and *P. anserina* (B2B2X0), respectively. Similarities increase when comparing the protein kinase domain (PK) of SmVPS15 solely. Identities of 95, 81, 72, 62, 62 and 36% with *N. crassa*, *P. anserina*, *M. oryzae*, *A. nidulans*, *A. oryzae* and *S. cerevisiae* respectively, are given (Fig. 9).

Orthologues of Vps34 and Vps15 were identified in *S. macrospora*, indicating a conservation of their functional domains among ascomycetes.

3.1.2 Construction of heterokaryotic *Smvps34* and *Smvps15* deletion strains. To examine the involvement of *Smvps34* and *Smvps15* in fruiting-body formation, deletion strains were generated using the *S. macrospora* Δku70 strain which is enhanced in homologous recombination. Generation of plasmids pRS-ΔSmvps34 and pRS-ΔSmvps15 containing the deletion cassette was conducted using the homologous recombination mechanism of *S. cerevisiae*. Gene deletion occurred by replacement of the target gene with a hygromycin resistance cassette.

To achieve *Smvps34* deletion, bases 54-2430 out of 2809 bp were exchanged and for *Smvps15* deletion, bases 1069-3782 out of 4831 bp were replaced (Fig. 10 and 11). After transformation of deletion cassettes into *S. macrospora* two heterokaryotic strains for each deletion construct were obtained. Verification via PCR confirmed the integration of the deletion cassettes at the desired gene locus as well as the presence of the *Smvps34* and *Smvps15* wt genes, confirming generation of heterokaryotic deletion strains (Fig. 12A and B).

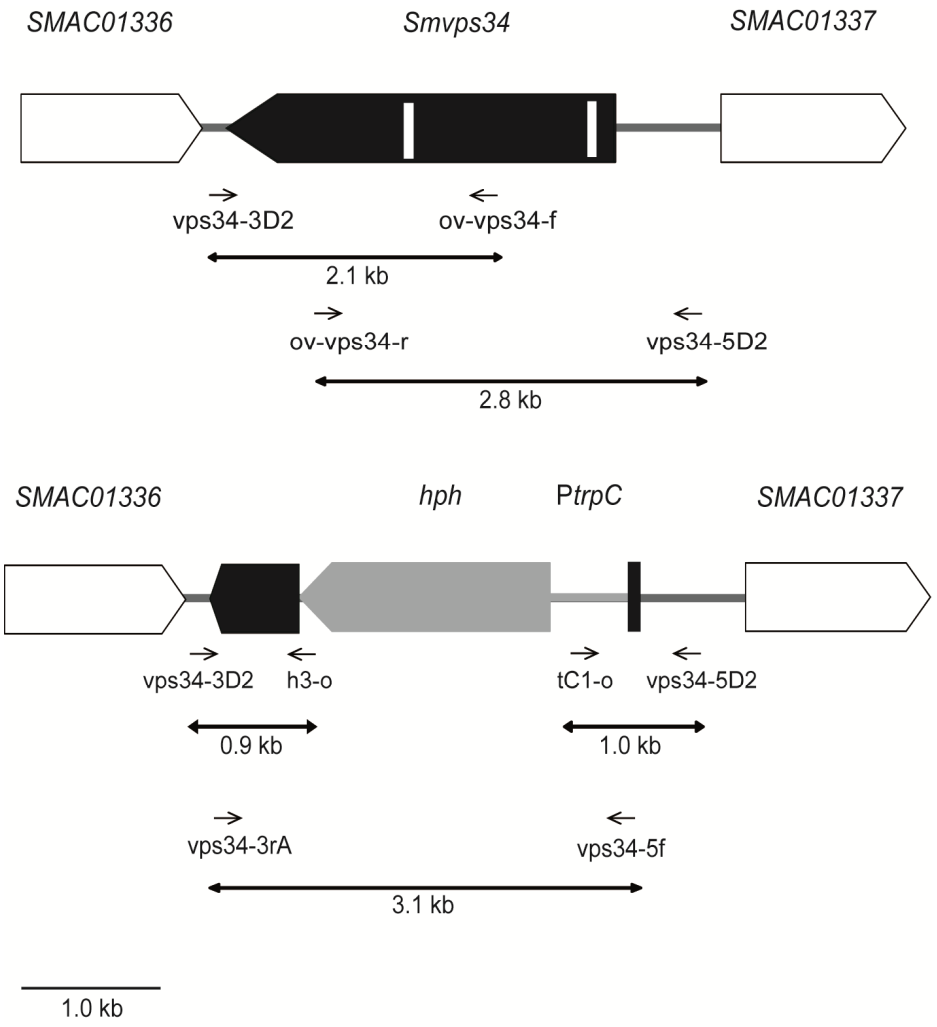

Figure 10. Construction of a ΔSmvps34 deletion mutant. Scheme of the *Smvps34* locus before and after gene replacement. Positions of primers confirming deletion and presence of the *Smvps34* wt gene are indicated by small arrows. Sizes of PCR fragments for deletion verification and deletion cassette amplification are given. White frames, adjacent genes; black frame, target gene; grey frame, *hph* gene for hygromycin resistance; grey line, *trpC* promoter of *A. nidulans*; white rectangles, introns; dark grey lines, intergenic regions.

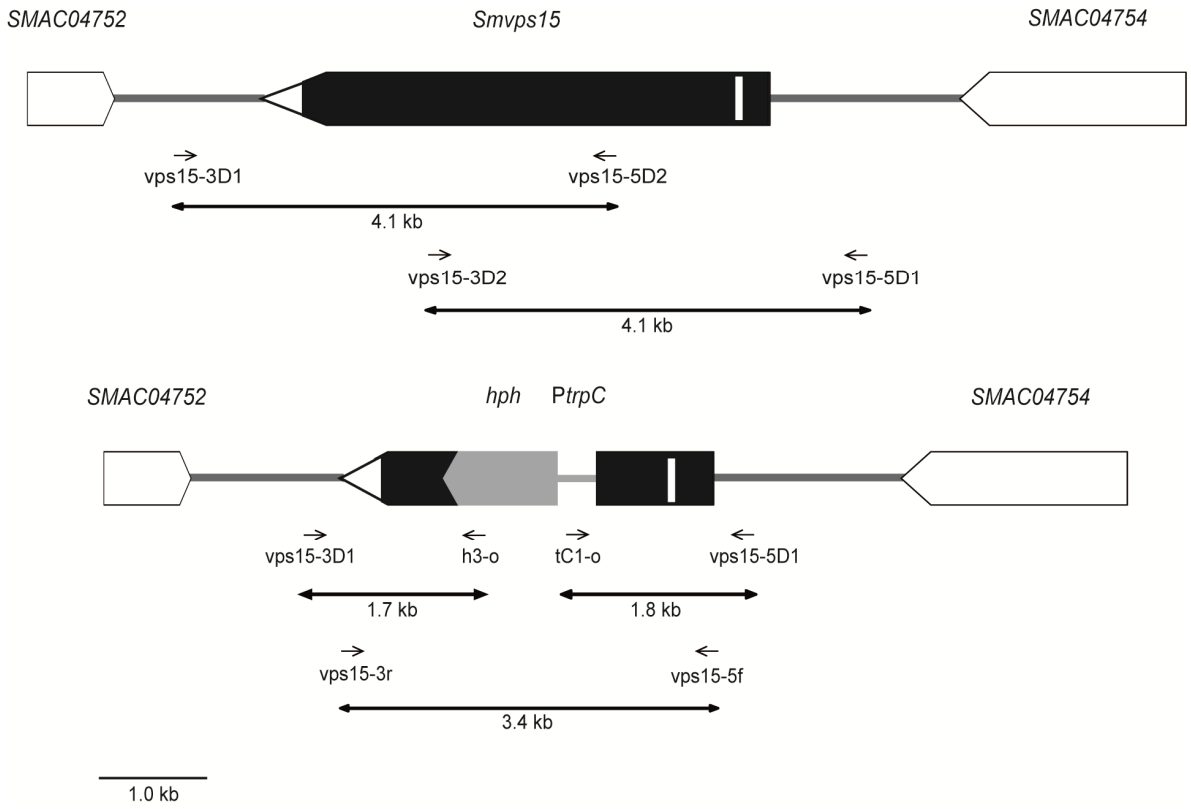

Figure 11. Generation of a ΔSmvps15 deletion strain. Illustration of the *Smvps15* gene locus before and after gene replacement. Primers positions confirming deletion and presence of the *Smvps15* wt gene are indicated by small arrows. Sizes of PCR fragments for deletion verification as well as amplification of the deletion cassette are shown. White frames, adjacent genes; black frame, target gene; grey frame, *hph* gene for hygromycin resistance; grey line, *trpC* promoter of *A. nidulans*; white rectangles and triangles, introns; dark grey lines, intergenic regions.

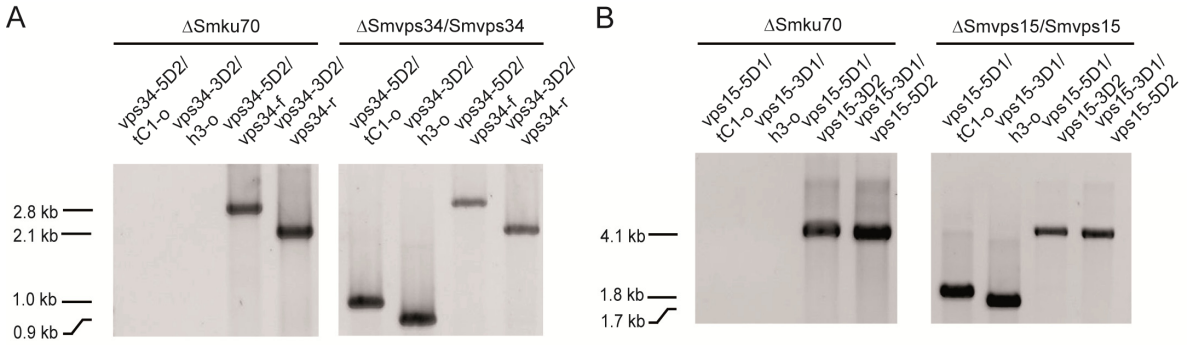

Figure 12. Deletion verification of heterokaryotic ΔSmvps34/Smvps34 and ΔSmvps15/Smvps15 strains. (A) and (B) Deletion and wt gene presence was confirmed by PCR. Fragment sizes according to primer pairs appeared as expected and are displayed in Fig. 10 and 11.

For the verification of the deletion via PCR, primer pairs vps34-3D2/h3-o and vps34-5D2/tC1-o were chosen, which bind in the 5'- or 3'-flanking regions of the target genes and in the hygromycin resistance cassette (for details, Fig. 10). Using ov-vps34-r/vps34-5D2 and ov-vps34-f/vps34-3D2, which bind in flanking regions as well as in *Smvps34*, presence of the wt gene was proven. In the same manner, applying primer combinations vps15-3D1/h3-o and vps15-5D1/tC1-o as well as vps15-3D1/vps15-5D2 and vps15-5D1/vps15-3D2, (for details, Fig. 11), the integration of the deletion cassette at the desired locus and the presence of *Smvps15* was affirmed.

Validated by PCR, heterokaryotic ΔSmvps34/Smvps34 and ΔSmvps15/Smvps15 strains were generated.

3.1.3 In *S. macrospora Smvps34* and *Smvps15* are required for viability. Deletion of the target genes was conducted in the *S. macrospora* Δku70 strain and the derived primary transformants contained a heterokaryotic genotype. Thus, in ΔSmvps34/Smvps34 nuclei with a ΔSmvps34*::hph*/Δku70::*nat* or Smvps34/Δku70::*nat* genotype are found. In ΔSmvps15/Smvps15 nuclei with a ΔSmvps15*::hph*/Δku70::*nat* or Smvps15/Δku70::*nat* genotype are present (Fig. 12A and B).

In order to determine the phenotype of the deletion strains it is crucial that the Δku70 and wt background are removed from the heterokaryotic primary transformants. For this purpose, crosses with spore-color mutants were performed. Interestingly, in several attempts it was not

possible to generate homokaryotic ΔSmvps34 or ΔSmvps15 deletion strains. To elucidate if both genes are required for viability a germination-efficiency assay was conducted. *S. macrospora* is a homothallic fungus that produces self-fertile perithecia. The discrimination between self-fertile and hybrid perithecia in crosses of wt strains is difficult. To circumvent this problem, spore-color mutants can be used in crosses. Crosses between wt and spore-color mutants result in hybrid perithecia in the contact zone, with asci containing four black wt spores and four colored spores. Spores from hybrid perithecia were isolated, and tested with regard to colony formation and hygromycin resistance. Hybrid perithecia are obtained by crossing of the primary transformants with the spore-color mutant fus1-1 strain. This strain has a mutation in the *fus1* gene encoding an enzyme of the melanine biosynthesis. Mutation of this gene leads to the production of brown ascospores (NOWROUSIAN *et al.* 2012). To compare germination rates of all crosses, spores were only isolated from hybrid perithecia.

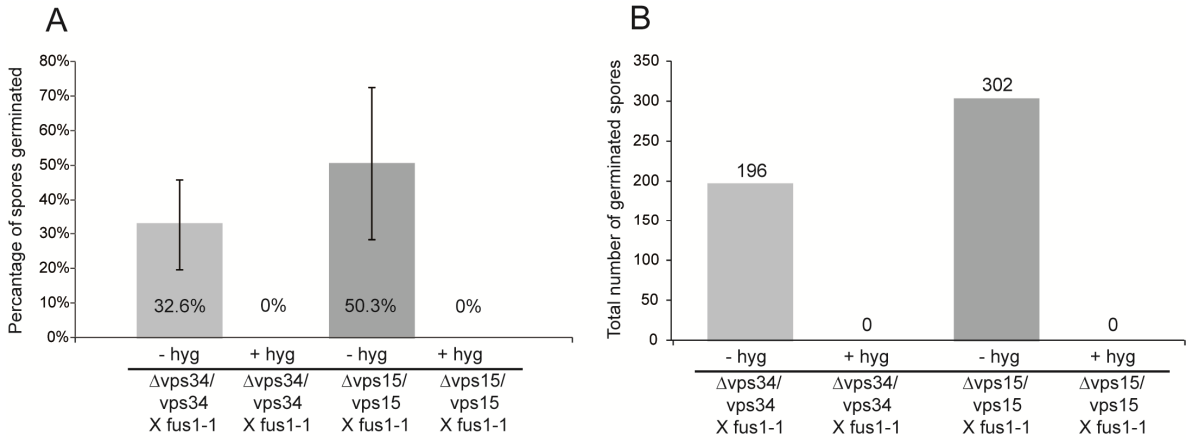

Figure 13. Germination-efficiency assay determined requirement of *Smvps34* and *Smvps15* for viability. (A) Determination of germination efficiency of ascospores. Deletion strains were crossed with the spore-color mutant fus1-1, as stated in Materials and Methods. In total 200 (100 spores of each color) were isolated from hybrid perithecia and inoculated on BMM supplemented with 0.5% of sodium acetate and another 200 spores (100 of each color) were inoculated on BMM supplemented with sodium acetate and hygromycin (110 U/ml). Determination of germinated spores in percent was conducted for each strain. Averages of three experiments are shown and error bars indicate standard deviations. (B) Screening for hygromycin resistant spores. Colonies obtained from ascospores germinated on BMM + sodium acetate were transferred to hygromycin containing BMM medium and tested for growth. Numbers of germinated spores represent the sum of three experiments.

Out of three experiments a total number of 600 ascospores each derived from hybrid perithecia of the crossing of ΔSmvps34/Smvps34 X fus1-1 and ΔSmvps15/Smvps15 X fus1-1 were isolated and transferred to solid BMM + sodium acetate and another 600 ascospores, also out of three experiments, to BMM + sodium acetate containing hygromycin. When transferred to BMM + sodium acetate medium, 196 spores (32.6%) of the ΔSmvps34/Smvps34 X fus1-1 and 302 spores (50.3%) of ΔSmvps15/Smvps15 X fus1-1 hybrid perithecia germinated (Fig. 13A). When transferred to medium containing hygromycin, no colony derived from either ΔSmvps34/Smvps34 X fus1-1 or ΔSmvps15/Smvps15 X fus1-1 hybrid perithecia was capable to grow indicating none of the germinated spores contained the Δ*Smvps34::hyg* or Δ*Smvps15::hyg* background (Fig. 12B). When spores of hybrid perithecia were isolated on BMM + sodium acetate containing hygromycin, not even one spore germinated when incubated for 4 days (Fig. 13B). This is true for spores isolated from ΔSmvps34/Smvps34 X fus1-1 and ΔSmvps15/Smvps15 X fus1-1 hybrid perithecia indicating that spores containing a Δ*Smvps34::hyg* or Δ*Smvps15*::*hyg* genotype are not able to germinate.

Taken together, of 1200 isolated spores out of three independent experiments, none was able to grow on hygromycin containing medium, showing that *Smvps34* and *Smvps15* are required for viability of *S. macrospora*.

3.2 Characterization of *Smatg8* and *Smatg4*

3.2.1 Isolation of *S. macrospora Smatg8* and *Smatg4* genes. To isolate a gene encoding a homologue of the autophagosomal protein ATG8 from *S. macrospora,* a TBLASTN search of the *S. macrospora* gene was performed with the *S. cerevisiae* Atg8 (YBL078C) protein as a query sequence. The 503 bp ORF *SMAC02305* (CCC07296.1) encoding a putative homologue of *S. cerevisiae* Atg8 was identified. Splicing of two predicted introns (69 and 68 bp) was confirmed by sequencing of the cDNA. *SMAC02305* encodes a protein of 121 amino acids with a predicted mass of 14.1 kDa and a theoretical isoelectric point of 6.15.

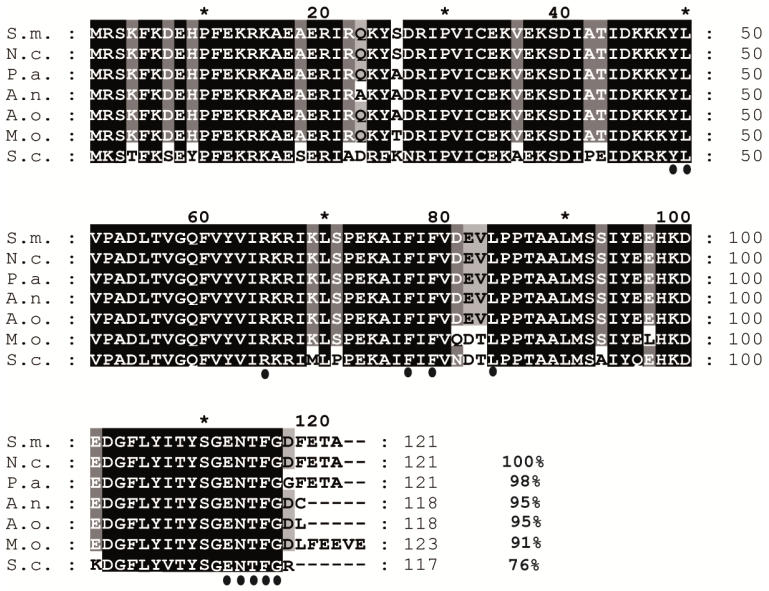

Figure 14. **Multiple sequence alignment of the Atg8 proteins from members of the Ascomycota.** The ClustalX alignment was created using the following sequences: S.m., *Sordaria macrospora*, F7VP68; N.c., *Neurospora crassa*, Q8WZY7; P.a., *Podospora anserina*, Q8J282; A.n., *Aspergillus nidulans*, Q5B2U9; A.o., *Aspergillus oryzae*, Q2UBH5; M.o., *Magnaporthe oryzae*, Q51MW4; S.c. *Saccharomyces cerevisiae*, P38182. Conserved residues important for the interaction with Atg4 and Atg7 in other organisms are indicated by dots below the alignment. Identical amino acids, which are conserved in all proteins, are shaded in black; residues conserved in at least 6 of 7 sequences are shaded in dark grey and residues conserved in at least four sequences are shaded in light grey. Amino-acid identity in % is given at the right margin.

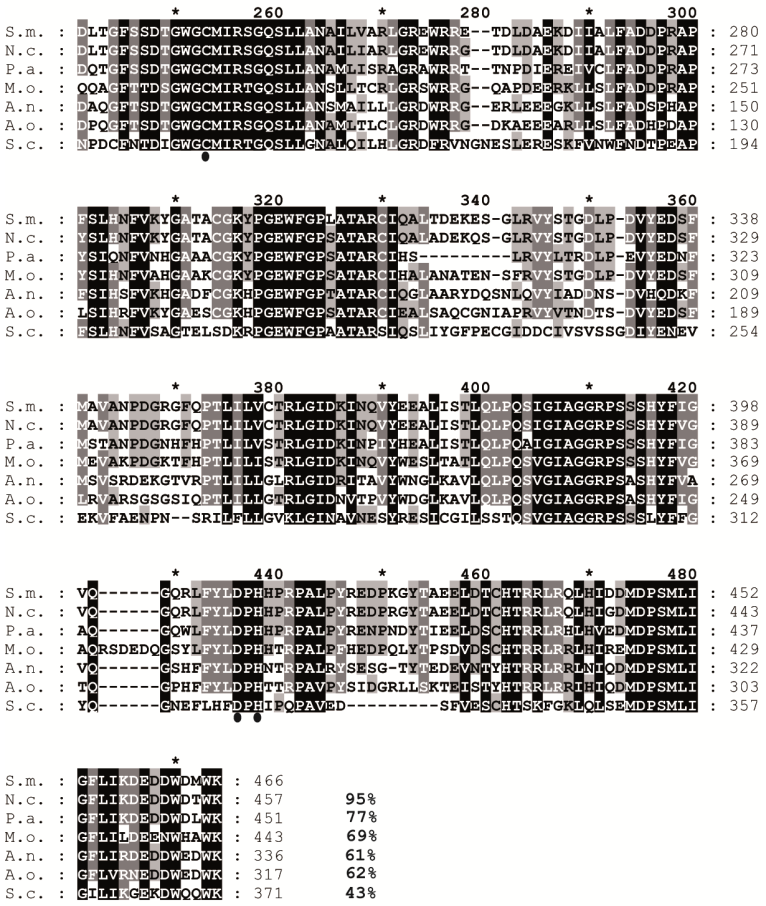

Figure 15. **Multiple sequence alignment of the Atg4 C54 catalytic domain from members of the acomycetes.** ClustalX alignment of catalytic C54 domain of Atg4 starting with Asp^{223} to Lys^{466} of the *S. macrospora* ATG4. Following sequences were utilized in the alignment: S.m., F7VV83; N.c., Q7S3X7; P.a., Q86ZL5; M.o., Q523C3; A.n., Q5B7L0; A.o., Q2U5B0; S.c., P53867. The conserved Cys, Asp, and His residues of the catalytic triad of the C54 domain are marked with dots under the alignment. Identical amino acids, conserved in all proteins, are shaded in black; conserved residues in at least 6 of 7 sequences are shaded in dark grey and residues conserved in at least four sequences are shaded in light grey. Identity of amino acid in % is given at the right margin.

Because the encoded protein shares 76% amino-acid identity to the *S. cerevisiae* Atg8 protein, the gene was named *Smatg8*. Amino-acid alignment of SmATG8 with homologues of other members of the phylum Ascomycota showed that this protein is highly conserved. Only the C-terminal residues after G116, which is predicted to be C-terminally exposed after processing by Atg4, display a low level of identity (Fig. 14). The alignment revealed that

SmATG8 shared 100, 98, 95, 95 and 91% identity with orthologues of *N. crassa* (Q8WZY7), *P. anserina* (Q8J282), *A. nidulans* (Q5B2U9), *A. oryzae* (Q2UBH5), and *M. oryzae* (Q51MW4), respectively (Fig. 14).

To isolate an orthologue of the gene encoding the cysteine protease Atg4, which is required for Atg8 processing and recycling, *S. cerevisiae* Atg4 (YNL223W) was used for a TBLASTN search and identified the 1789 bp *SMAC08321* (CCC09424.1) sequence, encoding a protein of 515 amino acids with a predicted mass of 56.16 kDa and a theoretical pI of 4.88. The ORF is predicted to contain three introns of 83, 90 and 68 bp. Intron splicing was confirmed by cDNA sequencing.

The encoded protein showed 43% identity in 254 aa overlap when compared to the *S. cerevisiae* homologue. The alignment of the predicted C54 peptidase domain (pfam03416) of the protein demonstrated that this domain is rather conserved among Atg4 orthologues of different ascomycetes (Fig. 15). This domain includes an active cysteine residue that was previously identified in the Atg4 protease of *M. oryzae* (Fig. 15) (LIU *et al.* 2010). Due to this high degree of sequence identity, the isolated gene was named *Smatg4*.

Orthologues of Atg8 and Atg4 were identified in *S. macrospora*. The entire SmATG8 protein is conserved among Ascomycota. But in SmATG4, solely the C54 peptidase domain shares similarities with orthologues of ascomycetes.

3.2.2 Functional characterization of *Smatg8* and *Smatg4* in *S. cerevisiae* autophagy mutants. In order to confirm functional conservation of *Smatg8* and *Smatg4* and their yeast counterparts, a complementation experiment using *Smatg8* and *Smatg4* cDNA under control of a *MET25* promoter was performed in *S. cerevisiae* to rescue *atg8Δ* and *atg4Δ* deletion strains, respectively.

In *S. cerevisiae*, maturation of the precursor proaminopetidase I (prApe1) to the mature enzyme (Ape1) depends on the autophagy proteins Atg8 and Atg4. Rescue of autophagy of the *S. cerevisiae* mutants was monitored using an aminopeptidase I (Ape1) maturation assay (HARDING *et al.* 1995).

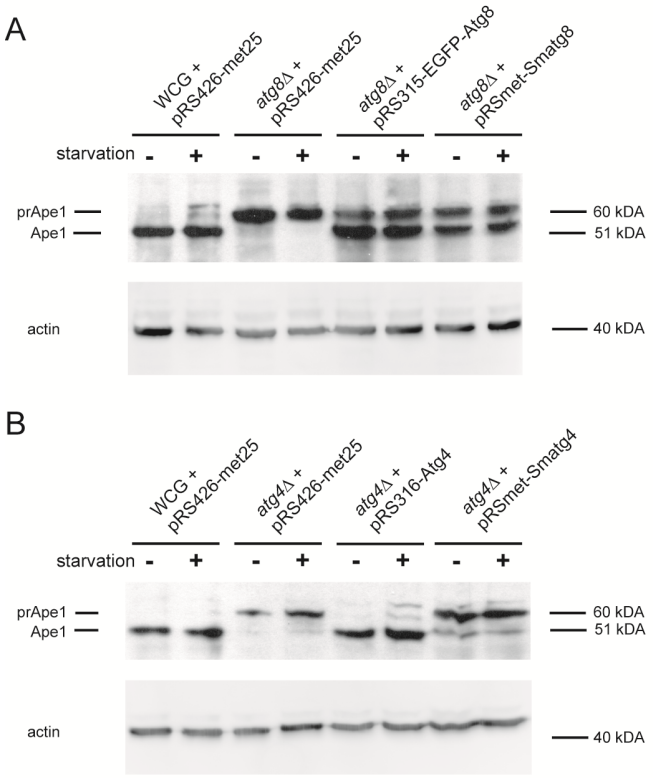

Figure 16. **Complementation of the *S. cerevisiae* autophagy mutants with *S. macrospora* autophagy genes.** Complementation of respective yeast strains with *Smatg8* and *Smatg4* was analyzed using an aminopeptidase I (Ape1) maturation assay (HARDING *et al.* 1995). In *S. cerevisiae*, the cytosolic 61 kDa precursor of Ape1 (prApe1) is delivered to the vacuole via the Cvt pathway which involves intact Atg4 and Atg8 proteins. Upon delivery to the vacuole prApe1 is processed to the mature Ape1 enzyme (Ape1). Identical amounts of yeast cell extracts (0.2 OD_{600} equivalents of cells) isolated before (-) and after starvation on SD-N medium for 4 hours (+) were separated on 15% SDS-PAGE. After blotting, PVDF membranes were probed with an anti-Ape1 antibody as stated in Materials and Methods. To verify equal protein concentrations after stripping of the membrane anti-actin antibody was used as loading control. Numbers at the right indicate the molecular mass. prApe1, Ape1 precursor, Ape1, mature Ape1. (A) Complementation of *S. cerevisiae atg8*Δ with *Smatg8* under control of the yeast *MET25* promoter (pRSmet-Smatg8). As positive control the *S. cerevisiae* wt strain WCG was transformed either with the empty plasmid pRS426-met25 or *S. cerevisiae atg8*Δ was transformed with the yeast *egfp-ATG8* gene (pRS315-EGFP-Atg8). *S. cerevisiae atg8*Δ transformed with the empty vector pRS426-met25 served as a negative control. (B) Complementation of *S. cerevisiae atg4*Δ with *Smatg4* under control of the yeast *MET25* promoter (pRSmet-Smatg4). As positive control, the *S. cerevisiae* wt WCG was transformed with the empty plasmid pRS426-met25 or *S. cerevisiae atg4*Δ was transformed with the yeast *ATG4* gene (pRS316-Atg4). *S. cerevisiae atg4*Δ transformed with the empty vector pRS426-met25 served as negative control.

We generated the yeast strains WCG + pRS426-met25, *atg8*Δ + pRS315-EGFP-Atg8, as well as *atg4*Δ + pRS316-Atg4 as positive controls, and *atg8*Δ + pRS426-met25 as well as *atg4*Δ + pRS426-met25 as negative controls (Table 1). Yeast strains *atg8*Δ + pRS-met-Smatg8 and *atg4*Δ + pRS-met-Smatg4 were used to assess whether the *S. macrospora* genes could rescue Ape1 processing in the yeast deletion strains. Yeast strains were grown over night in selective dropout (SD) minimal medium and adjusted to OD_{600} = 1. One set of cells was used for protein extraction, while another set was grown for four hours in SD minimal medium lacking nitrogen (SD-N) that induces amino-acid starvation and, in turn, autophagy in *S. cerevisiae*.

The effect of starvation was not as drastic as expected, which might have been due to the fact that cells were grown to an OD_{600} of 1, where the cells were stationary and already starved. Fig. 16A shows that prApe1 maturation occurred to the same extend when *S. cerevisiae ATG8* or *Smatg8* was expressed in *atg8Δ*, which indicated the capability of *Smatg8* to complement the yeast *atg8*Δ strain. However, *Smatg4* apparently complemented the yeast *atg4*Δ strain only partially. In the negative control (*atg4*Δ + pRS426-met25), in addition to the Ape1 precursor form, a very faint band of Ape1 was visible under starvation conditions, indicating low Ape1 processing activity in the yeast *atg4*Δ mutant. Extracts from cells expressing the heterologous *Smatg4* showed a clearly visible Ape1 signal, but when compared to the positive control signal of the strain expressing the endogenous *ATG4* gene (*atg4*Δ + pRS316-Atg4) the signal was weaker (Fig. 16B).

SmATG8 and SmATG4 are able to complement yeast deletion strains *atg8*Δ and *atg4*Δ, respectively.

3.2.3 SmATG8 interacts with SmATG4 in the Yeast Two-Hybrid system. A direct protein-protein interaction of Atg8 and Atg4 has been described in *S. cerevisiae* by KIRISAKO *et al.* (2000) and was recently demonstrated in *M. oryzae* (LIU *et al.* 2010). To confirm that SmATG8 and SmATG4 interact with each other, a Yeast Two-Hybrid analysis was performed.

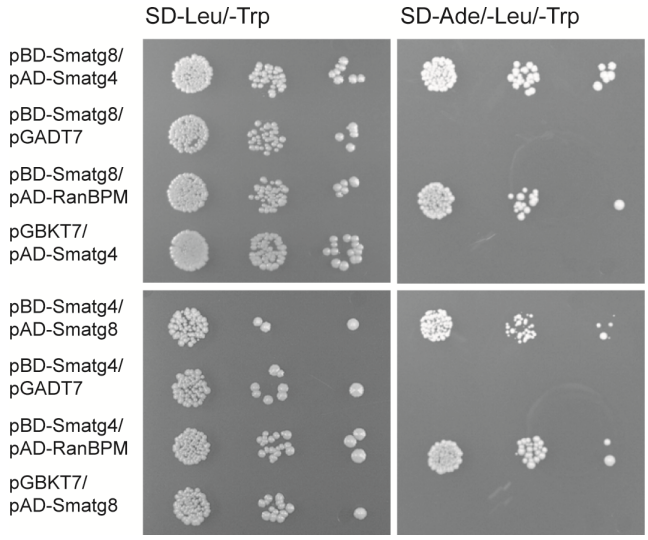

Figure 17. Yeast Two-Hybrid interaction of SmATG8 and SmATG4. Full-length cDNAs of *Smatg8* and *Smatg4* were used to generate Gal4 DNA binding domain (BD) and activation domain (AD) plasmids. Yeast strains Y187 and AH109 were transformed either with bait plasmids pGBKT7, pBD-Smatg8 and pBD-Smatg4 or with prey plasmids pGADT7, pAD-RanBPM, pAD-Smatg8 and pAD-Smatg4, respectively. After mating of both strains in all possible combinations diploid cells were selected on SD-Leu/-Trp media. Strains carrying empty plasmids pGADT7 and pGBKT7 served as negative controls. To determine whether the bait proteins are expressed appropriately for an interaction to be detected we used as a positive control a test, based on interaction with the Gal4 BD with protein RanBPM (TUCKER *et al.* 2009). Serial dilutions were made either on SD-Leu/-Trp to select for the presence of both plasmids (left) or on selection medium lacking adenine (SD-Ade/-Leu/-Trp) to verify the interaction of SmATG8 with SmATG4 (right).

For this purpose, *Smatg8* and *Smatg4* cDNA was cloned into the two-hybrid vectors pGBKT7 and pGADT7, respectively. The resulting bait plasmids were transformed into yeast strain Y187 and prey plasmids into the yeast strain AH109. Transactivation of pBD-Smatg8 and pBD-Smatg4 was tested by mating them with yeast strain AH109 carrying the empty pGADT7 vector. Mating of yeast strain Y187 carrying the empty pGBKT7 with yeast strain AH109 containing either pAD-Smatg8 or pAD-Smatg4 served as further negative control (transactivation). As a positive control and to test the appropriate expression of the proteins encoded by the bait plasmids, mating of bait plasmids carrying strains with the pAD-RanBPM containing yeast strain AH109 was conducted (TUCKER *et al.* 2009). The two-hybrid experiments clearly demonstrated an interaction of SmATG8 and SmATG4 (Fig. 17).

SmATG8 and SmATG4 interact in a heterologous expression system.

3.2.4 SmATG8 interaction studies via Y2H and GFP-Trap identified 70 putative interaction partners. Interaction partners of SmATG8 were supposed to be identified by protein interaction screens using Y2H (heterologous expression system) and GFP-Trap (*in vivo* expression).

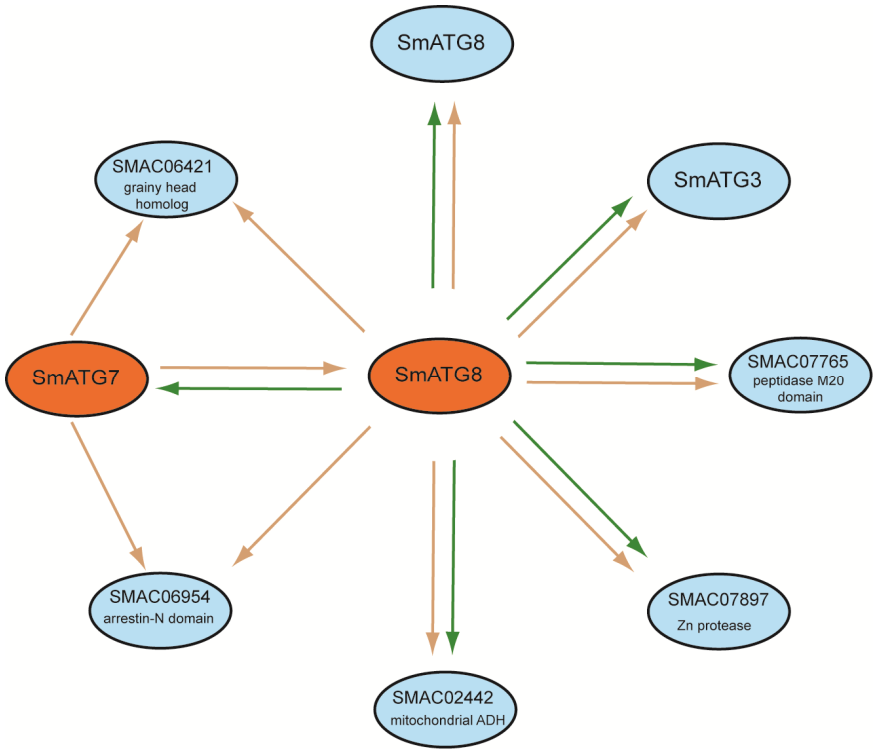

Figure 18. Scheme of interaction partners found in more than one screen. Schematic illustration of common interaction partners found in a Y2H screen with SmATG7 and SmATG8 in a *S. macrospora* cDNA library. Interaction partners of SmATG8 identified in a Y2H (beige arrow) and GFP-Trap screen (green arrow). Proteins in orange indicate bait proteins and proteins in light blue indicate identified interaction partners.

As previously mentioned the bait plasmid pBD-Smatg8 was confirmed to be expressed accurately and showed no transactivation (Fig. 17). Therefore it was used in a Y2H screen with a *S. macrospora* cDNA library. Functionality of the EGFP-SmATG8 fusion protein used for the GFP-Trap analysis was approved by complementation of the *Smatg8* deletion mutant and by microscopy (shown in chapter 3.2.9). Strains used in the GFP-Trap screen were ΔSmatg8::egfp-Smatg8^{ect} and ΔSmatg4::egfp-Smatg8^{ect}. The latter strain was used to elucidate if a different interaction pattern occurs when processing of EGFP-SmATG8 is abolished.

In total, 75 potential interaction partners could be identified, 56 by Y2H (Tab. 4) and 19 in a GFP-Trap screen (Tab. 5). 5 putative interactions were found in the Y2H as well as in the GFP-Trap screen. Thus, 70 unique interactions were identified combining the results of both screens. By BLASTP searches of the *N. crassa*, *S. cerevisiae* and *H. sapiens* databases (Broad Institute, SGD and NCBI) with the *S. macrospora* amino-acid sequence putative gene functions were determined. Validity of interaction was confirmed by a search for the LIR (LC3 interacting region) motif in the amino-acid sequence of the putative SmATG8 interaction partners and is discussed in chapter 4.3.2 (SMACs of proteins with putative LIR motifs are highlighted in light grey).

The five interactions found in both screens (Fig. 18) were identified as SmATG8, SmATG3, SMAC07765 (peptidase M20 domain), SMAC07897 (Zn protease) as well as SMAC02442 (alcohol dehydrogenase I). The interactions are also highlighted in bold in Tab. 4 and 5.

Interactions found in the Y2H screen with the highest number of hits were: SMAC00918 (phospolipase B, 16x), SMAC01312 (predicted Woronin body protein, 7x), SMAC09075 (conserved protein, 6x), SMAC02442 (alcohol dehydrogenase I, 6x), SMAC07505 (conserved protein, 5x), SMAC04326 (cell wall synthesis protein, 4x), SMAC00851 (transmembrane protein 184B, 4x), SMAC01818 (conserved protein, 4x) and SMAC02037 (α-1,2-mannosyltransferase, Kre5 of *N. crassa*, 4x).

Further interesting interactions with regard to the function of interacting proteins were: SMAC08632 (UDP-glucose sterol glucosyltransferase, Atg26 of *S. cerevisiae*, 3x), SMAC01351 (serine protease p2, 2x), SMAC07459 (F-box domain-containing protein, 1x) and SMAC09556 (hypothetical protein with caspase domain, cysteine-dependent aspartate-directed protease that mediates programmed cell death [apoptosis], 1x).

Another interesting finding of the Y2H screen was, that out of 56 putatively interacting proteins 25 proteins are enzymes, meaning that synthases, phosphatases, kinases, transferases, dehydrogenases and other degrading proteins were found (SMACs highlighted in italics, Tab. 4). Regarding the results of the GFP-Trap experiments these observations were confirmed. Here, 10 out of 19 identified interaction partners are enzymes, too (SMACs highlighted in italics, Tab. 5). Combining the results of the Y2H and GFP-Trap analysis, 32 out of 70 identified interactions were with enzymes.

In addition, Y2H and GFP-Trap analysis identified interactions with conserved autophagy proteins SmATG3 and SmATG7 (SMAC05399 and SMAC06539), confirming the interactions as described in *S. cerevisiae*. SmNBR1 was identified as further interesting interaction partner and is similar to the cargo receptor for selective autophagy in mammals and was identified as LC3 (mammalian Atg8) interaction partner. The proteins with the highest sequence coverage found in the GFP-Trap screen were SmATG3 (SMAC05399, 57.8%), SmATG7 (SMAC06539, 40.5%), SmNBR1 (SMAC0744, 37.3%), SmATG8 (SMAC02305, 34.7%) and SMAC07765 (ATP-dependent Zn protease, 29.4%), respectively. Interestingly, interaction of SmATG8 with SmATG4 could not be confirmed in both screens, even though a direct Y2H interaction experiment verified their interaction. On the other hand interaction with SmATG3 and SmATG7 could be shown, indicating an interaction pattern of SmATG8 similar to that of *S. cerevisiae*.

SmATG8 interacts with SmATG3 as well as SmATG7 and with 32 different enzymes.

Table 4. SmATG8 interaction partner identified by Y2H.

No.	No. of hits	SMAC	NCU	e-value*	S.c.	e-value**	name/function	reference
1	16	*SMAC00918*	NCU08298	0.0	YMR008C	$1.90e^{-11}$	phospholipase B (S.c.)	LEE *et al.* (1994)
2	7	SMAC01312	NCU00627	0.0	--	--	predicted Woronin body protein (N.c.)	MANAGADZE *et al.* (2010)
3	6	SMAC09075	NCU02164	0.0	--	--	conserved protein (N.c.)	--
4	6	***SMAC02442***	NCU01754	0.0	YMR083W	$1.60e^{-112}$	alcohol dehydrogenase I (N.c.)	BAKKER *et al.* (2000)
5	5	SMAC07505	NCU05900	$3.55055e^{-10}$	--	--	conserved protein (N.c.)	--
6	4	*SMAC04326*	NCU02668	0.0	--	--	cell wall synthesis protein (*P. chrysogenum*)	VAN DEN BERG *et al.* (2008)
7	4	SMAC00851	NCU07701	$5.63316e^{-25}$	YKR051W	$1.10e^{-54}$	transmembrane protein 184B (H. s.)	MATSUDA *et al.* (2003)
8	4	SMAC01818	NCU07978	$2.18509e^{-21}$	--	--	conserved protein (N.c.)	--
9	4	*SMAC02037*	NCU05680	0.0	YNL029C	$5.30e^{-99}$	α-1,2-mannosyltransferase Kre5 (N.c.)	SANCAR *et al.* (2011)
10	3	*SMAC08406*	NCU04885	$4.82277e^{-16}$	YBR229C	$2.50e^{-19}$	α-xylosidase (N.c.)	GALAGAN *et al.* (2003)
11	3	*SMAC08632*	NCU09301	0.0	YLR189C	$1.10e^{-199}$	UDP-glucose sterol glucosyltransferase (Atg26) (S.c.)	KLIONSKY *et al.* (2003)

No.	No. of hits	SMAC	NCU	e-value*	S.c.	e-value**	name/function	reference
12	3	SMAC00653	NCU04070	1.85476e^{-18}	--	--	conserved protein (N.c.)	--
13	3	*SMAC00308*	NCU10658	0.0	--	--	SGNH hydrolase (*N. tetrasperma*)	ELLISON *et al.* (2011)
14	3	***SMAC07897***	NCU05160	1.1e^{-44}	YLL034C	5.20e^{-18}	ATP-dependent Zn protease (N.c.)	GALAGAN *et al.* (2003)
15	2	*SMAC00875*	NCU07678	0.0	--	--	molybdenum cofactor sulfurase (*H.s.*)	ICHIDA *et al.* (2001)
16	2	SMAC06421	NCU06095	0.0	--	--	grainy-head homologue (CP2 transcription factor) (N.c.)	SMITH *et al.* (2010)
17	2	*SMAC05782*	NCU02580	1.56e^{-22}	YEL047C	3.80e^{-79}	fumarate reductase Osm1 (peroxisomal/glyoxysomal protein with PTS2 sequence) (N.c.)	MANAGADZE *et al.* (2010)
18	2	**SMAC05399**	NCU01955	0.0	YNR007C	8.70e^{-56}	ATG3/E2-like enzyme (N.c.)	VIDEIRA *et al.* (2009)
19	2	*SMAC00703*	NCU05490	2.94e^{-31}	YMR269W	0.0099	conserved protein (nicotinate-nucleotide-dimethylbenzimidazole phosphoribosyltransferase domain)*** (N.c.)	--
20	2	**SMAC02305**	NCU01545	8.4e^{-44}	YBL078C	9.80e-^{49}	ATG8/ubiquitin like protein (N.c.)	FU *et al.* (2011)
21	2	SMAC07851	NCU04276	2.69e^{-14}	--	--	conserved protein (N.c.)	--
22	2	*SMAC02523*	NCU03646	0.0	YOR008C	1.60e^{-05}	β-1, 3 exoglucanase (plant peroxidase like and WSC domains)*** (N.c.)	MADDI and FREE (2010)
23	2	*SMAC01351*	NCU00673	0.0	YEL060C	5.30e^{-105}	serine protease p2 (N.c.)	GREENWALD *et al.* (2010)

No.	No. of hits	SMAC	NCU	e-value*	S.c.	e-value**	name/function	reference
24	2	SMAC01783	NCU04360	0.0	--	--	conserved protein (N.c.)	--
25	1	***SMAC07765***	NCU07100	0.0	--	--	peptidase M20 domain-containing protein 2 (*H. s.*)	OTA *et al.* (2004)
26	1	*SMAC02434*	NCU01747	$3.08e^{-36}$	YPL110C	$3.20e^{-147}$	glycerophosphocholine phosphodiesterase Gde1 (N.c.)	GALAGAN *et al.* (2003)
27	1	SMAC00355	NCU07407	$6.67e^{-29}$	YHR120W	$2.7e^{-118}$	MutS2 protein (N.c.)	SMITH *et al.* (2010)
28	1	*SMAC08709*	NCU11963	$1.51e^{-30}$	YMR226C	$4.100e^{-18}$	short chain dehydrogenase (N.c.)	CORADETTI *et al.* (2012)
29	1	SMAC02139	NCU07864	0.0	YKL021C	$1.00e^{-09}$	60S ribosome biogenesis protein Mak11 (N.c.)	VIDEIRA *et al.* (2009)
30	1	*SMAC06499*	NCU00317	$4.03e^{-13}$	YMR154C	$3.80e^{-12}$	calpain-like protease palB/rim-13 (N.c.)	SUN *et al.* (2011)
31	1	SMAC07459	NCU06932	0.0	YML088W	--	F-box domain-containing protein (N.c.)	GALAGAN *et al.* (2003)
32	1	*SMAC06595*	NCU09533	0.0	--	--	NAD binding Rossmann fold oxidoreductase (N.c.)	SUN *et al.* (2012)
33	1	SMAC02166	NCU06405	0.0	YER159C	$6.50e^{-20}$	DNA polymerase epsilon subunit C (N.c.)	KASUGA and GLASS (2008)
34	1	SMAC04254	NCU02759	0.0	YNL097W-A	--	hypothetical protein (N.c.)	--
35	1	SMAC09150	NCU07769	$2.76e^{-16}$	YDL037C	0.0035	conserved protein (N.c.)	--
36	1	*SMAC03784*	NCU08048	0.0	--	--	L-2-hydroxyglutarate dehydrogenase, mitochondrial precursor (*H. sapiens*)	RZEM *et al.* (2004)

No.	No. of hits	SMAC	NCU	e-value*	S.c.	e-value**	name/function	reference
37	1	*SMAC09556*	NCU10001	$5.26e^{-39}$	--	--	hypothetical protein (caspase domain cysteine-dependent aspartate-directed proteases that mediate programmed cell death [apoptosis])*** (N.c.)	--
38	1	SMAC01108	NCU04493	$2.83e^{-32}$	--	--	extracellular serine rich GPI-anchored membrane protein (*A. fumigatus*)	NIERMAN *et al.* (2005)
39	1	SMAC06634	NCU06701	$1.68e^{-16}$	YLR176C	$6.70e^{-27}$	cephalosporin C regulator 1 (N.c.)	GALAGAN *et al.* (2003)
40	1	SMAC02013	NCU07542	0.0	YEL037C	$3.00e^{-22}$	rad23-like (XPC-binding and UBA domains)*** (N.c.)	MAERZ *et al.* (2010)
41	1	SMAC01676	NCU05314	$9.44e^{-36}$	YBR062C	0.00011	conserved protein (N.c.)	--
42	1	SMAC07137	NCU04025	$8.22e^{-24}$	--	--	hypothetical protein (N.c.)	--
43	1	SMAC01011	NCU06337	$8.11e^{-11}$	--	--	conserved protein (N.c.)	
44	1	*SMAC02626*	NCU03779	0.0	YML070W	$1.80e^{-94}$	dihydroxyacetone kinase-1 (N.c.)	NOGUCHI *et al.* (2007)
45	1	*SMAC08112*	NCU08703	$7.12e^{-4}$	YBR011C	$4.20e^{-57}$	inorganic pyrophosphatase (N.c.)	GALAGAN *et al.* (2003)
46	1	*SMAC02592*	NCU03741	0.0	YJR049C	$2.20e^{-83}$	NAD kinase/ATP NAD kinase (N.c.)	SMITH *et al.* (2010)
47	1	SMAC01640	NCU11506	$3.70e^{-20}$	YDL058W	--	conserved protein (dynamitin domain)*** (N.c.)	--

No.	No. of hits	SMAC	NCU	e-value*	S.c.	e-value**	name/function	reference
48	1	SMAC07526	NCU04628	0.0	YOR113W	$6.40e^{-05}$	zinc-finger transcription factor (zinc finger, C2H2 type)*** (S.c.)	STEIN *et al.* (1998)
49	1	SMAC00445	NCU09772	$1.36e^{-21}$	--	--	conserved protein (HET domain)*** (N.c.)	--
50	1	SMAC01818	NCU07976	$2.32e^{-10}$	--	--	conserved protein (N.c.)	--
51	1	SMAC06954	NCU05922	$1.44e^{-34}$	--	--	conserved protein (arrestin_N domain)*** (N.c.)	--
52	1	*SMAC00229*	NCU00951	$1.96e^{-18}$	YBR011C	$2.70e^{-110}$	inorganic pyrophosphatase (N.c.)	SEILER and PLAMANN (2003)
53	1	*SMAC00669*	NCU04089	$1.52e^{-38}$	YHR007C	0.00057	pisatin demethylase (CypX and P450 domains)*** (N.c.)	TIAN *et al.* (2009)
54	1	SMAC01892	NCU00457	$5.73e^{-5}$	YPR163C	$3.40e^{-15}$	translation initiation factor 4B (RRM and dnaA domains)*** (N.c.)	WANG *et al.* (2012)
55	1	SMAC08319	NCU02431	$1.05e^{-21}$	YNR013C	0.0042	RING-14 protein (SPX domain)*** (N.c.)	LEWIS *et al.* (2002)
56	1	SMAC05109	NCU08905	--	--	--	conserved protein (N.c.)	--

Order of interaction partners according to number of hits; highlighted in light grey, proteins with LIR motif; *, e-value determined by BLASTP of *S. macrospora* protein sequence in the *N. crassa* database; ** e-value determined by BLASTP of *S. macrospora* protein sequence in the *S. cerevisiae* genome database (SGD); *** domain determination by BLASTP of *S .macrospora* protein sequence in the NCBI database; highlighted in bold, hits found in Y2H and GFP-Trap screens; highlighted by underlining, hits found in SmATG8 and SmATG7 Y2H screens; highlighted in italics, enzymes; S.c., *S .cerevisiae*; N.c., *N. crassa*; H.s., *H. sapiens*.

Table 5. SmATG8 interaction partners identified by GFP-Trap.

SMAC	Protein Name (homologue)	Function	Mw (kDa)	No. of unique peptides	No. of experiments	Best Seq. coverage (%)	Best XCorr	Best P value
SMAC05399	ATG3 (N.c.)	E2-like enzyme	38.3	40	6	57.80	200.29	$1.11e^{-15}$
SMAC02305	ATG8 (N.c.)	ubiquitin-like protein	14.1	5	6	34.70	48.22	$3.33e^{-14}$
SMAC06539	SmATG7 (S.m.)	E1-like enzyme	78.3	24	4	40.50	206.27	$2.81e^{-13}$
SMAC07844	NBR1 (H.s.)	neighbor of BRCA1 gene 1	95.6	25	2	37.30	268.21	$8.77e^{-11}$
SMAC02605	aromatic amino-acid aminotransferase 1 (N.c.)	aromatic amino-acid aminotransferase 1	76.7	14	2	27.60	130.21	$1.38e^{-10}$
SMAC07897	ATP-dependent Zn protease (N.c.)	ATP-dependent Zn protease	55.2	13	2	29.40	110.20	$2.27e^{-12}$
SMAC07765	peptidase M20 domain-containing protein 2 (*H s.*)	peptidase M20 domain-containing protein 2	48.7	9	2	20.20	90.19	$5.68e^{-08}$
SMAC02442*	alcohol dehydrogenase I (N.c.)	alcohol dehydrogenase I	37.7	6	2	23.16	40.11	$1.50e^{-09}$
SMAC06980	β-galactosidase (N.c.)	β-galactosidase	116.5	8	1	10.40	74.15	$2.72e^{-10}$
SMAC02851	MSP1 (S.c.)	mitochondrial protein involved in sorting of proteins in the mitochondria	99.6	8	1	14.50	80.19	$1.42e^{-08}$

SMAC	Protein Name (homologue)	Function	Mw (kDa)	No. of unique peptides	No. of experiments	Best Seq. coverage (%)	Best XCorr	Best P value
SMAC00261*	von Willebrand domain-containing protein (N.c.)	von Willebrand domain-containing protein	99.4	4	1	4.60	38.16	$8.33e^{-07}$
*SMAC09126**	glycogen phosphorylase (N.c.)	glycogen phosphorylase	100.7	15	1	24.90	150.19	$6.17e^{-12}$
*SMAC06591**	alanine-glyoxylate aminotransferase 2-like 2 (H.s.)	alanine-glyoxylate aminotransferase 2-like 2	81.7	8	1	13.10	78.17	$2.60e^{-06}$
*SMAC05967**	pyruvate carboxylase (N.c.)	pyruvate carboxylase	126.0	3	1	4.25	26.12	$2.34e^{-07}$
SMAC04972**	heat shock protein 70 (N.c.)	heat shock protein 70	68.6	3	1	9.16	30.17	$5.49e^{-12}$
*SMAC06666***	calpain-3 isoform c (H.s.)	calpain-3 isoform c	115.6	6	1	9.30	60.18	$1.78e^{-06}$
SMAC05066**	sodium channel protein type 10 subunit alpha (H.s.)	sodium channel protein type 10 subunit alpha	37.3	2	1	5.50	20.13	$1.02e^{-04}$
*SMAC00353***	alpha-mannosidase (N.c)	alpha-mannosidase	124.4	9	1	9.40	88.24	$1.29e^{-08}$
SMAC00256**	60S acidic ribosomal protein P2 (N.c.)	60S acidic ribosomal protein P2	11.1	1	1	27.03	10.24	$5.25e^{-07}$

Order of interaction partners according to number of experiments; highlighted in light grey, proteins with LIR motif; highlighted in bold, hits found in Y2H and GFP-Trap screens; highlighted in italics, enzymes;*, hits found solely in ΔSmatg8::egfp-Smatg8^{ect}; **, hits found solely in ΔSmatg4::egfp-Smatg8^{ect}; N.c., *N. crassa*; S.m., *S. macrospora*; H.s., *H. sapiens*.

Table 6. SmATG7 interaction partner identified by Y2H.

No.	No. of hits	SMAC	NCU	e-value*	S.c.	e-value**	function	reference
1	19	SMAC02305	NCU01545	0.0	YBL078C	$9.80e^{-49}$	ATG8/ubiquitin like (N.c.)	FU *et al.* (2011)
2	5	SMAC06421	NCU06095	0.0	--	--	grainy-head homologue (CP2 transcription factor) (N.c.)	SMITH *et al.* (2010)
3	4	SMAC08700	NCU09355	$3.81e^{-5}$	--	--	nitrogen starvation-induced glutamine rich protein (*Colletotrichum gloeosporioides*)	STEPHENSON *et al.* (2005)
4	3	SMAC06998	NCU10049	0.0	YBR217W	$8.20e^{-13}$	ATG12/ubiquitin like (N.c.)	SUN *et al.* (2012)
5	1	SMAC06954	NCU05922	$1.21e^{-34}$	--	--	conserved protein (Arrestin_N domain)*** (N.c.)	--

Order of interaction partners according to number of hits; *, e-value determined by BLASTP of *S. macrospora* protein sequence in the *N. crassa* database; ** e-value determined by BLASTP of *S. macrospora* protein sequence in the *S. cerevisiae* genome database (SGD); *** domain determination by BLASTP of *S. macrospora* protein sequence in the NCBI database; highlighted by underlining, hits found in SmATG8 and SmATG7 Y2H screens; N.c., *N. crassa*; S.m., *S. macrospora*; H.s., *H. sapiens*.

3.2.5 In a Y2H screen SmATG7 interacts with SmATG8 and SmATG12. Interaction partners of SmATG7 were identified by a Y2H screen with a *S. macrospora* cDNA library. The bait plasmid pBD-Smatg7 was tested and affirmed to have no transactivation activity (personal communication, N. Nolting).

Overall 5 interactions were confirmed, of which 3 were also found in the SmATG8 Y2H screen also and are highlighted by underlining in Tab. 6. These include interactions with SmATG8 (SMAC02305, 19x), SMAC06421 (grainy-head homologue, 5x) and SMAC06954 (conserved protein with arrestin-N domain, 1x) as displayed in Fig. 18. The other identified interactions were with SMAC08700 (nitrogen starvation-induced glutamine rich protein, 4x) and SmATG12 (SMAC06998, 3x).

The Y2H screen confirmed the interaction of SmATG7 with SmATG8 and SmATG12 as described in *S. cerevisiae*.

3.2.6 Generation of *S. macrospora Smatg8* and *Smatg4* deletion and complementation strains. As aforementioned for *Smvps34* and *Smvps15,* deletion of the autophagy genes *Smatg8* and *Smatg4* were generated to elucidate the impact of autophagy on fruiting-body development.

After the construction of pRS-ΔSmatg8 and of pRS-ΔSmatg4 plasmids, deletion cassettes were amplified and transformed into the *S. macrospora* Δku70 strain resulting in 6 heterokaryotic ΔSmatg8/Smatg8 and 3 heterokaryotic ΔSmatg4/Smatg4 primary transformants. In ΔSmatg8/Smatg8, *Smatg8* was deleted from base 4-503 out of 503 bp and in ΔSmatg4/Smatg4 bases 1–1321 out of 1789 bp were deleted also (Fig. 19A and B). Both genes were deleted by replacement with a *hph* gene which mediates resistance to hygromycin. Deletions in both heterokaryotic strains were verified by PCR (data not shown).

Heterokaryotic ΔSmatg8 and ΔSmatg4 primary transformants were crossed with a fus1-1 strain to obtain single spore isolates without the Δku70 and the *Smatg8* and *Smatg4* wt background. For each deletion strain two single spore isolates were obtained and the integration of the *hph* gene at the desired locus and presence of the Δku70 wt genes were verified using primer combinations as displayed in Fig. 19.

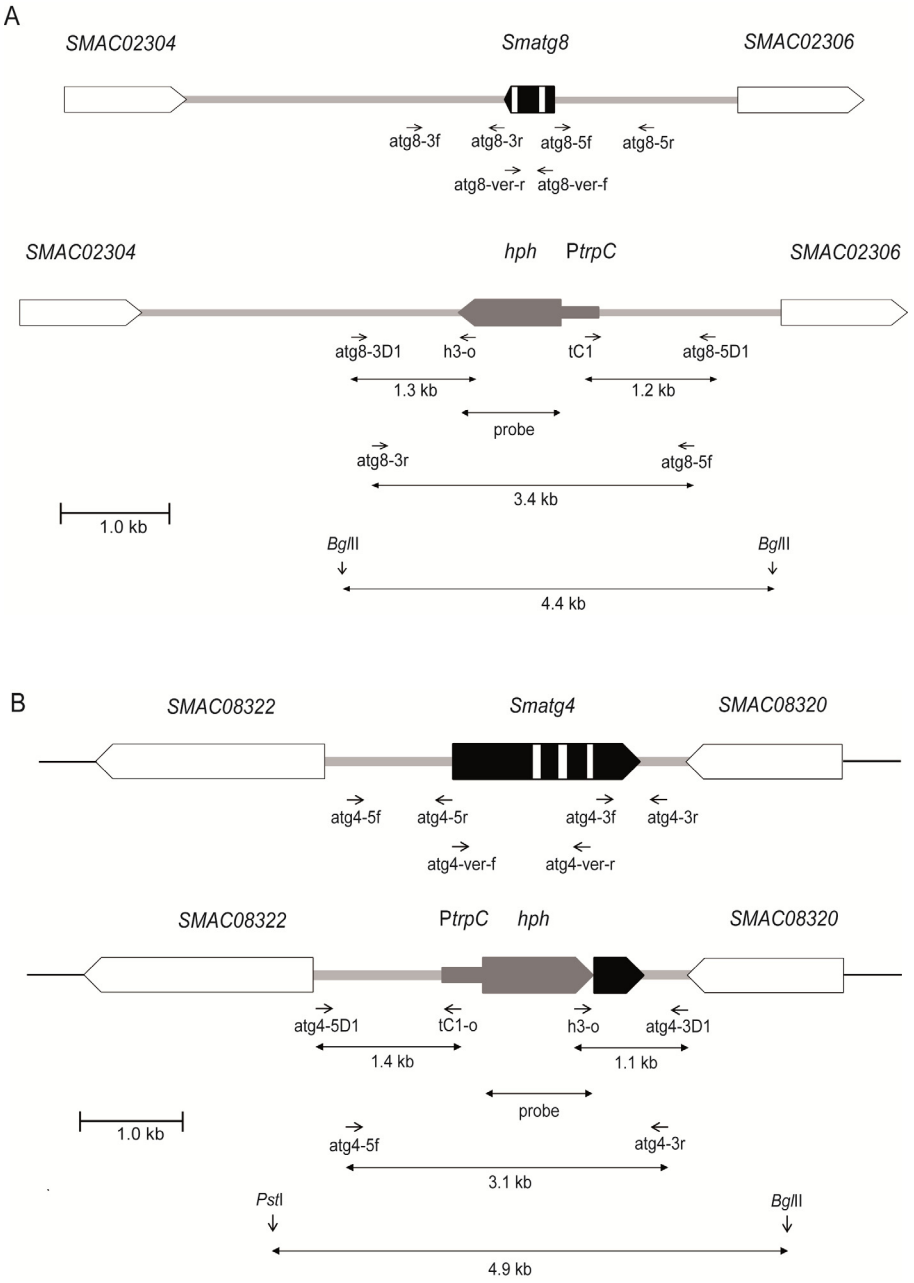

Figure 19. Generation and complementation of a ΔSmatg8 and ΔSmatg4 strain, respectively. (A) and (B) Schematic illustration of the *Smatg8* or *Smatg4* locus before and after homologous integration of the deletion cassette. Primer position used for the verification of the deletion and complementation of *Smatg8* or *Smatg4*, respectively, are indicated by small arrows. Sizes of PCR fragments for deletion/complementation verification and deletions cassette amplification are indicated. Fragments obtained after restriction enzyme cleavage are given also. Position and size of the probe used for Southern hybridization is indicated. White frames, adjacent genes; black frame, target gene; grey frame, *hph* gene for hygromycin resistance; grey line, *trpC* promoter of *A. nidulans*; white rectangles, introns; light grey lines, intergenic regions.

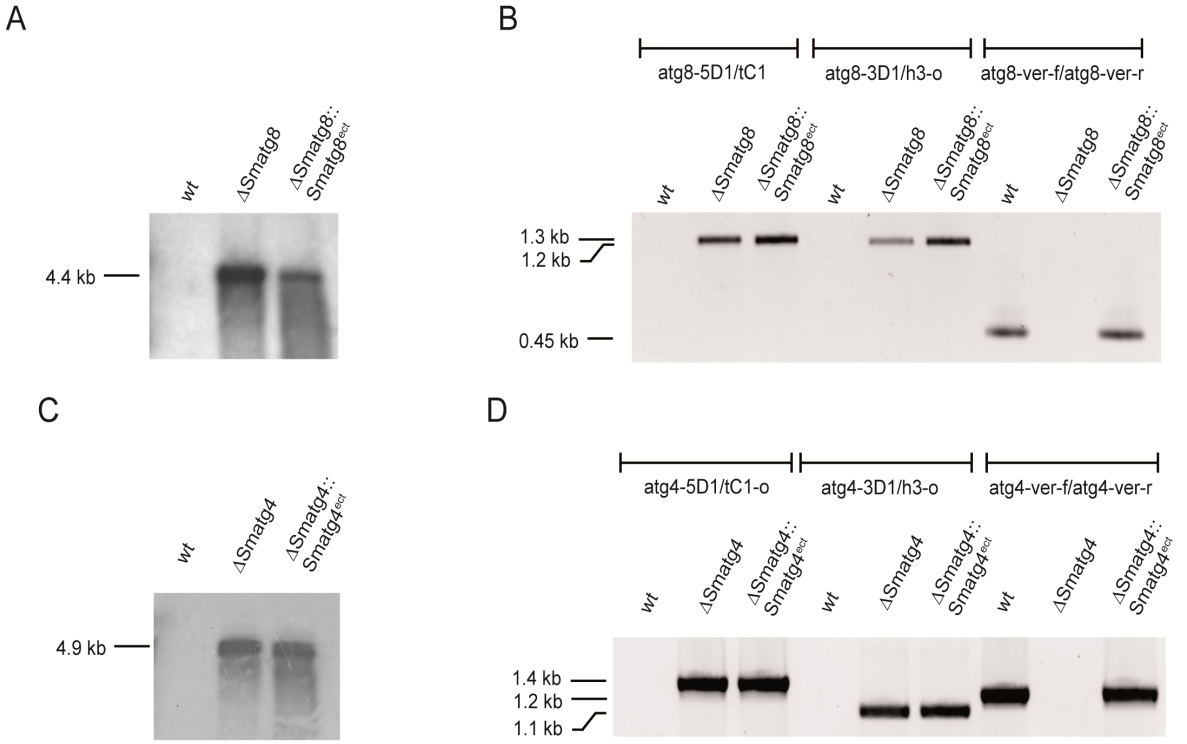

Figure 20. Deletion and complementation verification of ΔSmatg8 and ΔSmatg4, respectively. (A) Southern hybridization demonstrates the successful integration of the deletion cassette using a *hph* gene specific probe. The gDNA of wt, ΔSmatg8 and the complementation strain ΔSmatg8::Smatg8 was digested with *Bgl*II and hybridized with the *hph* gene specific probe. An expected signal of 4400 bp was detected in the deletion and the complemented strain. (B and D) Deletion and complementation was confirmed by PCR. Fragment sizes according to primer pairs appeared as expected and are displayed in Fig. 19. (C) Southern hybridization with *hph* probe to verify single copy integration of *Smatg4* deletion cassette. The gDNA of wt, ΔSmatg4 and the complemented strain ΔSmatg4::Smatg4 was digested with *Pst*I and *Bgl*II and hybridized with the *hph*-gene specific probe. An expected signal of 4900 bp was detected in the deletion and the complemented strain.

Construction of the complementation plasmids pRS-Smatg8-comp and pRS-Smatg4-comp was achieved with the 5f/3r primer pairs which were already used for the generation of the deletion cassettes (Fig. 19). After ectopic integration, two heterokaryotic *Smatg8* perithecia producing complementation strains were obtained of which 10 single spore isolates were derived. Six heterokaryotic fertile *Smatg4* complementation strains resulting in 11 single spore isolates were obtained also. The presence of the deletion cassettes and wt genes in the respective complementation strains was verified by PCR and the integration of the deletion

cassettes at the desired locus in the *S. macrospora* genome of the *Smatg8* and *Smatg4* deletion and complementation strains was additionally verified via Southern hybridization (Fig. 20A-D).

For each, *Smatg8* and *Smatg4*, deletion and complementation strains were generated.

3.2.7 *Smatg8* and *Smatg4* deletion strains are sterile and impaired in vegetative growth and ascospore germination. In order to analyze the effect of *Smatg8* and *Smatg4* on the viability and sexual reproduction of *S. macrospora*, ΔSmatg8 and ΔSmatg4 strains were generated for phenotypic characterization.

Microscopic analysis of the knockout strains revealed that both strains are blocked during fruiting-body development. Although, they were able to form the first stages of sexual development (ascogonia and protoperithecia), they failed to produce mature fruiting bodies (perithecia) or ascospores. Complementation by inserting an ectopic copy of *Smatg8* and *Smatg4* into the ΔSmatg8 and ΔSmatg4 mutant, respectively, fully restored the wt phenotype (Fig. 21A).

The term "foraging" is used here to describe the growth of a filamentous fungus over a non-nutritious surface to reach nutrient-rich regions. For this type of growth, the required nutrients are thought to be provided by basal hyphae (SHOJI and CRAVEN 2011). To assess the foraging capability of the deletion, wt and the complemented strain, agar plugs were transferred into an empty petri dish and incubated for 5 days. While the wt and the complemented strains displayed extensive mycelial growth, ΔSmatg8 and ΔSmatg4 knockout strains were unable to grow on an inert plastic surface (Fig. 21B). In addition to this phenotype, both mutants showed a significant decrease in vegetative growth velocity [1.9 (± 0.46) and 2.0 (± 0.29) cm/d compared to 3.1 (± 0.36) cm/d of the wt strain]. The vegetative growth defect was partially rescued in the complemented strains (Fig. 22). When histidine starvation was imposed by 3-AT (3-amino-1,2,4-triazole, histidine starvation), reduction of the growth velocity was more severe in the mutant strain than in the wt (Fig. 22).

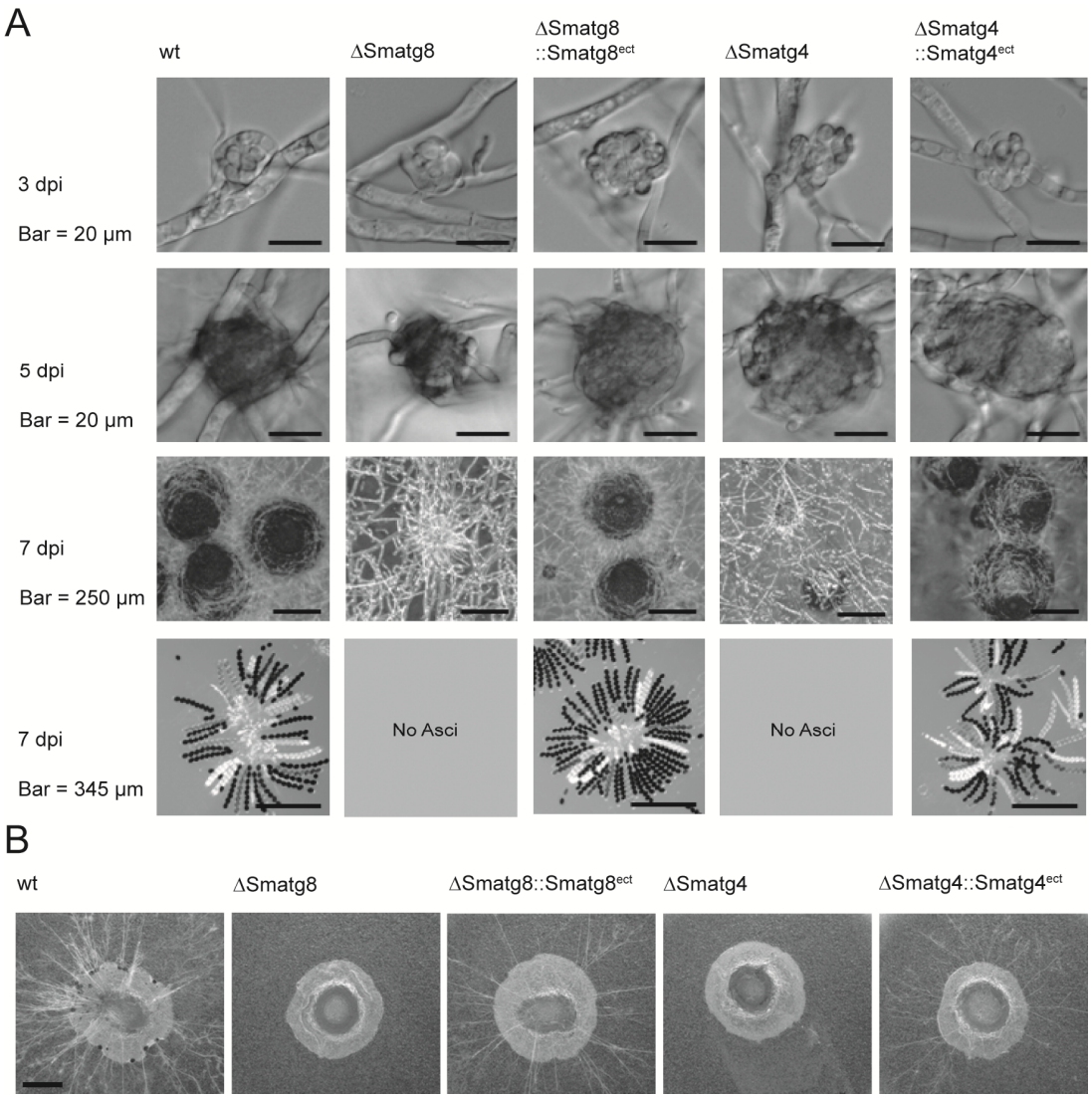

Figure 21. **Phenotypic analysis of *Smatg8* and *Smatg4* deletion and complementation strains.** (A) Microscopic investigation of sexual development in ΔSmatg8 and ΔSmatg4 compared to wt. Wt strains form ascogonia at day 3 which develop into protoperithecia at day 5 and mature perithecia after 7 days. Ascus rosettes are visible when cracking the perithecia. ΔSmatg8 and ΔSmatg4 generate only ascogonia and protoperithecia. Ectopically integrated copies of the *Smatg8* and *Smatg4* complement the mutant phenotype. (B) Deletion strains are unable to undergo foraging but wt and complemented strains exhibit the ability to grow on an inert plastic surface. Agar plugs of 5 mm diameter were transferred into empty petri dishes and incubated for 5 days in a damp chamber. Bar = 2 mm.

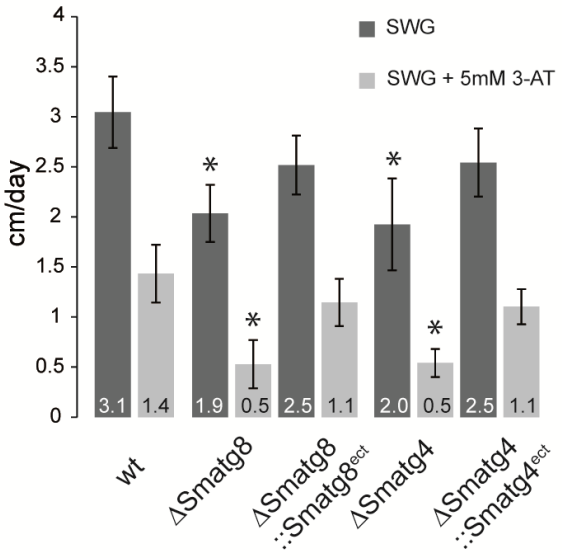

Figure 22. Growth velocity of deletion strains and complemented strains. In comparison to the wt the vegetative growth velocity of ΔSmatg8 and ΔSmatg4 is reduced by 39% and 36%, respectively. On medium containing 5 mM 3-AT this effect is increased. Growth-rate analysis was conducted in 30 cm race tubes. Growth rates shown are averages from nine independent measurements of three independent experiments (N=27), standard deviations are indicated by error bars. Values of the deletion mutants with asterisk differ significantly from wt and the complemented mutant according to Student's t-test (P<0.0000001).

Further investigation on hyphal fusion was conducted by crossing of two sterile strains. When two sterile strains are used in a cross, complementation of genetic defects results in the formation of fertile perithecia solely in the contact zone of two mutant mycelia, all of which are hybrid perithecia. Hyphal fusion events were examined in ΔSmatg8 and ΔSmatg4 mutants, also. Especially with regard to the *Smatg8* deletion, the question arises if this mutant is affected in hyphal fusion, since it was reported that a *N. crassa atg8* deletion strain exhibited defects in hyphal fusion (FU *et al.* 2011). Observation for intracolonial hyphal cell fusion events was analyzed microscopically. Affirmed by cytoplasmic flow at hyphal contact sites, ΔSmatg8 and ΔSmatg4 displayed neither defects in hyphal fusion nor in the number of hyphal fusion events when compared to wt (Fig. 23A).

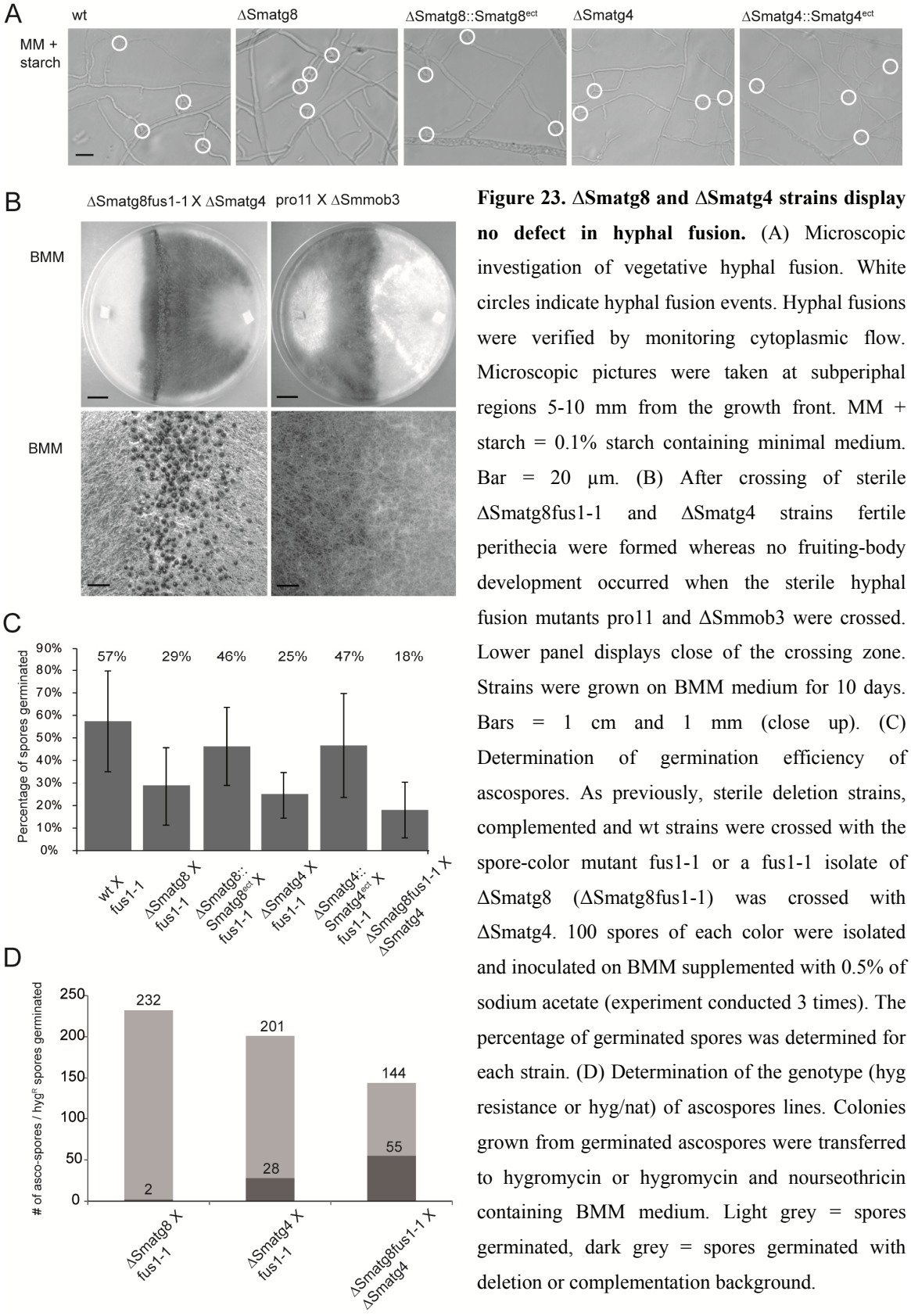

Figure 23. ΔSmatg8 and ΔSmatg4 strains display no defect in hyphal fusion. (A) Microscopic investigation of vegetative hyphal fusion. White circles indicate hyphal fusion events. Hyphal fusions were verified by monitoring cytoplasmic flow. Microscopic pictures were taken at subperiphal regions 5-10 mm from the growth front. MM + starch = 0.1% starch containing minimal medium. Bar = 20 µm. (B) After crossing of sterile ΔSmatg8fus1-1 and ΔSmatg4 strains fertile perithecia were formed whereas no fruiting-body development occurred when the sterile hyphal fusion mutants pro11 and ΔSmmob3 were crossed. Lower panel displays close of the crossing zone. Strains were grown on BMM medium for 10 days. Bars = 1 cm and 1 mm (close up). (C) Determination of germination efficiency of ascospores. As previously, sterile deletion strains, complemented and wt strains were crossed with the spore-color mutant fus1-1 or a fus1-1 isolate of ΔSmatg8 (ΔSmatg8fus1-1) was crossed with ΔSmatg4. 100 spores of each color were isolated and inoculated on BMM supplemented with 0.5% of sodium acetate (experiment conducted 3 times). The percentage of germinated spores was determined for each strain. (D) Determination of the genotype (hyg resistance or hyg/nat) of ascospores lines. Colonies grown from germinated ascospores were transferred to hygromycin or hygromycin and nourseothricin containing BMM medium. Light grey = spores germinated, dark grey = spores germinated with deletion or complementation background.

Hyphal fusion was also examined in ΔSmatg8 and ΔSmatg4 by crossing of these two sterile mutants. As depicted in Fig. 23B, both strains are capable of complementation of their genetic defects and form hybrid perithecia at the hyphal contact zone. Pro11 and ΔSmmob3 (both defective in hyphal fusion) served as a control and did not produce any hybrid perithecia (BERNHARDS and PÖGGELER 2011; BLOEMENDAL *et al.* 2012)

Furthermore, the role of SmATG8 and SmATG4 during ascospore germination was investigated and was conducted as described previously for ΔSmvps34 and ΔSmvps15. In comparison to wt, the germination efficiency of ΔSmatg8 and ΔSmatg4 decreased by about 50% when both mutants were crossed against the fertile fus1-1 mutant (Fig. 23C). The ascospore germination rate dropped even more when the two mutant strains were crossed against each other. To determine the percentage of germinated ascospores carrying the ΔSmatg8 and ΔSmatg4 deletion background, the mycelia of the spore isolates were transferred to BMM medium containing hygromycin. In the case of ΔSmatg8 X fus1-1, only 2 of the 232 ascospore isolates were hygromycin resistant and contained the ΔSmatg8 background, whereas in the ΔSmatg4 X fus1-1 cross, 28 of 201 spores displayed the ΔSmatg4 genotype. Crossing of ΔSmatg8fus1-1 X ΔSmatg4 resulted in 55 out of 144 hygromycin resistant ascospore isolates (Fig. 23D). Thus, the autophagy mutants of *S. macrospora* are capable of hyphal fusion but due to the impaired germination efficiency of the ascospores the majority of ascospore isolates carry the wt background.

In accordance to these experiments it is assumable that autophagy as a nutrient-providing process is necessary for fruiting-body development, foraging, vegetative growth and ascospore germination, but not for hyphal fusion.

3.2.8 EGFP-SmATG8 is processed by SmATG4. In *S. cerevisiae*, it was clearly demonstrated that the C-terminal arginine residue of Atg8 is removed by the cysteine protease Atg4 resulting in a processed Atg8 with a C-terminally exposed glycine residue (KIRISAKO *et al.* 2000). The alignment of SmATG8 with Atg8 homologues from *S. cerevisiae* and other fungi (Fig. 14) showed a high degree of amino-acid identity throughout the protein, except for the C-terminal amino acids after the G116 residue.

To verify that SmATG8 is cleaved by SmATG4, different versions of SmATG8 were labeled with EGFP. Figure 24 depicts characteristics of the different fusion protein versions generated in this study. In a processing scheme similar to *S. cerevisiae*, SmATG4 should cleave off the peptide DFETA at the C-terminus of SmATG8, exposing a glycine residue (Fig. 24A). The EGFP-SmATG8 fusion protein is processed in a similar manner and DFETA is cleaved off and an EGFP-SmATG8 protein with an exposed glycine remains (Fig. 24B). Cleavage of a SmATG8-EGFP fusion protein results in a glycine exposed SmATG8 and a DFETA-EGFP fusion protein (Fig. 24C). The EGFP-SmATG8^{G116} fusion protein is a version of EGFP-SmATG8 that is an already processed variant. Thus, cleavage mediated by SmATG4 is not necessary (Fig. 24D). Via PCR, the amino-acid sequence of SmATG8 was altered and F115, G116, D117 and F118 were substituted to alanine generating the SmATG8mut-EGFP fusion protein. Due to this alteration SmATG4 is supposed to be unable to process SmATG8 and SmATG8mut-EGFP remains uncleaved (Fig. 24E).

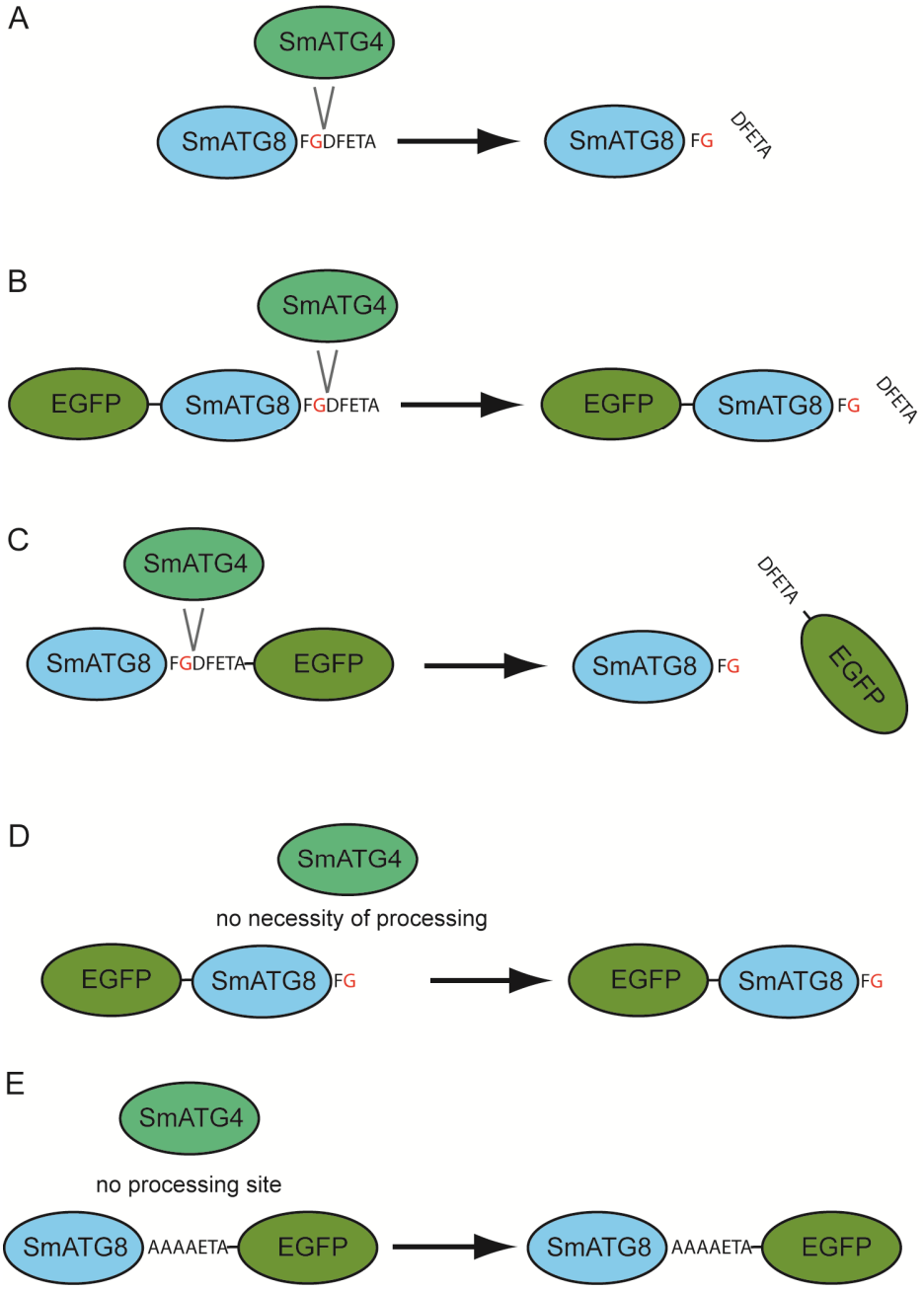

Figure 24. Processing scheme of different SmATG8-EGFP fusion proteins. A detailed description of the processing outcome is stated at chapter 3.2.8. (A) Theoretical scheme of SmATG8 processing by SmATG4. (B) Processing of N-terminal EGFP-SmATG8 fusion. (C) Processing of C-terminal SmATG8-EGFP fusion. (D) Processing of EGFP-SmATG8, expressed with an exposed glycine. (E) Processing of a SmATG8mut-EGFP fusion protein.

Protein extracts isolated from wt, ΔSmatg8 or ΔSmatg4 expressing the EGFP-tagged versions of SmATG8 were separated by sodium dodecyl sulfate-polyacrylamide gel electrophoresis (SDS-PAGE) and examined by western blot analysis using an anti-EGFP antibody. A wt strain expressing an ectopically integrated *egfp* gene and an untransformed wt were used as controls (Fig. 25).

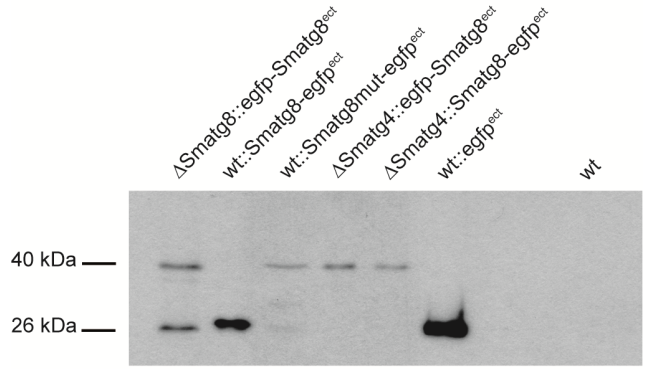

Figure 25. SmATG8 is C-terminally processed by SmATG4. Cleavage of EGFP-SmATG8 by SmATG4 was verified by western blotting using an anti-EGFP antibody. Protein crude extract of *S. macrospora* wt and mutant strains expressing EGFP, EGFP-SmATG8, SmATG8-EGFP or SmATG8mut-EGFP were separated on a 15% SDS-PAGE. The protein crude extract of the untransformed wt was used as a negative control. Cleaved or free EGFP is indicated by a 26 kDa band and fusion proteins of SmATG8 and EGFP are 40 kDa in size.

Signals of 40 kDa, representing the EGFP-SmATG8 fusion protein, and of the free kDa EGFP (26 kDa) were visible when proteins were extracted from ΔSmatg8::egfp-Smatg8^{ect}. In the wt expressing an ectopic *Smatg8-egfp* gene fusion (wt::Smatg8-egfp^{ect}) a signal that presumably represented the DFETA-EGFP apparently ran with retardation compared to free EGFP (Fig. 25). Only the unprocessed fusion protein was visible when a mutated version of SmATG8 was produced in the wt (wt::Smatg8mut-egfp^{ect}). In this construct, amino acids 115-118 (including G116) were exchanged for alanine. Similarly, only the 40 kDa signal was detected when N- or C-terminally EGFP-tagged versions of SmATG8 were produced in ΔSmatg4 (ΔSmatg4::egfp-Smatg8^{ect}, ΔSmatg4::Smatg8-egfp^{ect}).

Based on these results, it is assumable that SmATG4 is an essential protease for SmATG8 processing.

3.2.9 EGFP-SmATG8 localizes to autophagosomes and vacuoles, while SmATG4-EGFP is distributed within the cytoplasm. To analyze the cellular localization of SmATG8 and SmATG4 in *S. macrospora*, fluorescence microscopy was performed. Plasmids pRS-Smatg4-egfp and pRS-egfp-Smatg8 carrying *egfp* fusion genes under control of their endogenous promoters were transformed into the corresponding *S. macrospora* deletion mutant.

When compared to the wt, the obtained strains ΔSmatg8::egfp-Smatg8^{ect} and ΔSmatg4::Smatg4-egfp^{ect} showed no obvious differences in vegetative growth and sexual development, indicating that EGFP-SmATG8 and SmATG4-EGFP fusion proteins were functional (data not shown).

Fluorescence microscopy revealed that EGFP-SmATG8 was localized to punctate autophagosome-like structures in the cytoplasm and to the lumen of vacuoles, while SmATG4-EGFP was distributed diffusely within the cytoplasm (Fig. 26).

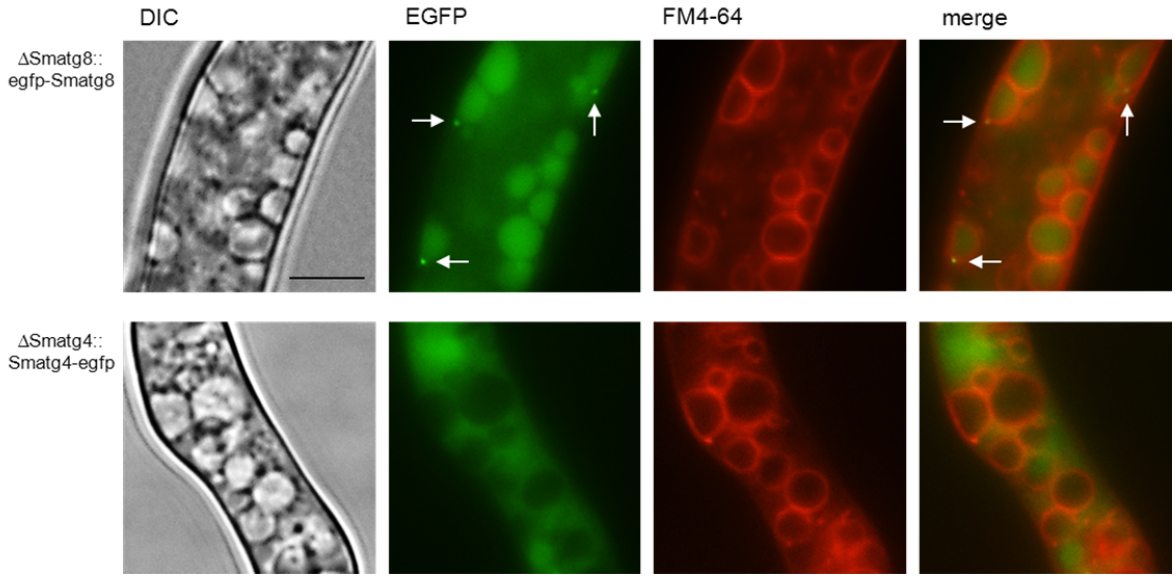

Figure 26. EGFP-SmATG8 localizes to autophagosomes and is degraded in vacuoles while SmATG4-EGFP is distributed in the cytoplasm. Fluorescence microscopic analysis of the *S. macrospora* ΔSmatg8 and ΔSmatg4 strain carrying plasmid pRS-egfp-Smatg8 and pRS-Smatg4-egfp, respectively. The upper panel shows that EGFP-SmATG8 localizes to autophagosomes and vacuoles. Autophagosomes are indicated by an arrow. SmATG4-EGFP expression in ΔSmatg4 leads to a diffuse cytoplasmic signal which is excluded from the vacuole. For the visualization of the vacuolar contours, vacuolar membranes were stained with FM4-64 as described in Materials and Methods. Strains were grown on SWG layered slides or on a cellophane layer on solid medium. Bar = 10 µm.

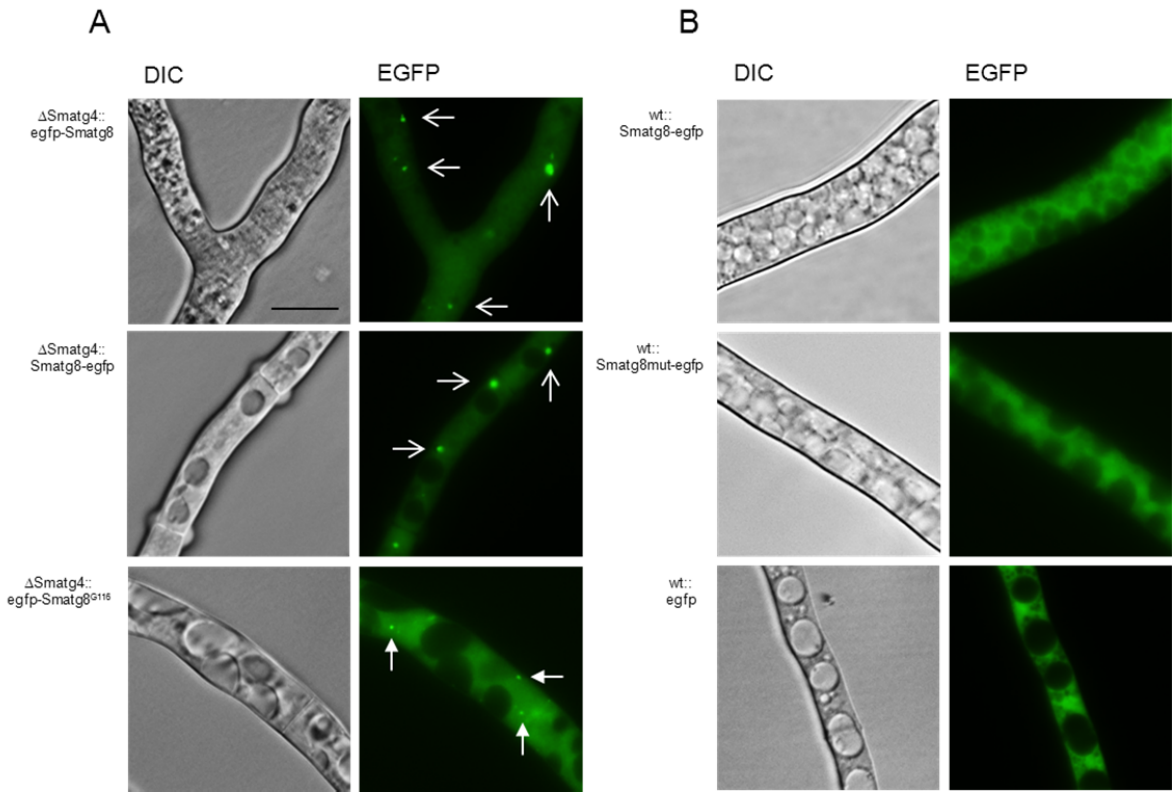

Figure 27. Localization of EGFP-tagged versions of SmATG8 in ΔSmatg4 and wt. (A) In the ΔSmatg4 mutant, EGFP-SmATG8 and SmATG8-EGFP localize to large aggregates (wide arrows) whereas a processed EGFP-SmATG8^{G116} version localizes to autophagosomes (narrow arrows). (B) In the wt, SmATG8-EGFP and its mutagenized version SmATG8mut-EGFP are mainly visible in the cytoplasm, similar to EGFP. Strains were grown on SWG layered slides or on a cellophane layer on solid medium. Bar = 10 µm.

In the mutant ΔSmatg4, EGFP-SmATG8 and the C-terminally tagged version SmATG8-EGFP were observed in large aggregates that were excluded from the vacuole. Thus, in both strains, an accumulation of EGFP was observed, but fluorescence of small autophagosomes and vacuoles was absent (Fig. 27A). In contrast, the C-terminally tagged SmATG8-EGFP in the wt seemed to be cleaved and displayed a similar distribution as the wt transformant expressing EGFP under control of the strong constitutive *gpd* promoter of *A. nidulans* (Fig. 27B). The same localization can be observed when the SmATG8-EGFP version with the mutated processing site is expressed in the wt (wt::Smatg8mut-egfp^{ect}) (Fig. 27B). To verify if a processed version of SmATG8 can complement the ΔSmatg4 mutant, a C-terminally truncated EGFP-SmATG8 version ending with G116 was constructed and the strain

ΔSmatg4::egfp-Smatg8^{G116ect} was generated (Fig. 27A). In this strain, the EGFP fluorescence localized to small autophagosome-like structures similar to those observed in ΔSmatg8::egfp-Smatg8^{ect} (Fig. 26). However, expression of the SmATG8^{G116} processed version did not complement sterility or the slow growth phenotype of ΔSmatg4 (data not shown). Thus recycling of SmATG8 by SmATG4 seems to be also important for vegetative growth and sexual development.

Taken together, these experiments indicate that SmATG4 is able to C-terminally process SmATG8 most probably by cutting the C-terminal motif DFETA, but it seems to be also required for SmATG8 recycling.

3.2.10 SmATG8 and SmATG4 are involved in pexophagy. Recently, it was demonstrated in *A. oryzae* that macroautophagy mediates degradation of nuclei, mitochondria and peroxisomes in basal cells of the mycelium to support the growth of tip cells (SHOJI *et al.* 2010).

In order to analyze the involvement of SmATG8 and SmATG4 in pexophagy, the plasmid pRS-egfp-Smatg8-DsRed-SKL was constructed encoding EGFP-SmATG8 together with DsRed fused to a C-terminal serine-lysine-leucine (SKL), the peroxisomal targeting sequence 1 (PTS1) signal for peroxisomal matrix import. Previously, it was demonstrated that in *S. macrospora*, expression of the *DsRed-SKL* fusion gene under the control of the *A. nidulans gpd* promoter led to protein import of DsRED into peroxisomes (ELLEUCHE and PÖGGELER 2008).

Plasmid pRS-egfp-Smatg8-DsRed-SKL was transformed into ΔSmatg8. DsRED and EFGP fluorescence was analyzed by fluorescence microscopy in the obtained strain ΔSmatg8::egfp-Smatg8-DsRed-SKL^{ect}. In the basal hyphae, EGFP signals were observed in the lumen of vacuoles, while the DsRED signal also localized to the lumen of vacuoles and to punctate peroxisomal structures (Fig. 28A, upper panel). The merged picture shows a yellow staining of the vacuolar lumen, indicating co-localization of DsRED and EGFP and the transport of these proteins into the vacuole. In the tip cells, EGFP-SmATG8 and DsRED-SKL localization differs from that in basal hyphae. The EGFP signal was mainly localized to autophagosomes and some small vacuoles, but excluded from larger vacuoles while DsRED signals displayed only punctate fluorescent patterns (Fig. 28A, lower panel). An overlay shows no co-

localization of EGFP and DsRED signals, indicating that pexophagy occurred in basal hyphae rather than in apical cells.

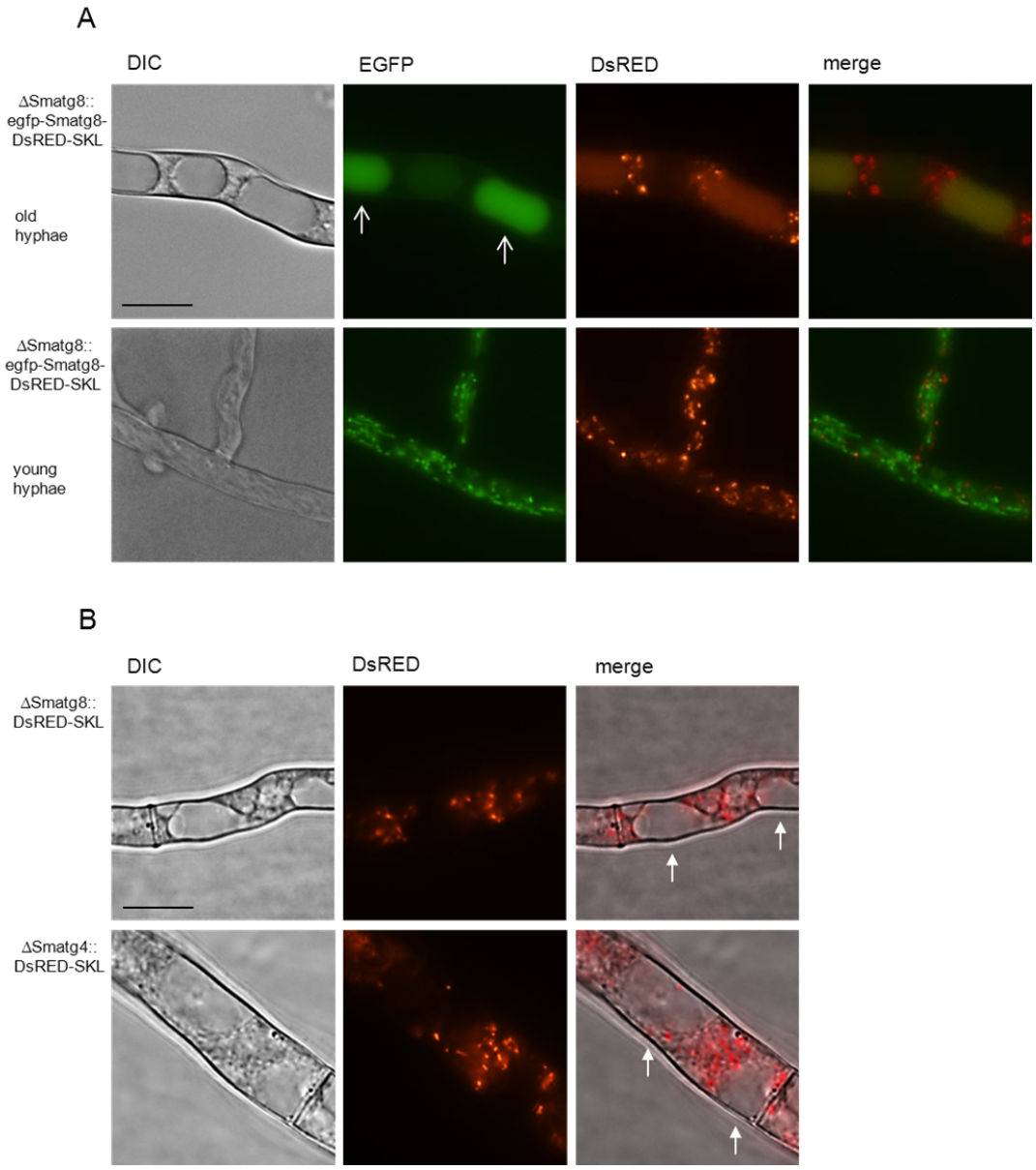

Figure 28. SmATG8 and SmATG4 are involved in pexophagy. (A) Localization of EGFP-SmATG8 and DsRED-SKL in basal hyphae (upper panel) and in apical hyphae (lower panel) of ΔSmatg8. Arrows indicate vacuoles. In basal hyphae DsRED-SKL and EGFP-SmATG8 are localized to the lumen of vacuoles. In apical hyphae peroxisomes are not degraded in the vacuoles. (B) DsRED-SKL is excluded from the vacuole in basal hyphae of ΔSmatg8 and ΔSmatg4. Arrows indicate vacuoles free of the DsRED-SKL fluorescence signals. Strains were grown on SWG layered slides or on a cellophane layer on solid medium. Bar = 10 µm.

To determine the impact of SmATG8 and SmATG4 on pexophagy, plasmid pDsRed-SKL was transformed into ΔSmatg8 and ΔSmatg4. Consistent with reports in *A. oryzae* (SHOJI *et al.* 2010), in the absence of *Smatg8* and *Smatg4*, DsRED fluorescence is only visible in small spots, but no DsRED signals were observed in the vacuoles of basal hyphae (Fig. 28B). Therefore, we concluded that pexophagy was arrested in *Smatg8* and *Smatg4* deletion mutants.

SmATG8 and SmATG4 are involved in pexophagy which is indicated by its absence in *Smatg8* and *Smatg4* deletion strains.

3.3 Characterization of *Smjlb1*

3.3.1 Isolation of *Smjlb1* in *S. macrospora*. In a microarray analysis of *S. macrospora* pro mutants, the IDI-4 orthologue of *P. anserina* was found to be downregulated. Since it was stated for IDI-4 of *P. anserina* that it is involved in regulation of autophagic-cell death, it seemed to be an interesting gene to be investigated in *S. macrospora* in regards of fruiting-body development. For identification of a *S. macrospora* homologue of the *P. anserina* bZIP transcription factor IDI-4, a TBLASTN search of the *S. macrospora* genome with the *P. anserina* amino-acid sequence was conducted. The 669 bp ORF *SMAC08510* (CCC14061.1) was isolated. The *SMAC08510* is predicted to contain no introns. This was confirmed by sequencing of the cDNA. The protein consisting of 222 amino acids has a predicted mass of 24.6 kDa and an isoelectric point of 9.12. SMAC08510 shared an identity of 27% with IDI-4 but was named SmJLB1 according to the *A. nidulans* transcription factor (see 4.3.1 for detailed explanation).

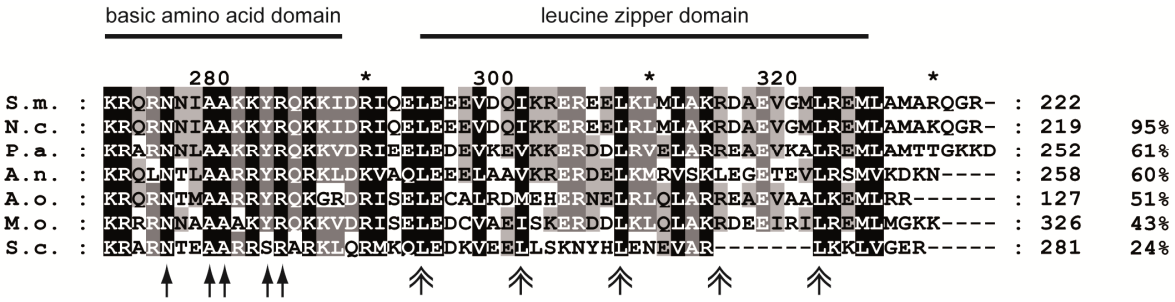

Figure 29. Multiple sequence alignment of the bZIP domain of SmJLB1 orthologues from Ascomycota members. The ClustalX alignment was created with following sequences: S.m., *S. macrospora*, F7W9S0; N.c., *N. crassa* Q7SGM8; P.a., *P. anserina*, Q6IUV0; A.n., *A. nidulans*, Q8TFD6; A.o., *A. oryzae*, Q2UER7; M.o., *M. oryzae*, G4MS16; S.c. *S. cerevisiae*, P03069 (Gcn4). Indicated above the alignment are the basic amino-acid domain (DNA binding) and the leucine-zipper domain (dimerization) (STRITTMATTER *et al.* 2001). Residues required for DNA contact are indicated by arrows (ELLENBERGER *et al.* 1992). Double arrows are pointing to residues of the heptad repeat (DEMENTHON *et al.* 2004). The functional amino acids, conserved in the bZIP domain of SmJLB1, are shaded in black; residues conserved in at least 6 of 7 sequences are shaded in dark grey and residues conserved in at least four sequences are shaded in light grey. Stated at the right margin are the amino-acid identities in %.

An amino-acid alignment of SmJLB1 with orthologues of other ascomycetes revealed identities of 79, 27, 17, 17, 15 and 10% when compared with putative homologues from *N. crassa* (Q7SGM8), *P. anserina* (Q6IUV0), *M. oryzae* (G4MS16), *A. nidulans* (Q8TFD6), *A. oryzae* (Q2UER7) and *S. cerevisiae* (Gcn4, P03069), respectively. In an amino-acid alignment of only the bZIP domain among ascomycetes identities of 95, 61, 60, 51, 43, and 24% in comparison with proteins of *N. crassa*, *P. anserina*, *A. nidulans*, *A. oryzae*, *M. oryzae* and *S. cerevisiae*, respectively, were determined (Fig. 29).

An orthologue of IDI-4/JlbA was identified in *S. macrospora*. Solely the bZIP domain of SmJLB1 is conserved among Ascomycota.

3.3.2 Generation of a *S. macrospora Smjlb1* deletion and complementation strain. To investigate whether SmJLB1, as a bZIP transcription factor, is involved in fruiting-body development, a deletion mutant was created. This included the construction of a plasmid pRS-ΔSmjlb1 carrying the deletion cassette. This was conducted in the same manner as described previously.

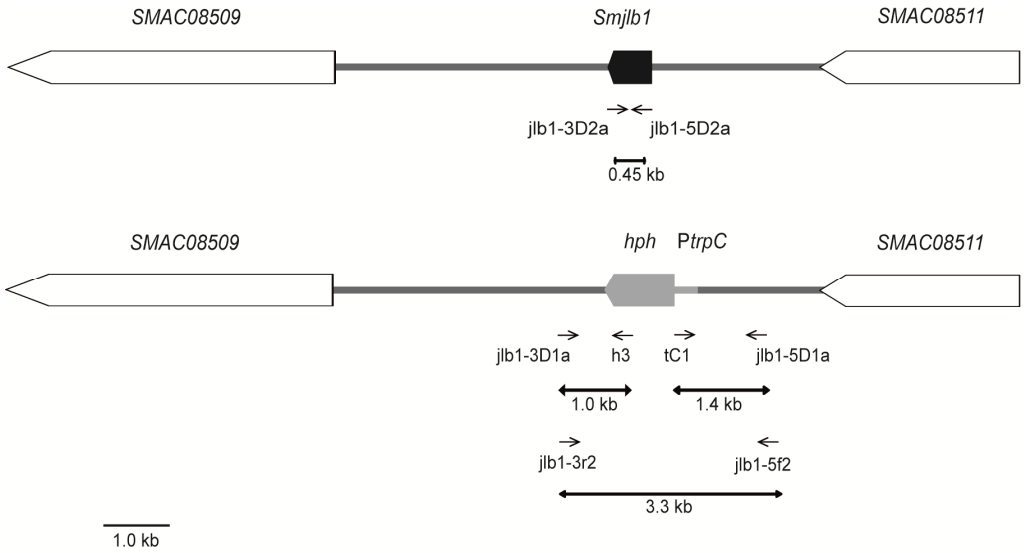

Figure 30. Generation and complementation of a ΔSmjlb1 strain. Scheme of the *Smjlb1* locus before and after homologous integration of the deletion cassette. Primers and their position used for the verification of the deletion and complementation are indicated by small arrows. PCR fragment sizes for deletion/complementation verification and deletions cassette amplification are indicated. White frames, adjacent genes; black frame, target gene; light grey frame, *hph* gene for hygromycin resistance; light grey line, *trpC* promoter of *A. nidulans*; grey lines, intergenic regions.

Bases 1-669 out of 669 bp were exchanged with a hygromycin-resistance cassette substituting *Smjlb1* completely (Fig. 30). Transformation with the deletion cassette resulted in three heterokaryotic ΔSmjlb1/Smjlb1 strains (verified by PCR, data not shown). These heterokaryotic strains were sterile and still contained the *Smjlb1* and the Δ*ku70* background. For removal of the Δ*ku70* background single spore isolates were isolated. This was achieved by crossing with a fus1-1 strain. Two single-spore isolates were obtained from hybrid perithecia, carrying the *Smjlb1* deletion background, without the Δ*ku70* background.

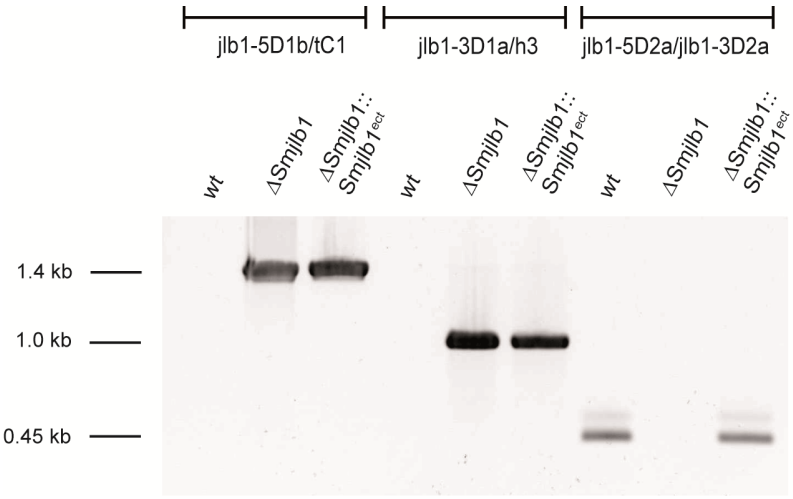

Figure 31. Deletion and complementation verification of the ΔSmjlb1 strain. Deletion and presence of *Smjlb1* was confirmed by PCR. Amplicon sizes according to primer pairs appeared as expected and are displayed in figure 30.

Genotype verification was conducted by PCR. Using primer pairs jlb1-3D1a/h3 and jlb1-5D1a/tC1, annealing in the 5'- and 3'-regions of *Smjlb1*, respectively, and in the *hph* cassette, insertion of the deletion cassette at the *Smjlb1* locus was verified. Primer combination jlb1-3D2a/jlb1-5D2a, annealing in *Smjlb1*, verified removal of the wt gene (Fig. 31). Complementation of ΔSmjlb1 was carried out to verify the observed phenotype of the ΔSmjlb1 deletion mutant. For this purpose pRS-Smjlb1-comp was constructed and inserted ectopically into ΔSmjlb1 and in total 10 ssi's were obtained carrying the Δ*Smjlb1/Smjlb1*^{ect} background. Conducted by PCR using the same primer combinations described for the knockout, revealed the presence of the deletion cassette and an ectopic integration of *Smjlb1* (Fig. 31).

3.3.3 Deletion of *Smjlb1* leads to sterility and impairment of vegetative growth. Phenotypical analysis of *Smjlb1* deletion was conducted to elucidate its impact on the sexual

development of *S. macrospora*. Strains wt::hph/nat^{ect}, ΔSmjlb1 (*hph*^{R}) and ΔSmjlb1::Smjlb1^{ect} (*hph/nat*^{R}) were grown on either BMM (complete medium) or SWG (fructification medium) solid medium. These media contained either 2.5 mM 3-AT, hygromycin (inhibition of protein biosynthesis) or no stress inducing agent.

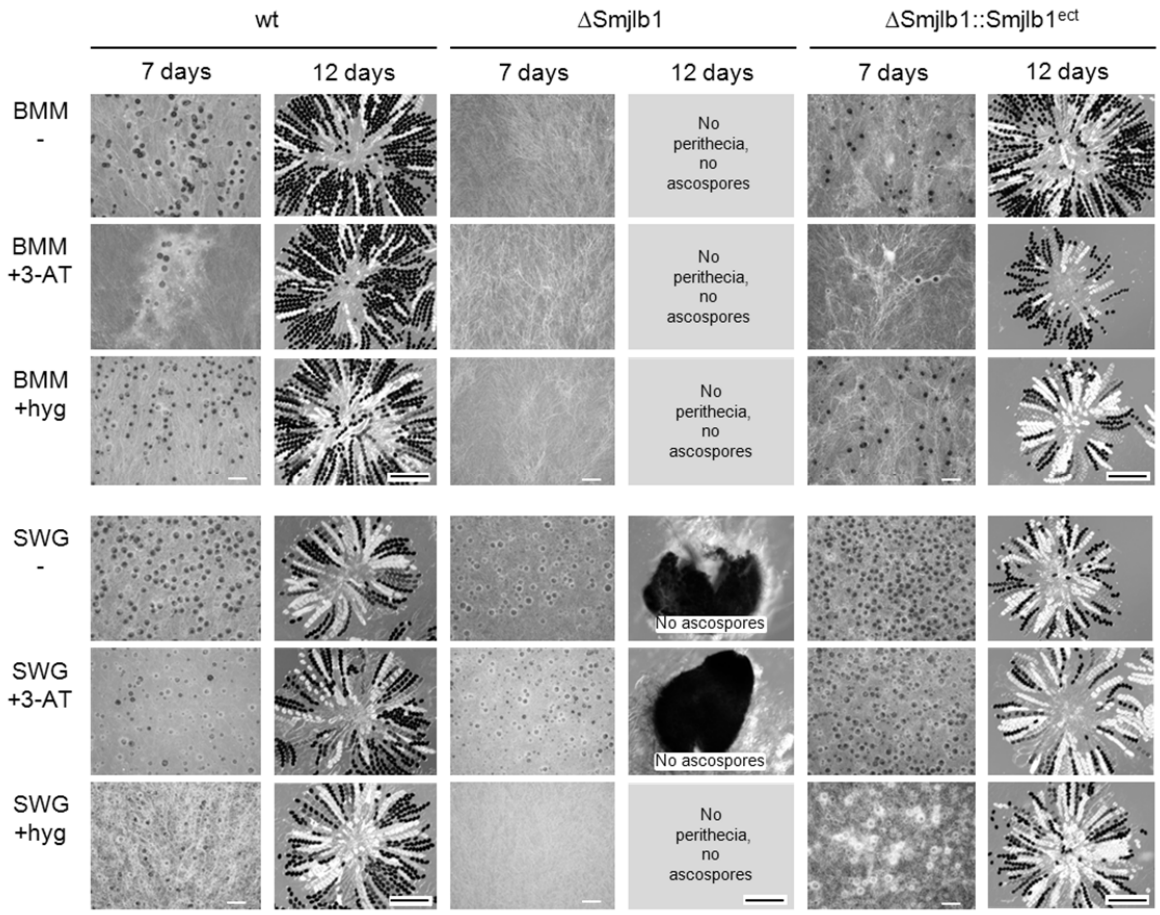

Figure 32. Phenotypic analysis of the sexual development of the ΔSmjlb1 deletion strain in comparison to wt and the complemented strain. Microscopic investigation of fruiting-body development and ascospore production in ΔSmjlb1, ΔSmjlb1::Smjlb1^{ect} and wt. Under laboratory conditions wt strains develop mature perithecia after 7 days. Ascus rosettes are made visible by cracking the perithecia. ΔSmjlb1 generate solely perithecia when grown on SWG and SWG containing 2.5 mM 3-AT. Ectopically integrated copies of the *Smjlb1* complemented the mutant phenotype. Bars = 1.0 mm (overview) and 200 µm (ascus rosettes).

Microscopical analysis revealed that ΔSmjlb1 produces no perithecia when grown on BMM medium (Fig. 32) with or without stress inducing agents. When grown on SWG

medium without a stress inducing agent or medium with 3-AT, ΔSmjlb1 was able to form perithecia but failed to produce ascospores. On SWG + hygromycin, ΔSmjlb1 was able to grow but incapable of perithecia development (Fig. 32). With regard to the sexual development the phenotype of the complemented strain was restored to wt level, except for the fact that it produces less mature ascospores on all media tested.

Furthermore, the question was addressed whether deletion of *Smjlb1* also leads to deficiency of the foraging capability as shown for the ΔSmatg8 and ΔSmatg4 mutants. The foraging capability of ΔSmjlb1 is abolished, while the wt and complementation strain exhibit extensive mycelial growth on an inert plastic surface (Fig. 33).

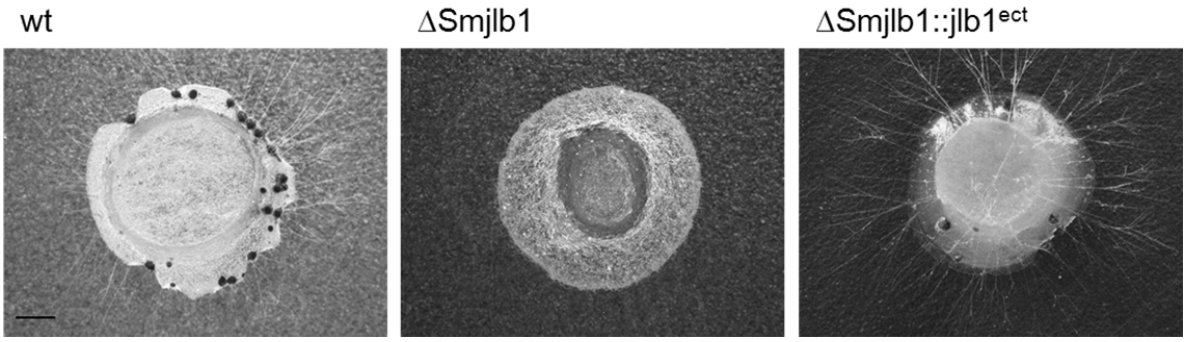

Figure 33. Phenotypic analysis of the ΔSmjlb1 deletion, complemented and wt strain by observation of foraging. Deletion strains are unable to undergo foraging but wt and complemented strains exhibit the ability to grow on an inert plastic surface. Agar plugs of 5 mm diameter were transferred into empty petri dishes and incubated for 10 days in a damp chamber. Bar = 1 mm.

In addition to the foraging growth defect, *Smjlb1* deletion leads to a decrease of vegetative growth velocity. Compared to wt [3.4 (± 0.19) cm/d], growth velocity of ΔSmjlb1 [1.4 (± 0.25) cm/d] is reduced to 41%. Under histidine starvation conditions (induced by 3-AT) growth is even more reduced to 20% comparing ΔSmjlb1 [0.5 (± 0.09) cm/d] to wt [2.5 (± 0.19) cm/d]. In the complemented strain, the growth defect was only slightly complemented when compared to the wt strain. This was most likely a result of the ectopic integration of the *Smjlb1* wt copy (Fig. 34).

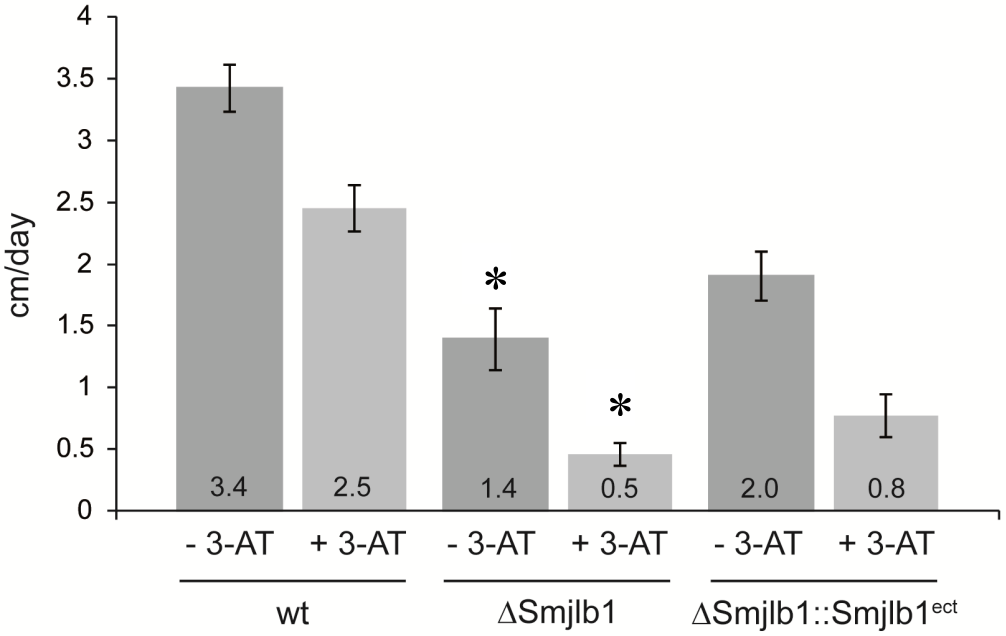

Figure 34. **Phenotypic analysis of *Smjlb1* deletion and complementation strains by determination of growth velocity.** Growth velocity of deletion and complemented strains. In comparison to the wt the vegetative growth velocity of ΔSmjlb1 is reduced to 41%. On medium containing 2.5 mM 3-AT this effect is more severe and decreased to 20% compared to wt. Growth-rate analysis was conducted in 30 cm race tubes. Growth rates shown are averages from nine independent measurements of three independent experiments (N=27), error bars indicate standard deviations. Values of the deletion mutants with asterisk differ significantly from wt and the complemented mutant according to Student's t-test ($p < 0.00001$).

To test if ΔSmjlb1 was capable of undergoing hyphal fusion, ΔSmjlb1 was analyzed microscopically for the presence of intracolonial hyphal cell fusion and monitored for cytoplasmic flow at putative hyphal fusion sites. In comparison to the wt and the complemented ΔSmjlb1::Smjlb1^{ect} strain, the ΔSmjlb1 strain displayed no hyphal fusion defect and thus a similar the number of hyphal fusion events (Fig. 35).

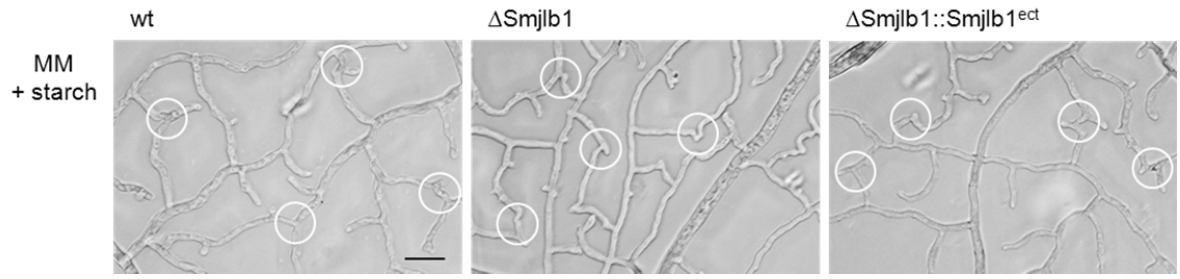

Figure 35. The ΔSmjlb1 strain is not impaired in hyphal fusion. Microscopic observation of vegetative hyphal fusion. White circles indicate hyphal fusion events. Hyphal fusions were confirmed by monitoring cytoplasmic flow. Microscopic pictures were taken at subperiphal regions 5-10 mm apart from the growth front. MM + starch, = 0.1% starch containing minimal medium. Bar = 20 µm.

The impact on hyphal fusion by a *Smjlb1* deletion was examined as described above for ΔSmatg8 and ΔSmatg4 mutants. As depicted in Fig. 36, crossing of the sterile mutant ΔSmjlb1 with either ΔSmatg8 or ΔSmatg4 resulted in the formation of hybrid perithecia in the crossing zone. In contrast, crossing of two hyphal fusion mutants, pro11 and ΔSmmob3, did not result in the formation of hybrid perithecia (BERNHARDS and PÖGGELER 2011; BLOEMENDAL *et al.* 2012).

To determine the role of SmJLB1 during ascospore germination, we investigated the ascospore-germination rate of ΔSmjlb1 in comparison to wt and the complemented strain by crossing them against a fertile fus1-1 strain (as described above).

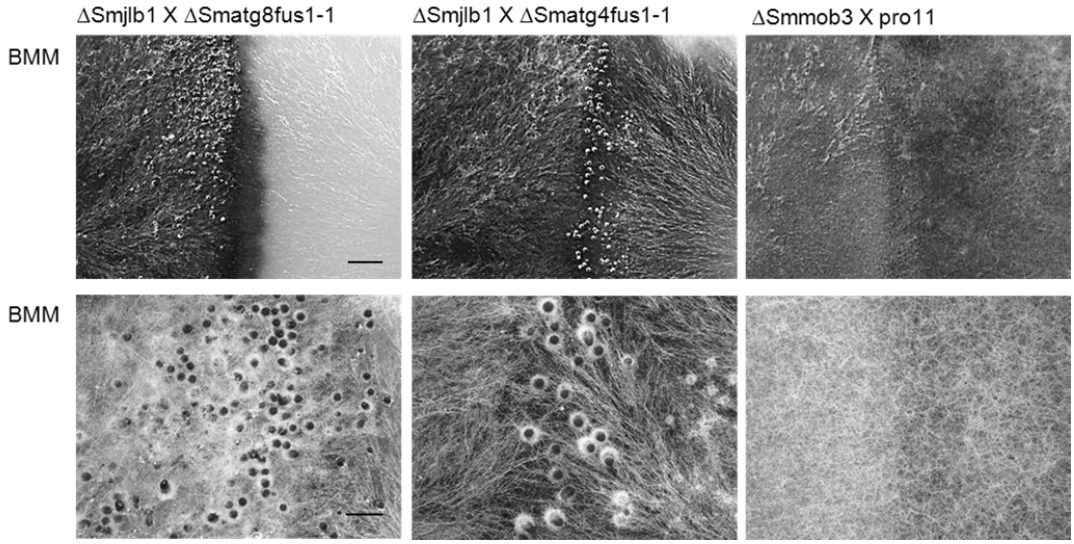

Figure 36. ΔSmjlb1 is able to form perithecia when crossed with sterile strains. Subsequent to crossing of sterile ΔSmjlb1 with either sterile ΔSmatg8 or ΔSmatg4 strains fertile perithecia were formed whereas no fruiting-body development could be observed when the sterile hyphal fusion mutants ΔSmmob3 and pro11were crossed. Lower panel displays close up of the crossing zone. Strains were grown on BMM medium for 10 days. Bars = 0.5 cm (upper panel) and 1.0 mm (lower panel).

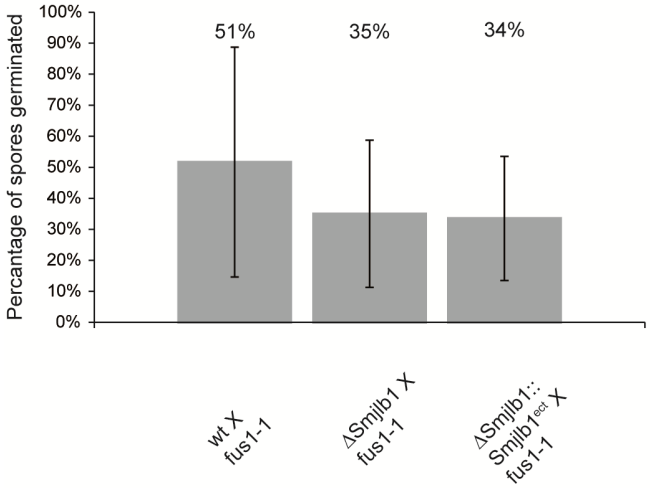

Figure 37. ΔSmjlb1 is not significantly reduced in germination. As described above, sterile deletion strains, complemented and wt strains were crossed with the spore-color mutant fus1-1 for determination of germination efficiency of ascospores. 100 spores of each color were isolated and inoculated on BMM supplemented with 0.5% of sodium acetate. The experiment was repeated four times. Germination rate of spores is given in percent. Mean of four experiments are shown, error bars display standard deviation.

The germination rate of ascospores isolated from ΔSmjlb1 X fus1-1, was decreased to 35%. However, the germination rate of ascospores isolated from the cross ΔSmjlb1::Smjlb1^{ect} X fus1-1 was decreased to the same range (34%) (Fig. 37). To elucidate the germination rate of ascospores with the *Smjlb1::hph* deletion background, mycelium of germinated spores was transferred to hygromycin containing BMM medium. A total of 67 out of 210 ascospore isolates where resistant to hygromycin and therefore carried the ΔSmjlb1 deletion background. This suggests that the many ascospores isolated from ΔSmjlb1 X fus1-1 hybrid perithecia carried the deletion background, indicating that the germination efficiency is not affected due to the *Smjlb1* deletion.

Taken together, the phenotypical analysis of the *Smjlb1* deletion mutant revealed that its deletion negatively influences the perithecia formation, vegetative growth and foraging but has no effect on germination efficiency and hyphal fusion.

3.3.4 Analysis of the transcriptional expression of *Smjlb1*, *Smatg8* and *Smatg4* in wt and the ΔSmjlb1 mutant. Previous studies have shown that IDI-4 of *P. anserina* is a transcription factor which regulates expression of *ATG8* and might therefore also be involved in the regulation of other *ATG* genes (DEMENTHON and SAUPE 2005; DEMENTHON *et al.* 2004). Expression of *Smjlb1*, *Smatg8* and *Smatg4* was examined in wt and ΔSmjlb1 by means of quantitative real-time PCR.

As the lifecycle of *S. macrospora* is completed within 7 days under laboratory conditions expression patterns were surveyed from day 3 (start of ascogonia formation) to 7 (completed perithecia development) either grown vegetatively or sexually to monitor alterations of the expression at different developmental stages.

Smjlb1, *Smatg8* and *Smatg4* appeared to be constitutively expressed since the transcript level of these genes does not differ significantly between sexual and vegetative growth (Fig. 38). Applying the relative expression software tool (REST), P values for significance were calculated (PFAFFL *et al.* 2002). According to the REST analysis the compared values are too similar to be considered significantly different and thus the genes are not regulated differently when sexual and vegetative growth is compared. Solely the expression of *Smjlb1* and *Smatg4* on the fifth day of the development is upregulated significantly different compared to vegetative growth. The fifth day of the *S. macrospora* lifecycle represents the

entry into fruiting-body development and therefore these genes might be upregulated on induction of perithecia development.

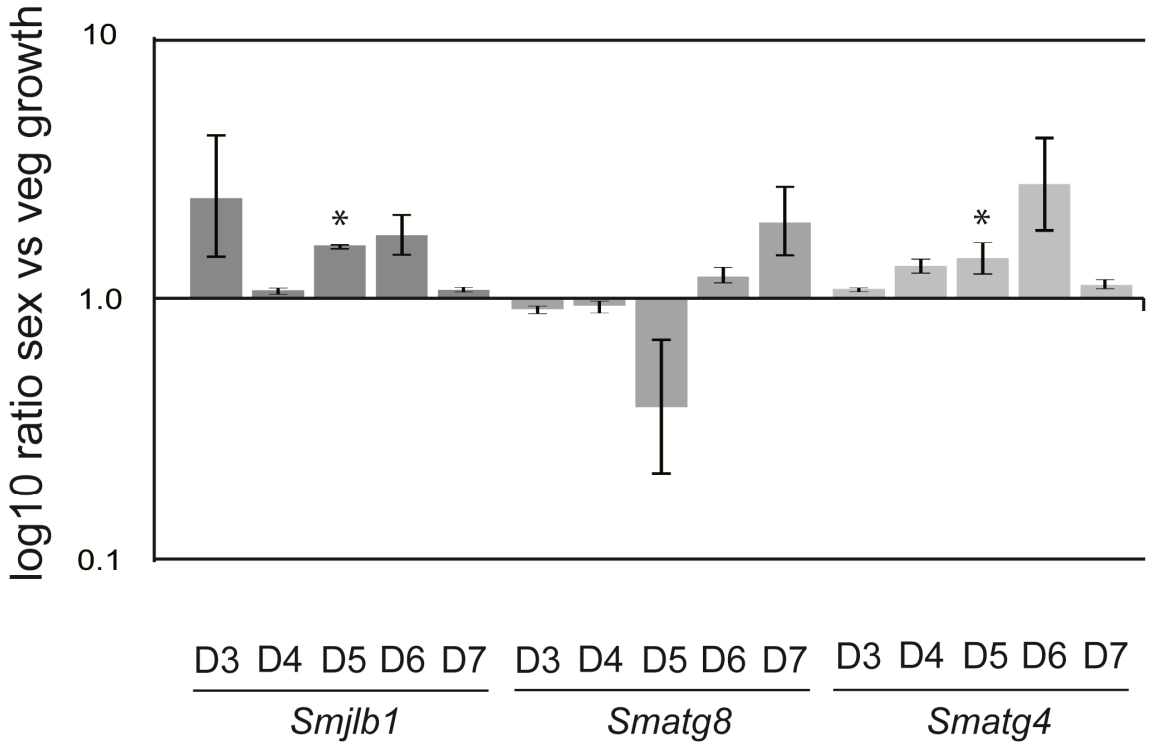

Figure 38. Analysis of the transcriptional expression of *Smjlb1*, *Smatg8* and *Smatg4* in wt background. Expression of *Smjlb1*, *Smatg8* and *Smatg4* was examined during vegetative growth and the sexual cycle of *S. macrospora* from day 3 (D3) to day 7 (D7) in relation to the *ssu* house keeping gene. Transcription level of *Smjlb1*, *Smatg8* and *Smatg4* is constitutive under the observed conditions except for the fifth day on which *Smjlb1* and *Smatg4* seem to be upregulated. Values of expression level are averages of at least 3 biologic independent measurements. sex, sexual development; veg, vegetative development; Significances are analyzed with the REST analysis and are highlighted with an asterisk ($P < 0.01$).

After determination of *Smjlb1*, *Smatg8* and *Smatg4* expression in the wt we were interested how *Smatg8* and *Smatg4*, two prominent autophagy related genes, were regulated in the ΔSmjlb1 mutant also. Additionally, expression of *Smjlb1* in the ΔSmjlb1 mutant was investigated as well. Expression levels of *Smjlb1* in ΔSmjlb1 had CT values around 30 and primer melting curves were similar to the negative control using water, indicating no

expression of *Smjlb1* in the deletion strain. The ratio of expression of *Smatg8* and *Smatg4* was compared between the wt and ΔSmjlb1 mutant strain.

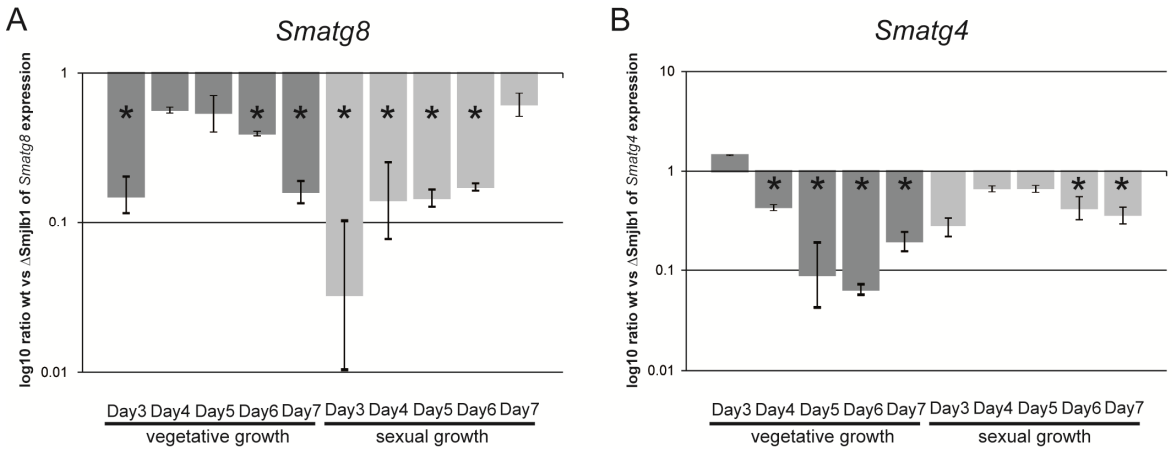

Figure 39. Analysis of the transcriptional expression of *Smatg8* and *Smatg4* in relation of wt to ΔSmjlb1. Expression of *Smatg8* and *Smatg4* was examined under vegetative and sexual growth conditions from day 3 to day 7 in wt and ΔSmjlb1 strains to test expressional influence of *Smjlb1* deletion. (A) and (B) Transcription levels of *Smatg8* and *Smatg4* are downregulated in wt compared to ΔSmjlb1 and do not differ significantly throughout all observed conditions. Values of expression level are averages of three measurements of biological independent samples. Error bars indicate standard deviations. Significances are analyzed with the REST application and are highlighted with an asterisk ($p < 0.05$).

As displayed in Fig. 39A, in comparison to ΔSmjlb1 *Smatg8* is significantly downregulated in the wt background by a maximal factor of 6 (day 3) during vegetative and 32 fold (day 3) during sexual growth. *Smatg4* is downregulated also significantly compared to ΔSmjlb1, by a max. factor of 15 (day 6) grown vegetatively and threefold (day 3) grown sexually (Fig. 39B). Significances in this assay ranged from $p = 0.046$ to $p = 0.001$ and were determined with the REST program.

***Smatg8*, *Smatg4* and *Smjlb1* are expressed constitutively in the wt and *Smatg8*, *Smatg4* are upregulated in ΔSmjlb1.**

3.3.5 SmJLB1-EGFP is localized to nuclei. For subcellular localization of SmJLB1 fluorescence microscopy was conducted. First, *Smjlb1* was introduced into the plasmid pDS23-EGFP and fused to the *egfp* gene resulting in pRS-Smjlb1-egfp. By transforming this plasmid in the *S. macrospora* ΔSmjlb1 strain, *Smjlb1* is constitutively expressed under the control of the glycerin aldehyde 3-phosphate dehydrogenase promoter (*gpd*) of *A. nidulans*. The ectopically integrated plasmid pRS-Smjlb1-egfp did not restore the phenotype of the deletion mutant. Thus, the functionality of the SmJLB1 fusion protein is not confirmed.

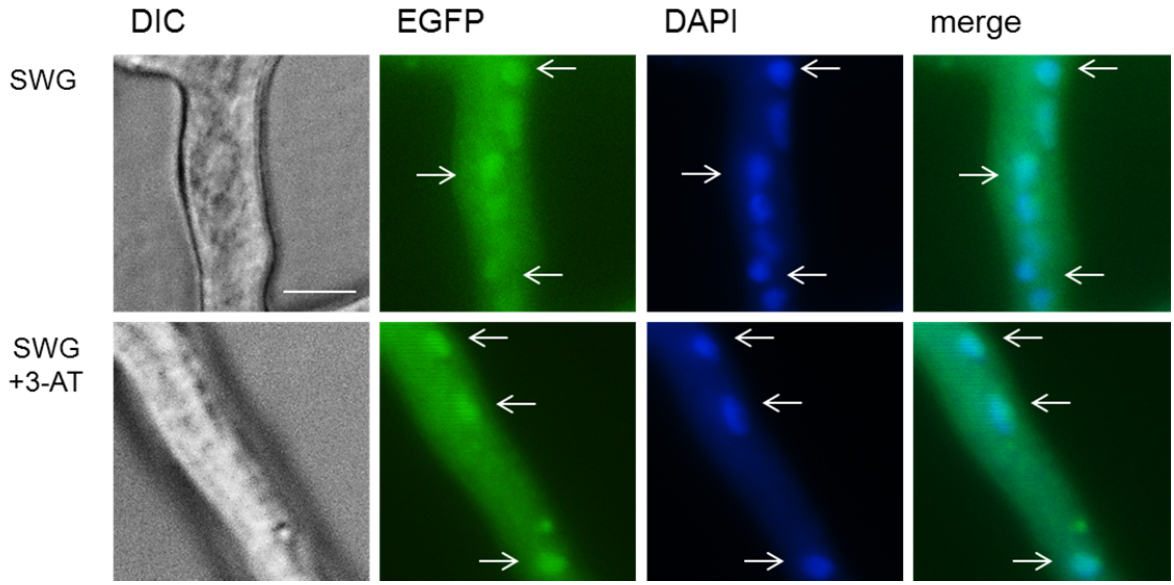

Figure 40. SmJLB1-EGFP localizes to nuclei. Subcellular localization by fluorescence microscopy of the *S. macrospora* ΔSmjlb1 strain with an ectopic integrated pRS-Smjlb1-egfp plasmid. The upper and lower panels display localization of SmJLB1-EGFP to nuclei. Nuclei are indicated by an arrow. For the visualization of the nuclei, DAPI staining was applied as described in Materials and Methods. Strains were grown on SWG or SWG + 3-AT layered slides or on a cellophane layer on solid medium. Bar = 5 µm.

Fluorescence microscopy revealed that SmJLB1-EGFP is localized to nuclei, which is confirmed by DAPI staining of the nuclei (Fig. 40). This is true for growth on SWG and SWG + 3-AT medium. Thus growth on histidine starvation medium did not influence the localization of SmJLB1-EGFP. However, hyphae grown on SWG + 3-AT medium formed more vacuoles than hyphae grown on SWG medium (data not shown).

SmJLB1-EGFP displays a nuclear localization.

4. Discussion

4.1 SmVPS34 and SmVPS15 are required for viability

4.1.1 Catalytic domains of the vacuolar protein sorting proteins SmVPS34 and SmVPS15 are conserved. Vps34 is the core protein of both complex I (Atg6, Atg14, Vps15 and Vps34) and complex II (Atg6, Vps38, Vps15 and Vps34) and thus vital for vacuolar protein sorting and autophagy (Fig. 3). Vps34 has been shown to be involved in trimeric G-protein signaling as well as the mTor nutrient-sensing pathway (HERMAN and EMR 1990; KOELLE 2006; OBARA and OHSUMI 2011b; YAN and BACKER 2007). For these pathways its PI3K activity is indispensable.

Studies in *S. cerevisiae* have shown that the PI3K domain localizes at the C-terminus of Vps34 (BUDOVSKAYA *et al.* 2002). The same domain was also predicted by a domain search with the SmVPS34 amino-acid sequence in NCBI. An alignment of the PI3K domain using amino-acid sequences of Vps34 orthologues from different ascomycetes revealed a strong conservation of this domain (Fig. 8). An overall alignment indicated less conservation in the phylum Ascomycota (data not shown). Studies in *S. cerevisiae* revealed that the last ten aa 865-875 (red box, above alignment, Fig. 8) of Vps34 (consisting of 875 aa) are required for its kinase activity. Residues 837-864 (blue box, above alignment, Fig. 8) of the *S. cerevisiae* Vps34 have been shown to play a crucial role in binding of Vps34 to Vps15, and deletion of these residues abolished interaction with Vps15 (BUDOVSKAYA *et al.* 2002).

As shown in the alignment of Fig. 8, the amino-acid residues responsible for Vps15 interaction (red box, above alignment, Fig. 8) as well as those required for kinase activity are conserved (blue box, above alignment, Fig. 8), indicating a strong conservation of the PI3K domain of Vps34 orthologues among ascomycetes.

Vps15 is the regulatory subunit of Vps34 and controls its activity by phosphorylation. Fig. 9 displays an alignment of the Vps15 N-terminal region comparing the amino-acid sequences among related ascomycetes. Vps15 of *S. cerevisiae* (consisting of 1454 aa) has been described to contain 4 domains: a myristoylation consensus site (aa 1-10, red box, above alignment, Fig. 9), the serine/threonine kinase domain (aa 11-262, blue box, above alignment, Fig. 9), HEAT repeats (Huntingtin, elongation factor 3, the PR65/A subunit of protein

phosphatase 2A and the lipid kinase Tor, aa 400-700, Fig. 9), and WD-40 domains at the C-terminus of Vps15 (PANARETOU *et al.* 1997; YAN and BACKER 2007).

Referring to common protein kinase domain sequences, Vps15 shares significant similarities to catalytic domains of these and it has been reported that Vps15 of *S. cerevisiae* possesses two residues conserved in most kinase motifs (Asp165 and Glu200, Fig. 9) (HERMAN *et al.* 1991b). It was shown that alteration of these two residues abolishes kinase activity of the *S. cerevisiae* Vps15 (HERMAN *et al.* 1991a). As displayed in Fig. 9 these two residues are also conserved among ascomycetes (indicated by arrows). The conservation of Vps15 among members of the Ascomycota is solely restricted to the N-terminus. Conservation includes the myristoylation consensus site and the kinase domain, but after the first 100 amino acids of the HEAT domain sequence similarities decrease. This indicates less conservation of the C-terminus of Vps15 orthologues among ascomycetes.

The PI3K domain of SmVPS34 and the protein kinase domain of SmVPS15 are conserved among members of the Ascomycota.

4.1.2 Deletion of *Smvps34* and *Smvps15* is lethal. The generation of the heterokaryotic ΔSmvps34/Smvps34 and ΔSmvps15/Smvps15 deletion strains was achieved subsequent to identification and isolation of both genes. The generation of single-spore isolates via crossing failed.

By a germination assay it was shown that combined out of three experiments, 1,200 ascospores derived of hybrid perithecia from crosses between the heterokaryotic Δvps mutants and spore-color mutant fus1-1 were not able to germinate on hygromycin containing medium (Fig. 13). This indicated that ascospores carrying the ΔSmvps34 or ΔSmvps15 background are incapable to germinate. In *S. cerevisiae* and *Candida albicans*, deletion of *VPS34* leads to a temperature sensitive phenotype, thus deletion mutants are unable to grow at elevated temperatures (GUNTHER *et al.* 2005; HERMAN and EMR 1990). This phenotype was defined also for a *HpPDD1* (*VPS34* orthologue) null mutant in *Hansenula polymorpha*, a methylothropic yeast species (KIEL *et al.* 1999). Additionally to the temperature sensitivity of the yeast *VPS34* gene deletion mutants, their vacuolar protein sorting machinery was impaired also (HERMAN and EMR 1990). Similar to the *VPS34* knockout phenotype, *VPS15* deletions in

S. cerevisiae and *Pichia pastoris* resulted in temperature sensitive mutants and impairment of vacuolar protein sorting (HERMAN *et al.* 1991a; STASYK *et al.* 1999).

The incubation of ascospore isolates from crosses between ΔSmvps34/Smvps34 X fus1-1 and ΔSmvps15/Smvps15 X fus1-1 crosses was conducted at 27°C which is not described as a restrictive temperature for *S. macrospora*. This excludes the assumption that spores with either ΔSmvps34 or ΔSmvps15 background were not able to germinate due to restrictive temperatures.

In mice knockdown of p110-β, a *vps15* orthologue resulted in impaired autophagy in embryonic fibroblasts, liver, and heart which leads to growth retardation (DOU *et al.* 2010). Furthermore, it has been shown that homozygous *Drosophila melanogaster* Δvps15 mutants died at early L3 larval stage (LINDMO *et al.* 2008). In *Arabidopsis thaliana* Vps15 has been shown to be vital for pollen development and germination. The working group around XU (2011) failed to find homozygous progenies with the *AtVPS15* deletion. Additionally, an *AtVPS34* deletion caused growth retardation of seedlings, and plants died in several occasions indicating lethality connected to *VPS34* deletion (WELTERS *et al.* 1994).

The reports of *A. thaliana* are similar to our findings that deletion of either *Smvps34* or *Smvps15* impairs ascospore germination. The findings reported for *D. melanogaster* confirm our assumption that deletion of either *Smvps34* or *Smvps15* is lethal. As stated previously, involvement of Vps34 and Vps15 in vacuolar protein sorting, autophagy, trimeric G-protein signaling and mTor nutrient-sensing pathway have been reported (HERMAN and EMR 1990; KOELLE 2006; OBARA and OHSUMI 2011b; YAN and BACKER 2007). In accordance to these reports, it is assumable that deletion of either *Smvps34* or *Smvps15* would cause impairment of multiple pathways, drastically influencing the metabolism of *S. macrospora*. Previously, our group could show that deletion of *S. macrospora Smatg7*, involved in the Atg8 and Atg12 conjugation pathway, is lethal (NOLTING *et al.* 2009). If deletion of a gene involved in two conjugation systems causes a lethal phenotype it is assumable that deletions of genes involved in multiple pathways have even more consequences for the viability of *S. macrospora*.

Taken together, deletion of either *Smvps34* or *Smvps15* leads to loss of viability.

4.2 Deletion of autophagy genes *Smatg8* and *Smatg4* impairs fruiting-body development

4.2.1 Autophagy proteins SmATG8 and SmATG4 are highly conserved and can rescue *S. cerevisiae* mutants. The ubiquitin-like *S. macrospora* protein SmATG8 reveals a high degree of sequence identity when compared to the *S. cerevisiae* Atg8 and other fungal Atg8 orthologues. This includes the conserved core of hydrophobic side chains Phe77, Phe79, as well as Leu84 and Arg65, which in *S. cerevisiae* and the human LC3 (an ATG8 homologue) were shown to be part of the recognition site for the cysteine protease Atg4 and the E1-enzyme Atg7.

In *S. cerevisiae*, Atg7 interacts via a salt bridge and a network of hydrogen bonds with the conserved residues Glu112, Asn113 and Thr114 of the Atg8 tail region. Furthermore, Tyr49 and Leu50, which were demonstrated to be essential for Atg8 function, and Phe115 and Gly116, which are required for the Atg4-dependent processing, were also perfectly conserved in the Atg8 homologues of filamentous ascomycetes (AMAR *et al.* 2006; NODA *et al.* 2011; SATOO *et al.* 2009). However, the last C-terminal amino acids after the conserved Gly116 residues display a high variability (Fig. 14).

In contrast to Atg8, the overall amino-acid identity of Atg4 homologues was less conserved. Only the predicted peptidase C-54 domain at the C-terminus was conserved among fungal Atg4 orthologues (Fig. 15). Recently, studies in *M. oryzae* have shown that Cys206 of the C-54 domain is the catalytic center of MoAtg4, required for processing of MoAtg8 (LIU *et al.* 2010). This cysteine residue (Cys206) as well as two other residues of the catalytic triad of cysteine proteases (Asp348 and His350) were conserved in SmATG4 and in other fungal Atg4 orthologues (Fig. 15) (SUGAWARA *et al.* 2005).

The functional conservation of the *Smatg8* and *Smatg4* orthologues was confirmed by rescue of *S. cerevisiae atg8*Δ and *atg4*Δ deletion strains. Complementation of the deletion strains was monitored using an Ape1 maturation assay (HARDING *et al.* 1995). The *Smatg8* cDNA was able to complement Ape1 maturation of the *atg8*Δ strain to the same extent as the endogenous *S. cerevisiae EGFP-ATG8* (Fig. 16A). This result was not surprising, considering the high degree of sequence identity between SmATG8 and the budding yeast Atg8 (76%), and the conservation of residues essential for interaction with Atg7 and Atg4.

In a previous study, it was demonstrated that *Smatg7* was capable of partially complementing ascospore-formation deficiency in a *S. cerevisiae* atg7Δ mutant (NOLTING *et al.* 2009). Similarly, complementation of the Ape1 maturation defect in the *S. cerevisiae atg4*Δ mutant was only partially rescued by expression of the *Smatg4* cDNA (Fig. 16B). Recently, it was demonstrated that the *M. oryzae MoATG4* cDNA rescued starvation sensitivity of an *S. cerevisiae atg4*Δ mutant. However, it was unclear whether this was a partial or a full complementation since the determination of the Ape1 maturation efficiency seems to be more precise than the rescue of starvation sensitivity (LIU *et al.* 2010). Expression of the *A. thaliana AtATG8a* and *AtATG8*d orthologues only partially rescued Ape1 maturation of a *S. cerevisiae atg8*Δ, whereas *AtATG4b* almost completely complemented an *atg4*Δ strain (KETELAAR *et al.* 2004).

In accordance with studies performed using Atg8 and Atg4 orthologues of *M. oryzae* and *A. thaliana,* we demonstrated, by means of a Yeast-Two Hybrid study, that SmATG8 and SmATG4 interact with each other, as their yeast orthologues (KETELAAR *et al.* 2004; LIU *et al.* 2010). Recently, LIU *et al.* (2010) tried to confirm *in vivo* interaction of *M. oryzae* MoAtg4 and MoAtg8 by means of a bimolecular fluorescence complementation assay, but detected an interaction only in vegetative hyphae grown under nitrogen starvation conditions.

Furthermore, we demonstrated that SmATG8 is C-terminally processed by SmATG4. Western blot experiments revealed that the SmATG8-EGFP fusion protein can be processed in the wt, but not in the ΔSmatg4 deletion strain or when the putative processing site was mutated (Fig. 25). These results corroborate that SmATG8 and SmATG4 might also interact *in vivo*.

SmATG8 and SmATG4 are conserved among ascomycetes and corresponding cDNAs can rescue respective *S. cerevisiae* deletion mutants. Interaction of SmATG8 and SmATG4 was confirmed as well as *in vivo* processing of SmATG8 by SmATG4.

4.2.2 SmATG8 interacts with SmATG3, SmATG7 and with a number of different enzymes. In *S. cerevisiae*, an interaction of Atg8 with the E1 enzyme Atg7 and the E2 enzyme Atg3 has been described (GENG and KLIONSKY 2008). In this study by means of Y2H and GFP-Trap analysis, an interaction of SmATG8 with SmATG3 was demonstrated. The interaction of SmATG8 with SmATG7 was only affirmed by GFP-Trap experiments. However, using SmATG7 as bait to screen a *S. macrospora* cDNA library, SmATG8 was found as interaction partner.

In mammals and in yeast an amino-acid sequence motif has been described in LC3 and Atg8 proteins, respectively. This motif is designated as LC3 interacting region (LIR) or Atg8-family interacting motif (AIM) and contains the consensus sequence WXXL or variants of this motif such as WXXI, WXXV, YXXL, YXXI and YXXV (NODA *et al.* 2010; PANKIV *et al.* 2007). In our analysis 56 out of 70 putative SmATG8 interaction partners have at least one putative LIR motif. The relative high numbers of LIR motif containing proteins indicate that the identified proteins might be true SmATG8 interaction partners. Interaction partners which contain this motif are highlighted in light grey in Tab. 4.

In the Y2H studies, proteins interacting with both, SmATG8 and SmATG7 were SmATG8, SMAC06421 and SMAC06954 (Fig. 18). As SmATG7 is proposed to be the E1-like enzyme, which activates SmATG8, this interaction was expected. Previously, it has been shown in *S. cerevisiae* that multimerization of Atg8-PE mediates tethering and hemifusion of membranes and thus autophagosome formation *in vivo*. Furthermore, it was reported that mutation of amino-acid residues in Atg8 abolishes tethering and hemifusion (NAKATOGAWA *et al.* 2007). Therefore, the interaction between SmATG8 and SmATG8 could also be expected. The *N. crassa* orthologue of SMAC06421 (*grhl*, NCU06095) has been described as a grainy head homologue which is involved in the development and remodeling of the cell wall and the transcription of genes involved in virulence and defense. Additionally, a *N. crassa* deletion mutant showed a defect in the dispersal of conidiospores (PARE *et al.* 2012). A gene function of SMAC06954 and its orthologue NCU05922 of *N. crassa* has not yet been identified but a BLAST search in the NCBI database indicated the presence of an arrestin-N domain (pfam00339). Proteins carrying an arrestin-N domain are involved in the regulation of G protein coupled receptor activity (PALCZEWSKI 1994).

SmATG3, SMAC07765, SMAC07897 and SMAC02442 are putative interaction partners of SmATG8 found in both, the Y2H and the GFP-Trap screens (Fig. 18). In yeast, Atg3 is the E2-like enzyme for Atg8 conjugation to PE and its interaction with SmATG8 was not surprising (KLIONSKY 2005). The orthologue of SMAC07765 in *H. sapiens* contains a peptidase M20 domain representing a glutamate carboxypeptidase (OTA *et al.* 2004; RAWLINGS and BARRETT 1995). NCU05160, the *N. crassa* orthologue of SMAC07897, has been described as an ATP-dependent Zn protease while NCU01754 is the orthologue of SMAC02442 and has been described as a mitochondrial alcohol dehydrogenase isoenzyme III (BAKKER *et al.* 2000; GALAGAN *et al.* 2003; SUN and GLASS 2011).

A very interesting interaction partner, only identified by GFP-Trap is SmNBR1 (neighbor of BRCA1 gene 1, SMAC07844). In mammals, NBR1 was identified as a cargo receptor for ubiquitinated protein aggregates and was recently identified as binding partner of LC3, the human SmATG8 orthologue (KIRKIN *et al.* 2009).

As listed in the results part, putative interaction partners of SmATG8 identified in the Y2H analysis with the most hits were: SMAC00918, SMAC01312, SMAC09075, previous mentioned SMAC02442, SMAC07505, SMAC04326, SMAC00851, SMAC01818 and SMAC02037. SMAC00918 is an orthologue of YMR008C which is predicted to be a cytosolic phospholipase A2 zeta (LEE *et al.* 1994). BLASTP search revealed that SMAC01312 is an orthologue of the *N. crassa* NCU00627. The *N. crassa* protein has previously been demonstrated to be localized in woronin bodies (MANAGADZE *et al.* 2010). Interaction of SmATG8 with SMAC01312 indicates that a specific form of autophagy might exist, responsible for selective degradation of woronin bodies which has not been described to date. Functions of SMAC09075, SMAC07505 and SMAC01818 and their orthologues are not described but a BLASTP searches at UniProt (http://www.uniprot.org/blast/uniprot/) revealed that these proteins are conserved among ascomycetes. The SmATG8 interaction partners SMAC04326, SMAC00851 and SMAC02037 were found to be highly similar to a cell wall synthesis protein of *P. chrysogenum*, a transmembrane protein 184B of *H. sapiens* and an α-1,2-mannosyltransferase Kre5 of *N. crassa* (MATSUDA *et al.* 2003; SANCAR *et al.* 2011; VAN DEN BERG *et al.* 2008).

Additionally, four proteins interacting with SmATG8 should be mentioned: SMAC08632, SMAC01351, SMAC07459 and SMAC00875. SMAC08632 is a putative orthologue of the

S. cerevisiae autophagy protein Atg26 and (KLIONSKY *et al.* 2003). Interaction of Atg8 with Atg26 has not been described to date, but it was shown that Atg26 is required for pexophagy in *C. orbiculare*, (ASAKURA *et al.* 2009). Thus, it is assumable that interaction of Atg8 and Atg26 is required for pexophagy. SMAC01351 is orthologous to the *N. crassa* serine protease p2 (GREENWALD *et al.* 2010). Interaction of SmATG8 with a putative serine protease might indicate that hydrolases are delivered to the vacuole using the autophagic machinery. The putative *N. crassa* orthologue of SMAC07459 is described as an F-box domain containing protein and might mediate SmATG8 degradation (GALAGAN *et al.* 2003). The function of SMAC00875 and orthologous proteins have not been described so far, but a BLAST search at NCBI revealed the presence of a peptidase-14/caspase domain (pfam00656). This domain is found in proteins involved in apoptosis, thus examination of the interaction between SmATG8 and SMAC00875 might elucidate connection between autophagy and apoptosis (autophagic cell death) (MARCHLER-BAUER and BRYANT 2004).

Interestingly, the most prominent functional group of SmATG8 interaction partners are proteins with enzymatic functions. 32 out of 70 SmATG8 interaction partners are predicted to have enzymatic activities. These proteins are highlighted in italics in Tab. 4 and 5.

Reports, that the autophagic machinery is used to deliver enzymes into the vacuole, exist in *S. cerevisiae*. For instance, the CVT pathway of *S. cerevisiae*, delivers the precursors of aminopeptidase I and α-mannosidase to the vacuole and Atg8 is used as cargo receptor (KLIONSKY 2005; KLIONSKY *et al.* 2003).

Taken together, in Y2H and GFP-Trap screens experiments 70 putative interaction partners of SmATG8 were identified, of which 32 might have enzymatic activity.

4.2.3 *Smatg8* and *Smatg4* are involved in vegetative growth, fruiting-body development and ascospore germination. In contrast to *Smatg7*, we succeeded in deleting *Smatg8* and *Smatg4* to generate homokaryotic ΔSmatg8 and ΔSmatg4 knockout strains from ascospore isolates of the primary transformants. Previously, it was suggested that SmATG7-mediated autophagy is at least essential for ascospore germination and the establishment of mycelial growth during the regeneration of protoplasts (NOLTING *et al.* 2009). However, this study shows that germination of ascospores is not *per se* abolished in autophagy mutants, although germination efficiency of the ΔSmatg8 and ΔSmatg4 deletion strains was significantly

decreased (Fig. 23C and D). Thus, autophagy seems to be important for a proper nutrient supply in the germinating ascospore. Previously, it was demonstrated that in *A. oryzae* and the plant pathogen *M. grisea*, autophagy-related proteins ATG8 and ATG4 were involved in early stages of conidial germination (KERSHAW and TALBOT 2009; KIKUMA and KITAMOTO 2011; KIKUMA *et al.* 2006; LIU *et al.* 2007; SHOJI and CRAVEN 2011; VENEAULT-FOURREY *et al.* 2006). In *F. graminearum*, *FgATG8* deletion resulted only in the reduction of conidiospore production (JOSEFSEN *et al.* 2012).

However, despite that ascospores carrying the ΔSmatg8 or ΔSmatg4 background can germinate, the growth velocity of the received mycelium was significantly reduced under normal conditions, but was restricted even more under amino-acid starvation conditions or on an inert plastic surface when compared to wt (Fig. 21B and 22). This was similar to reports in other filamentous fungi, which showed that deletion of *atg8 or atg4* also led to a decrease in vegetative growth velocity. An *idi7* deletion, the *ATG8* orthologue in *P. anserina,* showed no influence on the linear growth rate, but only on the hyphal density (PINAN-LUCARRE *et al.* 2003). In *U. maydis*, *atg8* deletion affects survival during carbon starvation and pathogenic growth (NADAL and GOLD 2010). Thus, autophagy is required for vegetative growth of filamentous fungi in general, but seems to be indispensable for growth under nutrient-limiting conditions. Recently, SHOJI and CRAVEN (2011) found that autophagy-mediated degradation of basal cell components, including nuclei and other organelles, were closely connected to the tip growth of filamentous fungi.

In addition to the reduced growth velocity, filamentous fungi deficient in *atg4* and *atg8* display a reduced density of the aerial hyphae and an absent or decreased conidiation (KIKUMA and KITAMOTO 2011; KIKUMA *et al.* 2006; LIU *et al.* 2010; PINAN-LUCARRE *et al.* 2003; VENEAULT-FOURREY and TALBOT 2007). An altered morphology of aerial hyphae in the *S. macrospora* ΔSmatg8 and ΔSmatg4 mutants was not observed and the effect on conidiation cannot be analyzed because *S. macrospora* produces no asexual spores.

For *P. anserina*, *M. oryzae*, and *F. graminearum* it has been described that deletion of *atg8* and *atg4* affected sexual development (JOSEFSEN *et al.* 2012; LIU *et al.* 2010; PINAN-LUCARRE *et al.* 2003). Similarly, ΔSmatg8 and ΔSmatg4 mutants are incapable of perithecia and ascospore formation and generated only the precursors of fruiting bodies, protoperithecia, in low numbers (Fig. 22A).

In *S. macrospora*, many genes involved in fruiting-body development have been characterized and several have shown a phenotype similar to ΔSmatg8 and ΔSmatg4. They have been described as **pro**-mutants, whose sexual development ceases at the point of **pro**toperithecia formation (ENGH *et al.* 2010). Another characteristic shared by most pro-mutants is their incapability of hyphal fusion, which is thought to be essential for the formation of multicellular sexual structures in ascomycetes (BERNHARDS and PÖGGELER 2011; BLOEMENDAL *et al.* 2012; BLOEMENDAL *et al.* 2010). Surprisingly, hyphal fusion was not affected and hyphal fusion events occurred in equal numbers in ΔSmatg8 and ΔSmatg4 when compared to wt and complemented strains (Fig. 23A). In contrast to the crossing of the hyphal fusion mutants pro11 and ΔSmmob3, crossing of sterile ΔSmatg8 and ΔSmatg4 strains resulted in mature hybrid perithecia at the contact zone of both mycelia (Fig. 23B), implying that autophagy affects sexual development but not hyphal fusion. For *N. crassa*, it has recently been reported that deletion of *Ncatg8* (NCU01545) prevents intracolonial hyphal cell fusion but an effect on fruiting-body development was not analyzed in this study (FU *et al.* 2011).

In summary, deletion of either *Smatg8* or *Smatg4* caused impairment of fruiting-body development and vegetative growth as well as germination efficiency.

4.2.4 EGFP-SmATG8 is localized to autophagosomes, while SmATG4-EGFP is distributed in the cytoplasm. Cellular localization studies using functionally expressed EGFP-SmATG8 fusion proteins revealed that SmATG8 was found to be localized in small dots, assumingly representing autophagosomes, and to vacuoles, indicating degradation of EGFP-SmATG8 delivered to vacuoles as structural components of autophagosomes (Fig. 26, upper panel). As previously described in yeast, Egfp-Atg8 fusion proteins assemble to autophagosomes and are visible as fluorescent dots that were also observed in other filamentous fungi, including *P. anserina*, *M. oryzae* and *A. oryzae* and even in mammals (KERSHAW and TALBOT 2009; KIKUMA *et al.* 2006; KLIONSKY *et al.* 2007; MIZUSHIMA *et al.* 2001; PINAN-LUCARRE *et al.* 2005).

In contrast to EGFP-SmATG8, SmATG4-EGFP was not focused in dot-like structures but rather dispersed throughout the cytoplasm (Fig. 26, lower panel). The same findings have been reported for Atg4 localization experiments in *M. oryzae* and *A. oryzae,* whereas in *S. cerevisiae*, Atg4-Egfp was dispersed in the cytoplasm and localized to nuclei (KERSHAW

and TALBOT 2009; KIKUMA and KITAMOTO 2011; LIU *et al.* 2010; NAKATOGAWA *et al.* 2012). Nuclear localization of SmATG4-EGFP could not be detected in our study.

SmATG4 seems to be necessary for proper processing and autophagosome formation since expression of EGFP-SmATG8 and SmATG8-EGFP in the ΔSmatg4 mutant led to the formation of larger aggregates instead of small punctate autophagosomes. Similar to our results, an accumulation of EGFP-Atg8 into aggregates has been observed in *M. oryzae* and *A. oryzae ATG4* deletion strains (KERSHAW and TALBOT 2009; KIKUMA and KITAMOTO 2011). It remains unclear whether the accumulation of unprocessed EGFP-SmATG8 is formed by an aggregation of EGFP or SmATG8. However, when the wt expressed SmATG8-EGFP or the mutated version SmATG8mut-EGFP, the fluorescence was dispersed in the cytoplasm and did not accumulate in aggregates (Fig. 27).

Interestingly, the expression of the putatively processed form EGFP-SmATG8^{G116} in ΔSmatg4 led to the formation of small punctate autophagosome-like structures confirming our assumption that Gly116 of SmATG8 is C-terminally exposed by the catalytic activity of SmATG4 und can undergo lipidation. Similar observations have been reported in *S. cerevisiae*, where introduction of EGFP-ATG8^{G116} in an *atg4*Δ mutant also resulted in formation of wt-like autophagosomes. Expression of the glycine-exposed Atg8^{G116} in the yeast *atg4Δ* mutant displayed significant autophagy defects and in *H. sapiens* the deconjugation of Atg8 by Atg4 has been shown to be crucial for the functioning of autophagy (KIRISAKO *et al.* 2000; NAKATOGAWA *et al.* 2012; SATOO *et al.* 2009). Just like in yeast, we showed that expression of the putatively processed form of SmATG8 did not complement the ΔSmatg4 phenotype, suggesting that delipidation and recycling of SmATG8 is also an important function of SmATG4.

SmATG4-EGFP is localized to the cytoplasm and EGFP-SmATG8 is found in small puncta which represent autophagosomes.

4.2.5 Deletion of *Smatg8* and *Smatg4* prevents pexophagy. In order to investigate the involvement of SmATG8 and SmATG4 in selective macroautophagy, we examined the extent of pexophagy in young and old hyphae of deletion mutants. Transformation of pRS-egfp-Smatg8-DsRed-SKL into ΔSmatg8 complemented the phenotype of the mutant. Thus, this

construct allowed us to simultaneously follow fluorescence signals of DsRED-SKL-labeled peroxisomes and EGFP-labeled autophagosomes.

Only in basal hyphae but not in tip cells both fluorescence signals were co-localized to the vacuole indicating that peroxisomes were delivered to the vacuole as cargo of autophagosomes and were degraded together (Fig. 28A). As shown for *A. oryzae* and *P. chrysogenum*, our result suggested that autophagic degradation of peroxisomes preferentially takes place in old basal hyphae but not in the growing hyphal tips (BARTOSZEWSKA *et al.* 2011; SHOJI *et al.* 2010). In *Smatg8* and *Smatg4* deletion mutants, pexophagy was abolished (Fig. 28B). Similarly, it was recently shown that pexophagy was not observed in a *P. pastoris* Pp*ATG8* deletion mutant (FARRE *et al.* 2008). In *P. chrysogenum,* deletion of *atg1* has been shown to prevent pexophagy and, furthermore, resulted in a significantly increased number of peroxisomes in subapical hyphae (BARTOSZEWSKA *et al.* 2011). However, in *S. macrospora*, an increased number of peroxisomes was not observed in ΔSmatg8 and ΔSmatg4 mutants.

Microscopic analysis revealed the involvement of SmATG8 and SmATG4 in pexophagy.

4.3 SmJLB1 is a transcription factor involved in fruiting-body development

4.3.1 The bZIP domain of the SmJLB1 transcription factor is highly conserved and orthologous to IDI-4/JlbA. Previously, by means of cross-species microarray experiments, *SMAC08510* a homologue of the *N. crassa NCU08055* was shown to be downregulated in the sterile mutants ΔSmta-1, pro1, pro11 and pro22 mutants (NOWROUSIAN *et al.* 2005; PÖGGELER *et al.* 2006). The closest homologues of *NCU08055* and *SMAC08510* that have been molecularly characterized are the bZIP transcription factors of JlbA and IDI-4 of *A. nidulans* and *P. anserina*, respectively (DEMENTHON *et al.* 2004; NOWROUSIAN *et al.* 2005; PÖGGELER *et al.* 2006; STRITTMATTER *et al.* 2001).

In a study of DEMENTHON *et al.* (2004) IDI-4 was described to be involved in autophagy and apoptosis. Its involvement in autophagy occurs by upregulation of *idi-7* (*ATG8*) and thus triggering autophagy induced apoptosis (DEMENTHON and SAUPE 2005). Since the abbreviation idi means induced during incompatibility and it has been described by NOWROUSIAN *et al.* (2010) that *S. macrospora* lacks incompatibility genes it would be inappropriate naming the *S. macrospora* orthologue *idi-4*. In *A. nidulans*, a bZIP transcription factor was described showing 17% similarities in an overall alignment and 32% in a bZIP domain alignment with the *S. macrospora* orthologue. Since jlb abbreviates jun-like bZIP, it seemed more adequate to name the *S. macropsora* gene *Smjlb1* (STRITTMATTER *et al.* 2001).

When the C-terminal bZIP domain of SmJLB1 was compared to other fungal IDI-4/JlbA-like proteins, SmJLB1 displayed a high degree of conservation, while the N-terminus did not. This has also been described for the N-terminal region of *P. anserina*, and similarly IDI-4 shows no significant homology when compared to other bZIP domain containing proteins of related ascomycetes (DEMENTHON *et al.* 2004).

As described by STRITTMATTER *et al.* (2001) and presented in Fig. 29, the basic amino-acid and the leucine-zipper domains are conserved in IDI-4/JlbA-like proteins of ascomycetes. In SmJLB1 of *S. macrospora*, the residues Asn165, Ala168, Ala169 and Arg173 of the DNA-binding domain are also conserved among SmJLB1 orthologues of ascomycetes while Ser172 is only present in yeast Gcn4. These residues have been shown to contact DNA in the Gcn4 complex and are common among the majority of fungal bZIP transcription factors (ELLENBERGER *et al.* 1992).

Similarly, the leucine residues Leu183, Leu197 and Leu211 of SmJLB1 of the leucine-zipper domain are conserved among ascomycetes. Interestingly, Leu160 of yeast Gcn4 is not conserved among the SmJLB1 orthologues of the filamentous fungi, but altered to an isoleucine (Ile190). Arg204 of SmJLB1 is not present in Gcn4 but in orthologues of *N. crassa*, *P. anserina*, *A. oryzae* and *M. oryzae*, respectively.

Recently, TIAN *et al.* (2011) analyzed the phylogenetic relationship of bZIP transcription factors in *N. crassa*, and other ascomycetes. The clade which contains orthologues of the *S. cerevisiae* Gcn4 was shown to be split into three subclades. The first subclade is composed of Gcn4 homologues of yeasts, the *S. cerevisiae* Gcn4, the *C. albicans* CaGCN4 and the *Yarrowia lipolytica* YALIOE27742g. The second subclade combines CPC1 of *N. crassa*, MG00602.4 of *M. grisiae* and AN3675.2, the *A. nidulans* CpcA which are considered to be Gcn4 orthologues. The third subclade displays AN1812.2 the *A. nidulans* JlbA, *M. grisiae* MG01990.4 and NCU08055, the *N. crassa* IDI-4, which is involved in the apoptotic machinery (FEDOROVA *et al.* 2005; STRITTMATTER *et al.* 2001). Regarding these facts, it is assumable that SmJLB1 is the orthologue of *A. nidulans* JlbA, *N. crassa* IDI-4 and *P. anserina* IDI-4 and therefore involved in the nutritional stress response (DEMENTHON *et al.* 2004; FEDOROVA *et al.* 2005). It is presumable that SmJLB1 is more similar to IDI-4/JlbA than to Gcn4 or CpcA since SmJLB1 similarity towards those is less compared to its similarity towards IDI-4/JlbA.

The SmJLB1 bZIP domain is strongly conserved including residues for DNA binding and dimerization. SmJLB1 is more similar to the *P. anserina* IDI-4 and *A. nidulans* JlbA than to *N. crassa* and *A. nidulans* Gcn4 orthologues.

4.3.2 Deletion of *Smjlb1* leads to impairment of vegetative growth and perithecia development but ascospore germination is not influenced. Generation of a homokaryotic ΔSmjlb1 strain revealed several phenotypic alterations of the mutant strain.

Deletion of *Smjlb1* resulted in retardation of the growth velocity. This effect is drastically increased under starvation condition (Fig. 34). Furthermore, vegetative growth is restricted also by loss of the foraging ability (Fig. 33). In *A. nidulans*, it was shown that the expression of *jlbA* was induced by amino-acid starvation (STRITTMATTER *et al.* 2001).

In addition to the reduced growth rate, deletion of *Smjlb1* resulted in a block of perithecia development which ceased at the stage of protoperithecia formation. Only when grown on SWG fructification medium and SWG containing 3-AT, the perithecia developed. However, as shown in Fig. 32, these fruiting bodies did not contain ascospores. Additionally, ΔSmjlb1 displayed no alteration in hyphal morphology as well as no change in pigmentation, hyphal density and aerial hyphae development. In contrast to *S. macrospora*, in *P. anserina*, deletion of *idi-4* led to no obvious phenotype. Neither the growth rate nor the pigmentation or aerial hyphae differentiation or male/female structures were changed (DEMENTHON *et al.* 2004).

In contrast to the autophagy mutants ΔSmatg8 and ΔSmatg4, the germination rate of ΔSmjlb1 was not reduced (Fig. 37). Additionally, hyphal fusion was not impaired in the deletion mutant indicating that *Smjlb1* is not involved in this process (Fig. 35 and 36). To date, no reports are available with regards to *Smjlb1* orthologues and their involvement in ascospore germination and hyphal anastomoses.

Deletion of *Smjlb1* impairs fruiting-body development and vegetative growth but has no impact on hyphal fusion and germination efficiency.

4.3.3 *Smjlb1*, *Smatg8* and *Smatg4* are expressed constitutively and *Smatg8* as well as *Smatg4* are upregulated in ΔSmjlb1. Quantitative real-time analysis revealed that *Smjlb1*, *Smatg8* and *Smatg4* are constitutively expressed throughout the sexual and vegetative growth (Fig. 38). Additionally, no significant differences in regulation were observed focusing on a certain stage of development except for the minor upregulated expression of *Smjlb1* and *Smatg4* and the fifth day of development. This indicates a similar expression pattern throughout all stages of development for *Smjlb1*, *Smatg8* and *Smatg4*. To date, no reports are available for *Smjlb1* orthologues regarding expression studies, under similar conditions. Only in *P. anserina* and *A. nidulans* upregulation of *idi-4* and *jlbA* upon amino-acid starvation was reported (DEMENTHON *et al.* 2004; STRITTMATTER *et al.* 2001).

Constitutive expression for yeast *ATG8* and *ATG4* orthologues have been reported for several organisms, consolidating the findings of this work. In *Triticum turgidum* (poulard wheat), *Oryza sativa* (rice) and *P. anserina* a constitutive expression for *ATG8* orthologues was verified by real-time PCR (KUZUOGLU-OZTURK *et al.* 2012; PINAN-LUCARRE *et al.* 2003; SU *et al.* 2006). In *O. sativa*, basal expression of *ATG4* was observed also (SU *et al.* 2006).

Similarly, in *M. oryzae* a constitutive expression of *MoATG4* throughout vegetative growth and fungal development was monitored by fluorescence microscopy using a *MoATG4-GFP* fusion gene under its native promoter (LIU *et al.* 2010).

Examination of *Smatg8* and *Smatg4* expression levels in ΔSmjlb1 revealed that, the genes are upregulated when compared to wt expression (Fig. 39). This leads to the conclusion that SmJLB1 might act as a repressor, regulating transcription negatively.

Interestingly, in *P. anserina* it has been reported that overexpression of *idi-4* leads to a tenfold upregulation of *idi-7* (*ATG8*) indicating that in *P. anserina* IDI-4 positively regulates transcription of *idi-7* and acts as an activator. In this study, DEMENTHON *et al.* (2003) could also show that expression of *idi-7* still occurs in the Δidi-4 strain. Unfortunately, they did not show whether this regulation is either up or down in comparison to wt (DEMENTHON *et al.* 2003). These findings do not exactly represent the findings of this study. However, reports of other organisms are missing regarding Atg8 or Atg4 regulation by a SmJLB1 orthologue.

Previous studies have shown that in *S. cerevisiae* the positive transcription factor Gcn4 regulates expression of its target genes by binding to their promoters at so called GCRE (Gcn4 protein recognition element) sequences (5'-TGACTC-3'). In later studies, this sequence was extended to 5'-(A)TGA(G/C)TCA(T)-3' and it was reported that Gcn4 is able to bind to variants of this motif such as 5'-TGATTCA-3', 5'-TGACTCT-3', 5'-TGACTGA-3', 5'-TGACTAT-3' and 5'-ATGACTCT-3' or to bind to half-sites of these GCRE motifs (ARNDT and FINK 1986; HOLLENBECK and OAKLEY 2000; NATARAJAN *et al.* 2001).

Interestingly, it has been described that JlbA contains sequence elements in its promoter region which share a high similarity with the CPRE (Cpc1 protein recognition element) motif and that this motif is equal to the GCRE sequence (STRITTMATTER *et al.* 2001). It has been reported that not only promoters of Gcn4-regulated genes but also the regulators themselves contain a CPRE/GCRE-like motif such as the *cpcA* promoter of *A. niger* (WANKE *et al.* 1997). Additionally, in a *cpcA*Δ strain induction of JlbA by 3-AT led to an increased expression level indicating a self-regulation of JlbA or at least a CpcA-independent regulation of *jlbA* (STRITTMATTER *et al.* 2001). Furthermore, in *P. anserina* positive auto regulation of *idi-4* and the *in vitro* interaction of the IDI-4 bZIP domain with the ATGANTCAT motif of the *idi-7* promoter region has been reported (DEMENTHON *et al.* 2004). According to these studies, it

seems that the regulation of *idi-7* expression (*ATG8*) is dependent on a 5'-ATGANTCAT-3'-like motif.

Using the LALIGN (http://www.ch.embnet.org/software/LALIGN_form.html) online tool, motifs similar to the GCRE sequence variants were identified in the promoter regions of *Smjlb1, Smatg8* and *Smatg4*. The identified motifs which were found in the promoter regions show minor alterations when compared to the GCRE motifs and are displayed in Tab. 7. The presence of these GCRE-like motifs in *Smjlb1, Smatg8*, and *Smatg4* leads to the assumption that expression of *Smatg8* and *Smatg4* is regulated by SmJLB1 and that expression of *Smjlb1* might be regulated by SmJLB1 itself.

Table 7 depicts motifs similar to the GCRE sequence found in the promoter region of *Smjlb1, Smatg8* and *Smatg4*, respectively.

Table 7. GCRE–like motifs in in the promoter regions of *Smjlb1, Smatg8* and *Smatg4*

promoter of gene:	TGATTCA	TGACTCT	TGACTGA	TGACTAT	ATGACTCT
Smjlb1	GATTCA 1485-1490	TGACTC 500-505 GACTCT 1674-1679	TGACTG 1005-1010 and 1344-1349	TGACTT 313-319 and 1931-1937 TGACTGT 1343-1349	AAGACTCT 1674-1681
Smatg8	TGATTCA 535-541	TGATTCA 1294-1299	---	TGACTA 863-868	TGATTCA 1294-1299
Smatg4	TAATTCA 490-496 TGCTTCA 729-735	GACTCT 1359-1364 and 2085-2090	TGACAGA 201-207 TGCCTGA 368-374 TGAATGA 735-759	TGACTA 365-370	GACTCT 1359-1364 and 2085-2090

Numbers represent positions of the identified motifs, upstream of the start codon of the respective gene; bases altered in comparison to the GCRE motif are indicated by underlining.

The deletion of *Smjlb1* was shown to upregulate expression of *Smatg8* and *Smatg4* and therefore autophagy as well. Therefore, it might be possible that autophagy is also induced in the ΔSmjlb1 mutant.

In the sterile mutants ΔSmta-1, pro1, pro11 and pro22 a microarray analysis revealed that *Smjlb1* was significantly downregulated and thus autophagy might be induced in these mutant strains (NOWROUSIAN *et al.* 2005; PÖGGELER *et al.* 2006). However, it cannot be unraveled if these similar phenotypes are caused by an upregulation of autophagy *per se* since deletion of *Smatg8* and *Smatg4* also leads to a sterile phenotype which is similar to pro-mutants.

Taken together, *Smjlb1*, *Smatg8* and *Smatg4* are constitutively expressed during the vegetative and sexual development. Upregulation of either *Smatg8* or *Smatg4* in ΔSmjlb1 indicates that SmJLB1 might act as a repressor of autophagy genes.

4.3.4 SmJLB1-EGFP displays a nuclear localization. The SmJLB1-EGFP fusion protein was localized to nuclei which can be expected for a transcription factor (Fig. 40). In *P. anserina* localization of EGFP-IDI-4bZIP to the nucleus was reported as well. However, a full length IDI-4-EGFP fusion protein expressed under control of its native promoter could not be observed (DEMENTHON *et al.* 2004).

Furthermore, it has been reported that basic domains of various bZIP transcription factors have a dual role in nuclear localization and DNA binding. Residues 190-206 in IDI-4 of *P. anserina* were predicted by *in silico* analysis to be a NLS (nuclear localization signal) (DEMENTHON *et al.* 2004). The amino-acid residues of this putative NLS correspond to residues 161-177 of SmJLB1, and are identical in sequence (Fig. 29), suggesting the presence of a nuclear localization signal in SmJLB1 as well. This was confirmed by *in silico* analysis using the online application NLStradamus with an adjustment called “4 state HMM static”. A NLS from residue 161 to 173, similar to the reports of *P. anserina*, was predicted in SmJLB1 as well (http://www.moseslab.csb.utoronto.ca/NLStradamus/).

It has to be taken into account that SmJLB1-EGFP was not able to complement the deletion phenotype of the ΔSmjlb1 strain, thus functionality was not verified. Interestingly, overexpression experiments of IDI-4 in *P. anserina* under the control of a constitutive *gpd* promoter revealed, that overexpression of *idi-4* is lethal in *P. anserina*. This was assumed because DEMENTHON *et al.* (2004) were not able to generate a mutant carrying the

overexpression construct. As stated previously, the *Smjlb1-egfp* fusion gene was also expressed under the control of a *gpd* promoter, but we were able to generate a homokaryotic strain carrying the overexpression construct. Thus, these results differ drastically to the reports of *P. anserina* (DEMENTHON *et al.* 2004).

SmJLB1-EGFP was localized to the nucleus and SmJLB1 contains a putative nuclear localization signal in its basic domain.

4.4 Outlook

The data gathered during this work implies an impact of autophagy on the fruiting-body development and vegetative growth of *S. macrospora*. An involvement of the kinases Vps34 and Vps15 not only in autophagy but also in vacuolar protein sorting, pheromone and Tor sensing has been reported (HERMAN and EMR 1990; KOELLE 2006; OBARA and OHSUMI 2011b; YAN and BACKER 2007). In this study, it was shown that the *S. macrospora* orthologues *Smvps34* and *Smvps15* are required for viability, since isolation of single-spore isolates failed. The generation of temperature-sensitive mutants would elucidate whether deletion of both genes is lethal or solely influence the germination. The temporary on and off switching of the genes would allow better phenotypical analysis than the permanent shutdown. Furthermore, using RNA interference under control of different constitutive promoters with different strength in expression would allow the successive downregulation of *Smvps34* and *Smvps15*, most likely revealing a partial deletion phenotype. Another approach would be to investigate if overexpression of *Smvps34* or *Smvps15* has a phenotypical impact. Localization studies of SmVPS34 and SmVPS15 under nutrient rich and starvation conditions would elucidate their involvement in autophagy and VPS (vacuolar protein sorting) since both proteins are localized to the PAS under starvation and to the endosome under nutrient-rich conditions (OBARA and OHSUMI 2011b). To elucidate if SmVPS34 and SmVPS15 are involved in pheromone sensing in *S. macrospora*, as described for *S. cerevisiae*, real-time experiments under pheromone treated and untreated conditions would show if pheromone treatment leads to upregulation. These further experiments would at least be an approximation to the functions of SmVPS34 and SmVPS15 and their involvement in fruiting-body development in *S. macrospora*.

In *P. anserina* it has been reported that the bZIP transcription factor IDI-4 is involved autophagic cell death and in regulation of *idi-7* (*ATG8*) by binding to a GCRE-like motif (DEMENTHON and SAUPE 2005; DEMENTHON *et al.* 2004). It has also been shown for the bZIP transcription factor JlbA in *A. nidulans* which is an orthologue of IDI-4 that it contains amino-acid residues able to bind this GCRE motif as well as sequence elements in its own promoter (STRITTMATTER *et al.* 2001). In this work, it was shown that *Smjlb1* deletion led to impairment in fruiting-body development and in vegetative growth. Furthermore, qRT-PCR experiments implied the regulation of *Smatg8* and *Smatg4* by SmJLB1. Analysis of the promoter region of *Smatg8*, *Smatg4* and *Smjlb1* revealed the presence of motifs similar to the GCRE sequence. The regulatory network of SmJLB1 could be further elucidated by searching for GCRE motifs in the promoter region of other autophagy related genes. In addition, genes involved in apoptosis should be examined for a GCRE motif to analyze if SmJLB1 might also regulate apoptotic genes as well. In an extended expression analysis expression of *Smjlb1* should be examined under amino-acid starvation conditions or other stress conditions. Microarray experiments performed in wt versus ΔSmjlb1 would unravel the regulatory network of SmJLB1. In *P. anserina* over-expression of IDI-4 was reported to be lethal (DEMENTHON *et al.* 2004). However, overexpression of *egfp-Smjlb1* was not lethal but failed to complement the deletion phenotype. Expression of SmJLB1 under control of the *gpd* promoter would reveal if the complementation of ΔSmjlb1 failed due to the *egfp* fusion or if overexpression of *Smjlb1* has a negative effect on *S. macrospora's* viability. A complementation experiment of a yeast *GCN4* deletion mutant with *Smjlb1* cDNA would finally reveal if SmJLB1 is a distant orthologue of Gcn4 or if it belongs to a separate group of bZIP transcriptions factors.

The importance of Atg8 for the autophagosome formation as structural component has been thoroughly investigated in *S. cerevisiae* and other ascomycets (GENG and KLIONSKY 2008). The cysteine protease Atg4 has been shown to be not only crucial for Atg8 processing but also for the deconjugation of Atg8 (KIRISAKO *et al.* 2000; YU *et al.* 2012). In this work, it was shown that deletion of both *Smatg8* and *Smatg4* leads to incapability of fruiting-body development and to an impairment of vegetative growth. Conservation of these genes among ascomycetes was confirmed in a yeast complementation experiment. Protein interaction experiments with SmATG8 revealed that it interacts with several enzymes. Interaction with the putative cargo receptor SmNBR1 and SMAC01312, a predicted woronin body protein,

seem to be the most interesting interaction partners of SmATG8 on the first sight. These interactions should be first verified by Y2H and GFP-Trap analysis. Further steps to verify involvement of SmNBR1 and SMAC01312 in autophagy by interaction with SmATG8 would be deletion of these genes and co-localization experiments.

Deletion of *Smjlb1*, *Smatg8* and *Smatg4* exhibited a similar phenotype which is the absence of fruiting-body development. In accordance to that, the question arises if *S. macrospora* is not able to form perithecia due to shortage of nutrients caused by breakdown of autophagy or if autophagy regulates processes involved in fruiting-body formation. An easy approach to answer this question would be growth tests. By a decrease of amino acid and nutrient supply, the wt could be analyzed for perithecia development, and restoration of perithecia formation should be surveyed in ΔSmjlb1, ΔSmatg8 and ΔSmatg4 upon increase of amino acid and nutrient supply.

5. Literature

ABELIOVICH, H., W. A. DUNN, JR., J. KIM and D. J. KLIONSKY, 2000 Dissection of autophagosome biogenesis into distinct nucleation and expansion steps. J Cell Biol **151:** 1025-1034.

AMAR, N., G. LUSTIG, Y. ICHIMURA, Y. OHSUMI and Z. ELAZAR, 2006 Two newly identified sites in the ubiquitin-like protein Atg8 are essential for autophagy. EMBO Rep **7:** 635-642.

AMBERG, D., D. BURKE and J. STRATHERN, 2005 *Methods in Yeast Genetics: A Cold Spring Harbor Laboratory Course Manual*. Cold Spring Harbor Laboratory Press.

ARNDT, K., and G. R. FINK, 1986 GCN4 protein, a positive transcription factor in yeast, binds general control promoters at all 5' TGACTC 3' sequences. Proc Natl Acad Sci USA **83:** 8516-8520.

ASAKURA, M., S. NINOMIYA, M. SUGIMOTO, M. OKU, S. YAMASHITA *et al.*, 2009 Atg26-mediated pexophagy is required for host invasion by the plant pathogenic fungus *Colletotrichum orbiculare*. Plant Cell **21:** 1291-1304.

BABA, M., M. OSUMI and Y. OHSUMI, 1995 Analysis of the membrane structures involved in autophagy in yeast by freeze-replica method. Cell Struct Funct **20:** 465-471.

BAKKER, B. M., C. BRO, P. KOTTER, M. A. LUTTIK, J. P. VAN DIJKEN *et al.*, 2000 The mitochondrial alcohol dehydrogenase Adh3p is involved in a redox shuttle in *Saccharomyces cerevisiae*. J Bacteriol **182:** 4730-4737.

BARTOSZEWSKA, M., J. A. KIEL, R. A. BOVENBERG, M. VEENHUIS and I. J. VAN DER KLEI, 2011 Autophagy deficiency promotes beta-lactam production in *Penicillium chrysogenum*. Appl Environ Microbiol **77:** 1413-1422.

BEAU, I., A. ESCLATINE and P. CODOGNO, 2008 Lost to translation: when autophagy targets mature ribosomes. Trends Cell Biol **18:** 311-314.

BECKER, D. M., and V. LUNDBLAD, 2001 Introduction of DNA into yeast cells. Curr Protoc Mol Biol **Chapter 13:** Unit13 17.

BERNHARDS, Y., and S. PÖGGELER, 2011 The phocein homologue SmMOB3 is essential for vegetative cell fusion and sexual development in the filamentous ascomycete *Sordaria macrospora*. Curr Genet **57:** 133-149.

BIRNBOIM, H. C., and J. DOLY, 1979 A rapid alkaline extraction procedure for screening recombinant plasmid DNA. Nucleic Acids Res **7:** 1513-1523.

BLOEMENDAL, S., Y. BERNHARDS, K. BARTHO, A. DETTMANN, O. VOIGT *et al.*, 2012 A homologue of the human STRIPAK complex controls sexual development in fungi. Mol Microbiol **84:** 310-323.

BLOEMENDAL, S., K. M. LORD, C. RECH, B. HOFF, I. ENGH *et al.*, 2010 A mutant defective in sexual development produces aseptate ascogonia. Eukaryot Cell **9:** 1856-1866.

BUDOVSKAYA, Y. V., H. HAMA, D. B. DEWALD and P. K. HERMAN, 2002 The C terminus of the Vps34p phosphoinositide 3-kinase is necessary and sufficient for the interaction with the Vps15p protein kinase. J Biol Chem **277:** 287-294.

BURSCH, W., 2004 Multiple cell death programs: Charon's lifts to Hades. FEMS Yeast Res **5:** 101-110.

BYFIELD, M. P., J. T. MURRAY and J. M. BACKER, 2005 hVps34 is a nutrient-regulated lipid kinase required for activation of p70 S6 kinase. J Biol Chem **280:** 33076-33082.

CAO, Y., H. CHEONG, H. SONG and D. J. KLIONSKY, 2008 In vivo reconstitution of autophagy in *Saccharomyces cerevisiae*. J Cell Biol **182:** 703-713.

CHEN, Y., and D. J. KLIONSKY, 2011 The regulation of autophagy - unanswered questions. J Cell Sci **124:** 161-170.

CHRISTIANSON, T. W., R. S. SIKORSKI, M. DANTE, J. H. SHERO and P. HIETER, 1992 Multifunctional yeast high-copy-number shuttle vectors. Gene **110:** 119-122.

COLOT, H. V., G. PARK, G. E. TURNER, C. RINGELBERG, C. M. CREW *et al.*, 2006 A high-throughput gene knockout procedure for *Neurospora* reveals functions for multiple transcription factors. Proc Natl Acad Sci USA **103:** 10352-10357.

COPPIN, E., R. DEBUCHY, S. ARNAISE and M. PICARD, 1997 Mating types and sexual development in filamentous ascomycetes. Microbiol Mol Biol Rev **61:** 411-428.

CORADETTI, S. T., J. P. CRAIG, Y. XIONG, T. SHOCK, C. TIAN *et al.*, 2012 Conserved and essential transcription factors for cellulase gene expression in ascomycete fungi. Proc Natl Acad Sci USA **109:** 7397-7402.

DEMENTHON, K., M. PAOLETTI, B. PINAN-LUCARRE, N. LOUBRADOU-BOURGES, M. SABOURIN *et al.*, 2003 Rapamycin mimics the incompatibility reaction in the fungus *Podospora anserina*. Eukaryot Cell **2:** 238-246.

DEMENTHON, K., and S. J. SAUPE, 2005 DNA-binding specificity of the IDI-4 basic leucine zipper factor of *Podospora anserina* defined by systematic evolution of ligands by exponential enrichment (SELEX). Eukaryot Cell **4:** 476-483.

DEMENTHON, K., S. J. SAUPE and C. CLAVE, 2004 Characterization of IDI-4, a bZIP transcription factor inducing autophagy and cell death in the fungus *Podospora anserina*. Mol Microbiol **53:** 1625-1640.

DOU, Z., M. CHATTOPADHYAY, J. A. PAN, J. L. GUERRIERO, Y. P. JIANG *et al.*, 2010 The class IA phosphatidylinositol 3-kinase p110-beta subunit is a positive regulator of autophagy. J Cell Biol **191:** 827-843.

DUPONT, N., N. TEMIME-SMAALI and F. LAFONT, 2010 How ubiquitination and autophagy participate in the regulation of the cell response to bacterial infection. Biol Cell **102:** 621-634.

ELLENBERGER, T. E., C. J. BRANDL, K. STRUHL and S. C. HARRISON, 1992 The GCN4 basic region leucine zipper binds DNA as a dimer of uninterrupted alpha helices: crystal structure of the protein-DNA complex. Cell **71:** 1223-1237.

ELLEUCHE, S., and S. PÖGGELER, 2008 Visualization of peroxisomes via SKL-tagged DsRed protein in *Sordaria macrospora*. Fungal Genet Reports **55:** 9-12.

ELLEUCHE, S., and S. PÖGGELER, 2009 Beta-carbonic anhydrases play a role in fruiting body development and ascospore germination in the filamentous fungus *Sordaria macrospora*. PLoS One **4:** e5177.

ELLISON, C. E., J. E. STAJICH, D. J. JACOBSON, D. O. NATVIG, A. LAPIDUS *et al.*, 2011 Massive changes in genome architecture accompany the transition to self-fertility in the filamentous fungus *Neurospora tetrasperma*. Genetics **189:** 55-69.

ENGH, I., M. NOWROUSIAN and U. KÜCK, 2010 *Sordaria macrospora*, a model organism to study fungal cellular development. Eur J Cell Biol **89:** 864-872.

EPPLE, U. D., I. SURIAPRANATA, E. L. ESKELINEN and M. THUMM, 2001 Aut5/Cvt17p, a putative lipase essential for disintegration of autophagic bodies inside the vacuole. J Bacteriol **183:** 5942-5955.

FARRE, J. C., R. MANJITHAYA, R. D. MATHEWSON and S. SUBRAMANI, 2008 PpAtg30 tags peroxisomes for turnover by selective autophagy. Dev Cell **14:** 365-376.

FEDOROVA, N. D., J. H. BADGER, G. D. ROBSON, J. R. WORTMAN and W. C. NIERMAN, 2005 Comparative analysis of programmed cell death pathways in filamentous fungi. BMC Genomics **6:** 177.

FU, C., P. IYER, A. HERKAL, J. ABDULLAH, A. STOUT *et al.*, 2011 Identification and characterization of genes required for cell-to-cell fusion in *Neurospora crassa*. Eukaryot Cell **10:** 1100-1109.

FUJITA, N., T. ITOH, H. OMORI, M. FUKUDA, T. NODA *et al.*, 2008 The Atg16L complex specifies the site of LC3 lipidation for membrane biogenesis in autophagy. Mol Biol Cell **19:** 2092-2100.

GALAGAN, J. E., S. E. CALVO, K. A. BORKOVICH, E. U. SELKER, N. D. READ *et al.*, 2003 The genome sequence of the filamentous fungus *Neurospora crassa*. Nature **422:** 859-868.

GENG, J., and D. J. KLIONSKY, 2008 The Atg8 and Atg12 ubiquitin-like conjugation systems in macroautophagy. 'Protein modifications: beyond the usual suspects' review series. EMBO Rep **9:** 859-864.

GIETZ, D., A. ST JEAN, R. A. WOODS and R. H. SCHIESTL, 1992 Improved method for high efficiency transformation of intact yeast cells. Nucleic Acids Res **20:** 1425.

GLASS, N. L., and I. KANEKO, 2003 Fatal attraction: nonself recognition and heterokaryon incompatibility in filamentous fungi. Eukaryot Cell **2:** 1-8.

GREENWALD, C. J., T. KASUGA, N. L. GLASS, B. D. SHAW, D. J. EBBOLE *et al.*, 2010 Temporal and spatial regulation of gene expression during asexual development of *Neurospora crassa*. Genetics **186:** 1217-1230.

GUNTHER, J., M. NGUYEN, A. HARTL, W. KUNKEL, P. F. ZIPFEL *et al.*, 2005 Generation and functional in vivo characterization of a lipid kinase defective phosphatidylinositol 3-kinase Vps34p of *Candida albicans*. Microbiology **151:** 81-89.

HANADA, T., N. N. NODA, Y. SATOMI, Y. ICHIMURA, Y. FUJIOKA *et al.*, 2007 The Atg12-Atg5 conjugate has a novel E3-like activity for protein lipidation in autophagy. J Biol Chem **282:** 37298-37302.

HARDING, T. M., K. A. MORANO, S. V. SCOTT and D. J. KLIONSKY, 1995 Isolation and characterization of yeast mutants in the cytoplasm to vacuole protein targeting pathway. J Cell Biol **131:** 591-602.

HERMAN, P. K., and S. D. EMR, 1990 Characterization of *VPS34*, a gene required for vacuolar protein sorting and vacuole segregation in *Saccharomyces cerevisiae*. Mol Cell Biol **10:** 6742-6754.

HERMAN, P. K., J. H. STACK, J. A. DEMODENA and S. D. EMR, 1991a A novel protein kinase homolog essential for protein sorting to the yeast lysosome-like vacuole. Cell **64:** 425-437.

HERMAN, P. K., J. H. STACK and S. D. EMR, 1991b A genetic and structural analysis of the yeast Vps15 protein kinase: evidence for a direct role of Vps15p in vacuolar protein delivery. EMBO J **10:** 4049-4060.

HOFFMAN, C. S., and F. WINSTON, 1987 A ten-minute DNA preparation from yeast efficiently releases autonomous plasmids for transformation of *Escherichia coli*. Gene **57:** 267-272.

HOFFMANN, B., O. VALERIUS, M. ANDERMANN and G. H. BRAUS, 2001 Transcriptional autoregulation and inhibition of mRNA translation of amino acid regulator gene *cpcA* of filamentous fungus *Aspergillus nidulans*. Mol Biol Cell **12:** 2846-2857.

HOLLENBECK, J. J., and M. G. OAKLEY, 2000 GCN4 binds with high affinity to DNA sequences containing a single consensus half-site. Biochemistry **39:** 6380-6389.

ICHIDA, K., T. MATSUMURA, R. SAKUMA, T. HOSOYA and T. NISHINO, 2001 Mutation of human molybdenum cofactor sulfurase gene is responsible for classical xanthinuria type II. Biochem Biophys Res Commun **282:** 1194-1200.

ICHIMURA, Y., T. KIRISAKO, T. TAKAO, Y. SATOMI, Y. SHIMONISHI *et al.*, 2000 A ubiquitin-like system mediates protein lipidation. Nature **408:** 488-492.

JAMES, P., J. HALLADAY and E. A. CRAIG, 1996 Genomic libraries and a host strain designed for highly efficient two-hybrid selection in yeast. Genetics **144:** 1425-1436.

JOSEFSEN, L., A. DROCE, T. E. SONDERGAARD, J. L. SORENSEN, J. BORMANN *et al.*, 2012 Autophagy provides nutrients for nonassimilating fungal structures and is necessary for plant colonization but not for infection in the necrotrophic plant pathogen *Fusarium graminearum*. Autophagy **8:** 326-37.

KANKI, T., K. WANG, M. BABA, C. R. BARTHOLOMEW, M. A. LYNCH-DAY *et al.*, 2009a A genomic screen for yeast mutants defective in selective mitochondria autophagy. Mol Biol Cell **20:** 4730-4738.

KANKI, T., K. WANG, Y. CAO, M. BABA and D. J. KLIONSKY, 2009b Atg32 is a mitochondrial protein that confers selectivity during mitophagy. Dev Cell **17:** 98-109.

KASUGA, T., and N. L. GLASS, 2008 Dissecting colony development of *Neurospora crassa* using mRNA profiling and comparative genomics approaches. Eukaryot Cell **7:** 1549-1564.

KAUSHIK, S., U. BANDYOPADHYAY, S. SRIDHAR, R. KIFFIN, M. MARTINEZ-VICENTE *et al.*, 2011 Chaperone-mediated autophagy at a glance. J Cell Sci **124:** 495-499.

KERSCHER, O., R. FELBERBAUM and M. HOCHSTRASSER, 2006 Modification of proteins by ubiquitin and ubiquitin-like proteins. Annu Rev Cell Dev Biol **22:** 159-180.

KERSHAW, M. J., and N. J. TALBOT, 2009 Genome-wide functional analysis reveals that infection-associated fungal autophagy is necessary for rice blast disease. Proc Natl Acad Sci USA **106:** 15967-15972.

KETELAAR, T., C. VOSS, S. A. DIMMOCK, M. THUMM and P. J. HUSSEY, 2004 *Arabidopsis* homologues of the autophagy protein Atg8 are a novel family of microtubule binding proteins. FEBS Lett **567:** 302-306.

KIEL, J. A., K. B. RECHINGER, I. J. VAN DER KLEI, F. A. SALOMONS, V. I. TITORENKO *et al.*, 1999 The *Hansenula polymorpha PDD1* gene product, essential for the selective degradation of peroxisomes, is a homologue of *Saccharomyces cerevisiae* Vps34p. Yeast **15:** 741-754.

KIKUMA, T., and K. KITAMOTO, 2011 Analysis of autophagy in *Aspergillus oryzae* by disruption of *Aoatg13*, *Aoatg4*, and *Aoatg15* genes. FEMS Microbiol Lett **316:** 61-69.

KIKUMA, T., M. OHNEDA, M. ARIOKA and K. KITAMOTO, 2006 Functional analysis of the *ATG8* homologue *Aoatg8* and role of autophagy in differentiation and germination in *Aspergillus oryzae*. Eukaryot Cell **5:** 1328-1336.

KIRISAKO, T., Y. ICHIMURA, H. OKADA, Y. KABEYA, N. MIZUSHIMA *et al.*, 2000 The reversible modification regulates the membrane-binding state of Apg8/Aut7 essential for autophagy and the cytoplasm to vacuole targeting pathway. J Cell Biol **151:** 263-276.

KIRKIN, V., T. LAMARK, Y. S. SOU, G. BJORKOY, J. L. NUNN *et al.*, 2009 A role for NBR1 in autophagosomal degradation of ubiquitinated substrates. Mol Cell **33:** 505-516.

KLIONSKY, D. J., 2005 The molecular machinery of autophagy: unanswered questions. J Cell Sci **118:** 7-18.

KLIONSKY, D. J., J. M. CREGG, W. A. DUNN, JR., S. D. EMR, Y. SAKAI *et al.*, 2003 A unified nomenclature for yeast autophagy-related genes. Dev Cell **5:** 539-545.

KLIONSKY, D. J., A. M. CUERVO and P. O. SEGLEN, 2007 Methods for monitoring autophagy from yeast to human. Autophagy **3:** 181-206.

KLIX, V., M. NOWROUSIAN, C. RINGELBERG, J. J. LOROS, J. C. DUNLAP *et al.*, 2010 Functional characterization of MAT1-1-specific mating-type genes in the homothallic ascomycete *Sordaria macrospora* provides new insights into essential and nonessential sexual regulators. Eukaryot Cell **9:** 894-905.

KOELLE, M. R., 2006 Heterotrimeric G protein signaling: Getting inside the cell. Cell **126:** 25-27.

KÜCK, U., 2005 *Praktikum der Molekulargenetik*, Berlin Heidelberg New York: Springer-Verlag.

KÜCK, U., S. PÖGGELER, M. NOWROUSIAN, N. NOLTING and I. ENGH, 2009 *Sordaria macrospora,* a model system for fungal development., pp. 17-39. in *THE MYCOTA XV, Physiology and Genetics: Selected Basic and Applied Aspects.*, edited by T. ANKE and D. WEBER. Springer Verlag, Heidelberg.

KUZUOGLU-OZTURK, D., O. CEBECI YALCINKAYA, B. A. AKPINAR, G. MITOU, G. KORKMAZ *et al.*, 2012 Autophagy-related gene, *TdAtg8*, in wild emmer wheat plays a role in drought and osmotic stress response. Planta Epub ahead of print.

LAEMMLI, U. K., 1970 Cleavage of structural proteins during the assembly of the head of bacteriophage T4. Nature **227:** 680-685.

LECELLIER, G., and P. SILAR, 1994 Rapid methods for nucleic acids extraction from Petri dish-grown mycelia. Curr Genet **25:** 122-123.

LEE, K. S., J. L. PATTON, M. FIDO, L. K. HINES, S. D. KOHLWEIN *et al.*, 1994 The *Saccharomyces cerevisiae PLB1* gene encodes a protein required for lysophospholipase and phospholipase B activity. J Biol Chem **269:** 19725-19730.

LEVINE, B., and D. J. KLIONSKY, 2004 Development by self-digestion: molecular mechanisms and biological functions of autophagy. Dev Cell **6:** 463-477.

LEVINE, B., and J. YUAN, 2005 Autophagy in cell death: an innocent convict? J Clin Invest **115:** 2679-2688.

LEWIS, Z. A., A. CORREA, C. SCHWERDTFEGER, K. L. LINK, X. XIE *et al.*, 2002 Overexpression of White Collar-1 (WC-1) activates circadian clock-associated genes, but is not sufficient to induce most light-regulated gene expression in *Neurospora crassa*. Mol Microbiol **45:** 917-931.

LINDMO, K., A. BRECH, K. D. FINLEY, S. GAUMER, D. CONTAMINE *et al.*, 2008 The PI 3-kinase regulator Vps15 is required for autophagic clearance of protein aggregates. Autophagy **4:** 500-506.

LIU, T. B., X. H. LIU, J. P. LU, L. ZHANG, H. MIN *et al.*, 2010 The cysteine protease MoAtg4 interacts with MoAtg8 and is required for differentiation and pathogenesis in *Magnaporthe oryzae*. Autophagy **6:** 74-85.

LIU, X. H., J. P. LU, L. ZHANG, B. DONG, H. MIN *et al.*, 2007 Involvement of a *Magnaporthe grisea* serine/threonine kinase gene, *MgATG1*, in appressorium turgor and pathogenesis. Eukaryot. Cell **6:** 997-1005.

LORD, K. M., and N. D. READ, 2011 Perithecium morphogenesis in *Sordaria macrospora*. Fungal Genet Biol **48:** 388-399.

MADDI, A., and S. J. FREE, 2010 alpha-1,6-Mannosylation of N-linked oligosaccharide present on cell wall proteins is required for their incorporation into the cell wall in the filamentous fungus *Neurospora crassa*. Eukaryot Cell **9:** 1766-1775.

MAERZ, S., Y. FUNAKOSHI, Y. NEGISHI, T. SUZUKI and S. SEILER, 2010 The *Neurospora* peptide:N-glycanase ortholog PNG1 is essential for cell polarity despite its lack of enzymatic activity. J Biol Chem **285:** 2326-2332.

MANAGADZE, D., C. WURTZ, S. WIESE, H. E. MEYER, G. NIEHAUS *et al.*, 2010 A proteomic approach towards the identification of the matrix protein content of the two types of microbodies in *Neurospora crassa*. Proteomics **10:** 3222-3234.

MARCHLER-BAUER, A., and S. H. BRYANT, 2004 CD-Search: protein domain annotations on the fly. Nucleic Acids Res **32:** W327-331.

MASSEY, A., R. KIFFIN and A. M. CUERVO, 2004 Pathophysiology of chaperone-mediated autophagy. Int J Biochem Cell Biol **36:** 2420-2434.

MATSUDA, A., Y. SUZUKI, G. HONDA, S. MURAMATSU, O. MATSUZAKI *et al.*, 2003 Large-scale identification and characterization of human genes that activate NF-kappaB and MAPK signaling pathways. Oncogene **22:** 3307-3318.

MEIJER, W. H., I. J. VAN DER KLEI, M. VEENHUIS and J. A. KIEL, 2007 ATG genes involved in non-selective autophagy are conserved from yeast to man, but the selective Cvt and pexophagy pathways also require organism-specific genes. Autophagy **3:** 106-116.

MIZUSHIMA, N., T. NODA, T. YOSHIMORI, Y. TANAKA, T. ISHII *et al.*, 1998 A protein conjugation system essential for autophagy. Nature **395:** 395-398.

MIZUSHIMA, N., A. YAMAMOTO, M. HATANO, Y. KOBAYASHI, Y. KABEYA *et al.*, 2001 Dissection of autophagosome formation using Apg5-deficient mouse embryonic stem cells. J Cell Biol **152:** 657-668.

NADAL, M., and S. E. GOLD, 2010 The autophagy genes *atg8* and *atg1* affect morphogenesis and pathogenicity in *Ustilago maydis*. Mol Plant Pathol **11:** 463-478.

NAKATOGAWA, H., Y. ICHIMURA and Y. OHSUMI, 2007 Atg8, a ubiquitin-like protein required for autophagosome formation, mediates membrane tethering and hemifusion. Cell **130:** 165-178.

NAKATOGAWA, H., J. ISHII, E. ASAI and Y. OHSUMI, 2012 Atg4 recycles inappropriately lipidated Atg8 to promote autophagosome biogenesis. Autophagy **8:** 177-186.

NATARAJAN, K., M. R. MEYER, B. M. JACKSON, D. SLADE, C. ROBERTS *et al.*, 2001 Transcriptional profiling shows that Gcn4p is a master regulator of gene expression during amino acid starvation in yeast. Mol Cell Biol **21:** 4347-4368.

NICHOLAS, K. B., H. B. NICHOLAS JR and D. W. DEERFIELD II, 1997 GeneDoc: Analysis and Visualization of Genetic Variation. EMBNET.news **4:** 1-4.

NIERMAN, W. C., A. PAIN, M. J. ANDERSON, J. R. WORTMAN, H. S. KIM *et al.*, 2005 Genomic sequence of the pathogenic and allergenic filamentous fungus *Aspergillus fumigatus*. Nature **438:** 1151-1156.

NOBUKUNI, T., M. JOAQUIN, M. ROCCIO, S. G. DANN, S. Y. KIM *et al.*, 2005 Amino acids mediate mTOR/raptor signaling through activation of class 3 phosphatidylinositol 3OH-kinase. Proc Natl Acad Sci USA **102:** 14238-14243.

NODA, N. N., Y. OHSUMI and F. INAGAKI, 2010 Atg8-family interacting motif crucial for selective autophagy. FEBS Lett **584:** 1379-1385.

NODA, N. N., K. SATOO, Y. FUJIOKA, H. KUMETA, K. OGURA *et al.*, 2011 Structural basis of Atg8 activation by a homodimeric E1, Atg7. Mol Cell **44:** 462-475.

NOGUCHI, R., S. BANNO, R. ICHIKAWA, F. FUKUMORI, A. ICHIISHI *et al.*, 2007 Identification of OS-2 MAP kinase-dependent genes induced in response to osmotic stress, antifungal agent fludioxonil, and heat shock in *Neurospora crassa*. Fungal Genet Biol **44:** 208-218.

NOLTING, N., Y. BERNHARDS and S. PÖGGELER, 2009 SmATG7 is required for viability in the homothallic ascomycete *Sordaria macrospora*. Fungal Genet Biol **46:** 531-542.

NOLTING, N., and S. PÖGGELER, 2006 A MADS box protein interacts with a mating-type protein and is required for fruiting body development in the homothallic ascomycete *Sordaria macrospora*. Eukaryot Cell **5:** 1043-1056.

NOWROUSIAN, M., and P. CEBULA, 2005 The gene for a lectin-like protein is transcriptionally activated during sexual development, but is not essential for fruiting body formation in the filamentous fungus *Sordaria macrospora*. BMC Microbiol **5:** 64.

NOWROUSIAN, M., S. MASLOFF, S. PÖGGELER and U. KÜCK, 1999 Cell differentiation during sexual development of the fungus *Sordaria macrospora* requires ATP citrate lyase activity. Mol Cell Biol **19:** 450-460.

NOWROUSIAN, M., C. RINGELBERG, J. C. DUNLAP, J. J. LOROS and U. KÜCK, 2005 Cross-species microarray hybridization to identify developmentally regulated genes in the filamentous fungus *Sordaria macrospora*. Mol Genet Genomics **273:** 137-149.

NOWROUSIAN, M., J. E. STAJICH, M. CHU, I. ENGH, E. ESPAGNE *et al.*, 2010 De novo assembly of a 40 Mb eukaryotic genome from short sequence reads: *Sordaria macrospora*, a model organism for fungal morphogenesis. PLoS Genet **6:** e1000891.

NOWROUSIAN, M., I. TEICHERT, S. MASLOFF and U. KÜCK, 2012 Whole-Genome Sequencing of *Sordaria macrospora* Mutants Identifies Developmental Genes. G3 (Bethesda) **2:** 261-270.

OBARA, K., and Y. OHSUMI, 2011a Atg14: a key player in orchestrating autophagy. Int J Cell Biol **2011:** 713435.

OBARA, K., and Y. OHSUMI, 2011b PtdIns 3-Kinase Orchestrates Autophagosome Formation in Yeast. J Lipids **2011:** Article ID 498768, 9 pages.

OHSUMI, Y., 2001 Molecular dissection of autophagy: two ubiquitin-like systems. Nat Rev Mol Cell Biol **2:** 211-216.

OKAMOTO, K., N. KONDO-OKAMOTO and Y. OHSUMI, 2009 Mitochondria-anchored receptor Atg32 mediates degradation of mitochondria via selective autophagy. Dev Cell **17:** 87-97.

OTA, T., Y. SUZUKI, T. NISHIKAWA, T. OTSUKI, T. SUGIYAMA *et al.*, 2004 Complete sequencing and characterization of 21,243 full-length human cDNAs. Nat Genet **36:** 40-45.

PALCZEWSKI, K., 1994 Structure and functions of arrestins. Protein Sci **3:** 1355-1361.

PANARETOU, C., J. DOMIN, S. COCKCROFT and M. D. WATERFIELD, 1997 Characterization of p150, an adaptor protein for the human phosphatidylinositol (PtdIns) 3-kinase. Substrate presentation by phosphatidylinositol transfer protein to the p150.Ptdins 3-kinase complex. J Biol Chem **272:** 2477-2485.

PANKIV, S., T. H. CLAUSEN, T. LAMARK, A. BRECH, J. A. BRUUN *et al.*, 2007 p62/SQSTM1 binds directly to Atg8/LC3 to facilitate degradation of ubiquitinated protein aggregates by autophagy. J Biol Chem **282:** 24131-24145.

PARE, A., M. KIM, M. T. JUAREZ, S. BRODY and W. MCGINNIS, 2012 The functions of grainy head-like proteins in animals and fungi and the evolution of apical extracellular barriers. PLoS One **7:** e36254.

PFAFFL, M. W., G. W. HORGAN and L. DEMPFLE, 2002 Relative expression software tool (REST) for group-wise comparison and statistical analysis of relative expression results in real-time PCR. Nucleic Acids Res **30:** e36.

PINAN-LUCARRE, B., A. BALGUERIE and C. CLAVE, 2005 Accelerated cell death in *Podospora* autophagy mutants. Eukaryot Cell **4:** 1765-1774.

PINAN-LUCARRE, B., and C. CLAVE, 2008 Monitoring autophagy in the filamentous fungus *Podospora anserina*. Methods Enzymol **451:** 251-270.

PINAN-LUCARRE, B., M. PAOLETTI, K. DEMENTHON, B. COULARY-SALIN and C. CLAVE, 2003 Autophagy is induced during cell death by incompatibility and is essential for differentiation in the filamentous fungus *Podospora anserina*. Mol Microbiol **47:** 321-333.

PÖGGELER, S., and U. KÜCK, 2004 A WD40 repeat protein regulates fungal cell differentiation and can be replaced functionally by the mammalian homologue striatin. Eukaryot Cell **3:** 232-240.

PÖGGELER, S., and U. KÜCK, 2006 Highly efficient generation of signal transduction knockout mutants using a fungal strain deficient in the mammalian *ku70* ortholog. Gene **378:** 1-10.

PÖGGELER, S., S. MASLOFF, B. HOFF, S. MAYRHOFER and U. KÜCK, 2003 Versatile EGFP reporter plasmids for cellular localization of recombinant gene products in filamentous fungi. Curr Genet **43:** 54-61.

PÖGGELER, S., M. NOWROUSIAN, S. JACOBSEN and U. KÜCK, 1997 An efficient procedure to isolate fungal genes from an indexed cosmid library. J. Microbiol. Methods **29:** 49-61.

PÖGGELER, S., M. NOWROUSIAN, C. RINGELBERG, J. J. LOROS, J. C. DUNLAP *et al.*, 2006 Microarray and real-time PCR analyses reveal mating type-dependent gene expression in a homothallic fungus. Mol Genet Genomics **275:** 492-503.

POLLACK, J. K., S. D. HARRIS and M. R. MARTEN, 2009 Autophagy in filamentous fungi. Fungal Genet Biol **46:** 1-8.

RAWLINGS, N. D., and A. J. BARRETT, 1995 Evolutionary families of metallopeptidases. Methods Enzymol **248:** 183-228.

READ, N. D., 1983 A scanning electron microscopic study of the external features of perithecium development in *Sordaria humana*. Can. J. Bot **61:** 3217-3229.

READ, N. D., and A. BECKETT, 1985 The anatomy of the mature perithecium in *Sordaria humana* and its significance for fungal multicellular development. Can. J. Bot **63:** 281-296.

REGGIORI, F., and D. J. KLIONSKY, 2002 Autophagy in the eukaryotic cell. Eukaryot Cell **1:** 11-21.

RICHIE, D. L., K. K. FULLER, J. FORTWENDEL, M. D. MILEY, J. W. MCCARTHY *et al.*, 2007 Unexpected link between metal ion deficiency and autophagy in *Aspergillus fumigatus*. Eukaryot Cell **6:** 2437-2447.

RZEM, R., M. VEIGA-DA-CUNHA, G. NOEL, S. GOFFETTE, M. C. NASSOGNE *et al.*, 2004 A gene encoding a putative FAD-dependent L-2-hydroxyglutarate dehydrogenase is mutated in L-2-hydroxyglutaric aciduria. Proc Natl Acad Sci USA **101:** 16849-16854.

SAMBROOK, J., and D. W. RUSSELL, 2001 *Molecular cloning : a laboratory manual / Joseph Sambrook, David W. Russell*. Cold Spring Harbor Laboratory, Cold Spring Harbor, N.Y.

SANCAR, G., C. SANCAR, B. BRUGGER, N. HA, T. SACHSENHEIMER *et al.*, 2011 A global circadian repressor controls antiphasic expression of metabolic genes in *Neurospora*. Mol Cell **44:** 687-697.

SASSE, C., E. M. BIGNELL, M. HASENBERG, K. HAYNES, M. GUNZER *et al.*, 2008 Basal expression of the *Aspergillus fumigatus* transcriptional activator CpcA is sufficient to support pulmonary aspergillosis. Fungal Genet Biol **45:** 693-704.

SATOO, K., N. N. NODA, H. KUMETA, Y. FUJIOKA, N. MIZUSHIMA *et al.*, 2009 The structure of Atg4B-LC3 complex reveals the mechanism of LC3 processing and delipidation during autophagy. EMBO J **28:** 1341-1350.

SATOO, K., N. N. SUZUKI, Y. FUJIOKA, N. MIZUSHIMA, Y. OHSUMI *et al.*, 2007 Crystallization and preliminary crystallographic analysis of human Atg4B-LC3 complex. Acta Crystallogr Sect F Struct Biol Cryst Commun **63:** 99-102.

SAUPE, S. J., 2000 Molecular genetics of heterokaryon incompatibility in filamentous ascomycetes. Microbiol Mol Biol Rev **64:** 489-502.

SAUPE, S. J., 2011 The [Het-s] prion of *Podospora anserina* and its role in heterokaryon incompatibility. Semin Cell Dev Biol **22:** 460-468.

SEILER, S., and M. PLAMANN, 2003 The genetic basis of cellular morphogenesis in the filamentous fungus *Neurospora crassa*. Mol Biol Cell **14:** 4352-4364.

SHINTANI, T., and D. J. KLIONSKY, 2004 Autophagy in health and disease: a double-edged sword. Science **306:** 990-995.

SHINTANI, T., N. MIZUSHIMA, Y. OGAWA, A. MATSUURA, T. NODA *et al.*, 1999 Apg10p, a novel protein-conjugating enzyme essential for autophagy in yeast. EMBO J **18:** 5234-5241.

SHOJI, J. Y., and K. D. CRAVEN, 2011 Autophagy in basal hyphal compartments: A green strategy of great recyclers. Fungal Biol Rev. **25:** 79-83.

SHOJI, J. Y., T. KIKUMA, M. ARIOKA and K. KITAMOTO, 2010 Macroautophagy-mediated degradation of whole nuclei in the filamentous fungus *Aspergillus oryzae*. PLoS One **5:** e15650.

SLESSAREVA, J. E., S. M. ROUTT, B. TEMPLE, V. A. BANKAITIS and H. G. DOHLMAN, 2006 Activation of the phosphatidylinositol 3-kinase Vps34 by a G protein alpha subunit at the endosome. Cell **126:** 191-203.

SMITH, K. M., G. SANCAR, R. DEKHANG, C. M. SULLIVAN, S. LI *et al.*, 2010 Transcription factors in light and circadian clock signaling networks revealed by genomewide mapping of direct targets for *neurospora* white collar complex. Eukaryot Cell **9:** 1549-1556.

STASYK, O. V., I. J. VAN DER KLEI, A. R. BELLU, S. SHEN, J. A. KIEL *et al.*, 1999 A *Pichia pastoris* VPS15 homologue is required in selective peroxisome autophagy. Curr Genet **36:** 262-269.

STEIN, T., J. KRICKE, D. BECHER and T. LISOWSKY, 1998 Azf1p is a nuclear-localized zinc-finger protein that is preferentially expressed under non-fermentative growth conditions in *Saccharomyces cerevisiae*. Curr Genet **34:** 287-296.

STEPHENSON, S. A., C. M. STEPHENS, D. J. MACLEAN and J. M. MANNERS, 2005 CgDN24: a gene involved in hyphal development in the fungal phytopathogen *Colletotrichum gloeosporioides*. Microbiol Res **160:** 389-397.

STRITTMATTER, A. W., S. IRNIGER and G. H. BRAUS, 2001 Induction of *jlbA* mRNA synthesis for a putative bZIP protein of *Aspergillus nidulans* by amino acid starvation. Curr Genet **39:** 327-334.

SU, W., H. MA, C. LIU, J. WU and J. YANG, 2006 Identification and characterization of two rice autophagy associated genes, *OsAtg8* and *OsAtg4*. Mol Biol Rep **33:** 273-278.

SUGAWARA, K., N. N. SUZUKI, Y. FUJIOKA, N. MIZUSHIMA, Y. OHSUMI *et al.*, 2004 The crystal structure of microtubule-associated protein light chain 3, a mammalian homologue of *Saccharomyces cerevisiae* Atg8. Genes Cells **9:** 611-618.

SUGAWARA, K., N. N. SUZUKI, Y. FUJIOKA, N. MIZUSHIMA, Y. OHSUMI *et al.*, 2005 Structural basis for the specificity and catalysis of human Atg4B responsible for mammalian autophagy. J Biol Chem **280:** 40058-40065.

SUN, J., and N. L. GLASS, 2011 Identification of the CRE-1 cellulolytic regulon in *Neurospora crassa*. PLoS One **6:** e25654.

SUN, J., C. TIAN, S. DIAMOND and N. L. GLASS, 2012 Deciphering transcriptional regulatory mechanisms associated with hemicellulose degradation in *Neurospora crassa*. Eukaryot Cell **11:** 482-493.

SUN, X., H. ZHANG, Z. ZHANG, Y. WANG and S. LI, 2011 Involvement of a helix-loop-helix transcription factor CHC-1 in CO(2)-mediated conidiation suppression in *Neurospora crassa*. Fungal Genet Biol **48:** 1077-1086.

SURIAPRANATA, I., U. D. EPPLE, D. BERNREUTHER, M. BREDSCHNEIDER, K. SOVARASTEANU *et al.*, 2000 The breakdown of autophagic vesicles inside the vacuole depends on Aut4p. J Cell Sci **113 (Pt 22):** 4025-4033.

SUZUKI, K., T. KIRISAKO, Y. KAMADA, N. MIZUSHIMA, T. NODA *et al.*, 2001 The pre-autophagosomal structure organized by concerted functions of *APG* genes is essential for autophagosome formation. EMBO J **20:** 5971-5981.

SUZUKI, K., and Y. OHSUMI, 2007 Molecular machinery of autophagosome formation in yeast, *Saccharomyces cerevisiae*. FEBS Lett **581:** 2156-2161.

TAKEDA, K., T. YOSHIDA, S. KIKUCHI, K. NAGAO, A. KOKUBU *et al.*, 2010 Synergistic roles of the proteasome and autophagy for mitochondrial maintenance and chronological lifespan in fission yeast. Proc Natl Acad Sci USA **107:** 3540-3545.

TANIDA, I., 2011 Autophagosome formation and molecular mechanism of autophagy. Antioxid Redox Signal **14:** 2201-2214.

TANIDA, I., N. MIZUSHIMA, M. KIYOOKA, M. OHSUMI, T. UENO *et al.*, 1999 Apg7p/Cvt2p: A novel protein-activating enzyme essential for autophagy. Mol Biol Cell **10:** 1367-1379.

TASDEMIR, E., M. C. MAIURI, N. TAJEDDINE, I. VITALE, A. CRIOLLO *et al.*, 2007 Cell cycle-dependent induction of autophagy, mitophagy and reticulophagy. Cell Cycle **6:** 2263-2267.

THOMPSON, J. D., T. J. GIBSON, F. PLEWNIAK, F. JEANMOUGIN and D. G. HIGGINS, 1997 The CLUSTAL_X windows interface: flexible strategies for multiple sequence alignment aided by quality analysis tools. Nucleic Acids Res **25:** 4876-4882.

TIAN, C., W. T. BEESON, A. T. IAVARONE, J. SUN, M. A. MARLETTA *et al.*, 2009 Systems analysis of plant cell wall degradation by the model filamentous fungus *Neurospora crassa*. Proc Natl Acad Sci USA **106:** 22157-22162.

TIAN, C., J. LI and N. L. GLASS, 2011 Exploring the bZIP transcription factor regulatory network in *Neurospora crassa*. Microbiology **157:** 747-759.

TOWBIN, H., T. STAEHELIN and J. GORDON, 1979 Electrophoretic transfer of proteins from polyacrylamide gels to nitrocellulose sheets: procedure and some applications. Proc Natl Acad Sci USA **76:** 4350-4354.

TUCKER, C. L., L. A. PETEYA, A. M. PITTMAN and J. ZHONG, 2009 A genetic test for yeast two-hybrid bait competency using RanBPM. Genetics **182:** 1377-1379.

UTTENWEILER, A., and A. MAYER, 2008 Microautophagy in the yeast *Saccharomyces cerevisiae*. Methods Mol Biol **445:** 245-259.

VAN DEN BERG, M. A., R. ALBANG, K. ALBERMANN, J. H. BADGER, J. M. DARAN *et al.*, 2008 Genome sequencing and analysis of the filamentous fungus *Penicillium chrysogenum*. Nat Biotechnol **26:** 1161-1168.

VENEAULT-FOURREY, C., M. BAROOAH, M. EGAN, G. WAKLEY and N. J. TALBOT, 2006 Autophagic fungal cell death is necessary for infection by the rice blast fungus. Science **312:** 580-583.

VENEAULT-FOURREY, C., and N. J. TALBOT, 2007 Autophagic cell death and its importance for fungal developmental biology and pathogenesis. Autophagy **3:** 126-127.

VIDEIRA, A., T. KASUGA, C. TIAN, C. LEMOS, A. CASTRO *et al.*, 2009 Transcriptional analysis of the response of *Neurospora crassa* to phytosphingosine reveals links to mitochondrial function. Microbiology **155:** 3134-3141.

WANG, Z., N. LEHR, F. TRAIL and J. P. TOWNSEND, 2012 Differential impact of nutrition on developmental and metabolic gene expression during fruiting body development in *Neurospora crassa*. Fungal Genet Biol **49:** 405-413.

WANKE, C., S. ECKERT, G. ALBRECHT, W. VAN HARTINGSVELDT, P. J. PUNT *et al.*, 1997 The *Aspergillus niger GCN4* homologue, *cpcA*, is transcriptionally regulated and encodes an unusual leucine zipper. Mol Microbiol **23:** 23-33.

WELTERS, P., K. TAKEGAWA, S. D. EMR and M. J. CHRISPEELS, 1994 AtVPS34, a phosphatidylinositol 3-kinase of *Arabidopsis thaliana*, is an essential protein with homology to a calcium-dependent lipid binding domain. Proc Natl Acad Sci USA **91:** 11398-11402.

YAMAMOTO, A., and A. SIMONSEN, 2010 The elimination of accumulated and aggregated proteins: A role for aggrephagy in neurodegeneration. Neurobiol Dis **43:** 17-28

YAN, Y., and J. M. BACKER, 2007 Regulation of class III (Vps34) PI3Ks. Biochem Soc Trans **35:** 239-241.

YORIMITSU, T., and D. J. KLIONSKY, 2005 Autophagy: molecular machinery for self-eating. Cell Death Differ **12 Suppl 2:** 1542-1552.

YU, Z. Q., T. NI, B. HONG, H. Y. WANG, F. J. JIANG *et al.*, 2012 Dual roles of Atg8-PE deconjugation by Atg4 in autophagy. Autophagy **8:** 883-92.

6. List of figures

7. List of tables

8. Curriculum vitae

Personal details
Oliver Voigt
born on April 15th, 1979
in Berlin, Germany

Address: Hannoversche Straße 102, 37077 Göttingen

Education

1984-1989	Marshall Shukow Oberschule
1989-1990	Grundschule Himmelsthür
1990-1992	Orientierungsstufe Himmelsthür
1992-1996	Realschule Himmelsthür
1996-1999	Gymnasium Himmelsthür (Graduation: Abitur)

Non educational engagement

1999-2000	Civilian service

Academic career

2001-2008	Study of biology at the Georg-August-University in Göttingen. Subject: Microbiology (main), Botany and Chemistry (side)
2007-2008	Diploma thesis "Characterization of the *f-box* genes *32,58,62* in the filamentous fungus *Aspergillus nidulans*" in the department of Molecular Microbiology and Genetics (Prof. Braus) at the Georg-August-University in Göttingen.
2008-2012	Scientific assistant and PhD student in the department: Genetics of eukaryotic microorganisms of Prof. Stefanie Pöggeler at the Georg-August-University in Göttingen. Thesis title: "The influence of autophagy on the fruiting-body development of the filamentous ascomycete *Sordaria macrospora*".

Göttingen, 14.09.2012